

Evaluating the transport and removal of coated microspheres as *Cryptosporidium*
surrogates in drinking water filtration

by

Jeffrey Seaman

A thesis submitted in partial fulfillment of the requirements for the degree of

Master of Science

in

Environmental Science

Department of Civil and Environmental Engineering
University of Alberta

© Jeffrey Seaman, 2015

Abstract

In this study, a glycopolymer-modified microsphere surrogate for *Cryptosporidium* was developed, characterized, and used in filtration experiments. Several surrogates were investigated (yeast, unmodified microspheres, glycoprotein-modified microspheres), and then compared to *Cryptosporidium* oocysts. Glycopolymer-modified microspheres were the most cost effective option, with a size and surface charge similar to viable *Cryptosporidium*. The effect of three common polyelectrolyte coagulant aids on glycopolymer-modified microspheres was investigated. Cationic epichlorohydrin amine (ECHA) was determined to be the most effective with regards to charge reversal and attachment to silica surfaces as evaluated by quartz crystal microbalance with dissipation monitoring (QCM-D). The glycopolymer-modified microspheres were then used in pilot-scale filtration experiments. Results indicate that influent conditions play an important role in the transport and removal of glycopolymer-modified microspheres, with increased turbidity having a negative impact on log-removal. Increased flow rate was also observed to have a negative impact on log-removal.

Acknowledgments

Completing this thesis was a continuous learning process that tested my persistence and patience. Many people helped carry out this research, and any success I achieved is due to their support.

First, I'd like to acknowledge to my parents and brother – thank you for instilling in me a work ethic and always supporting me. You have shaped the person I am, and for that I am so thankful.

I am grateful to my supervisor, Dr. Yang Liu, for letting me into graduate school and providing guidance and motivation along the way.

I'd like to acknowledge the fine people at EPCOR, I am deeply grateful for your help and humbled by your depth of knowledge, particularly the Process Development Team. This could not have been done without you. Dr. Steve Craik, Wendell James, Sadra Heidary-Monfrared, Garry Solonyanko, Dr. Rasha-Maal Bared.

Thanks to Yinan Wang and Dr. Ravin Narain for helping with the microsphere coating and characterization, and introducing me to the fascinating world of quartz crystal microbalance with dissipation monitoring.

Thanks to the organizations that provided funding. EPCOR and Natural Sciences and Engineering Research Council of Canada.

Lastly, I have amazing communities of friends and family in both Calgary and Edmonton. Thank you for supporting and caring for me. To those people in my life who always wondered what I was researching, read this thesis. I promise you it is exactly as boring as you thought.

Table of Contents

Chapter 1. Introduction.....	1
1.1 <i>Cryptosporidium</i> public health risks.....	1
1.2 Needs for <i>Cryptosporidium</i> removal.....	1
1.3 Monitoring of <i>Cryptosporidium</i>	2
1.4 Need for reliable <i>Cryptosporidium</i> surrogates.....	3
1.5 Overall study aims and thesis structure	4
1.6 References	5
Chapter 2. Literature Review	8
2.1 <i>Cryptosporidium</i> life cycle and infectivity	8
2.2 Drinking water treatment methods for <i>Cryptosporidium</i> removal	9
2.2.1 Chemical and UV treatment.....	10
2.2.2 Physical treatment	10
2.3 Review of removal mechanisms in granular filtration.....	10
2.3.1 Rapid filtration overview	10
2.3.2 Colloidal transport and removal mechanisms	11
2.4 Review of colloidal filtration models	13
2.4.1 Review of colloidal filtration models.....	13
2.4.2 Particle stability and DLVO theory	14
2.5 Role of pretreatment in removal.....	16
2.5.1 Coagulation and optimization for pathogen removal.....	16
2.5.2 Polymers.....	17
2.6 Review of <i>Cryptosporidium</i> detection and indicators	18
2.6.1 Overview of standard detection methods.....	18
2.6.2 <i>Cryptosporidium</i> indicators and surrogate	18
2.7 Review of engineered polystyrene microspheres	19
2.7.1 Role of surface properties in filtration	19
2.7.2 Polystyrene microsphere modification.....	20
2.8 Areas for further study	20
2.9 References	21
Chapter 3. Surrogate Development and Characterization	28
3.1 Introduction	28
3.2 Methods	29
3.2.1 Surrogate Development and Preparation	29
3.2.1.1 Unmodified carboxylate polystyrene microspheres.....	30
3.2.1.2 AGP-modified carboxylate microspheres	30
3.2.1.3 Glycopolymers-modified microspheres	31
3.2.1.4 Viable <i>C. parvum</i>	33

3.2.1.5 Non-viable <i>C. parvum</i>	33
3.2.1.5 Yeast at 1-, 2-, and 4-hour incubation.....	34
3.2.2 Zeta potential and particle size measurement methods.....	34
3.2.2.1 Zeta Potential.....	34
3.2.2.2 Particle Size.....	35
3.3 Results and Discussion	36
3.3.1 Fluoresbrite carboxylate polystyrene microspheres.....	36
3.3.1.1 Microsphere modification zeta potential results	36
3.3.3 Yeast.....	40
3.3.3.1 Yeast zeta potential (1, 2, and 4-hour incubation)	40
3.3.4 Comparison of potential surrogates	43
3.4 Conclusions	43
3.5 References	45
Chapter 4. Chemical pretreatment and polyelectrolyte optimization	48
4.1 Introduction	48
4.1.1 Background	48
4.1.3 Polyelectrolyte characteristics.....	49
4.1.3 QCM-D background	50
4.2 Methods and materials.....	53
4.2.1 Gel permeation chromatography.....	53
4.2.2 Zeta potential.....	53
4.2.3 QCM-D	54
4.2.3.1 Glycopolymer-modified microsphere preparation for QCM-D.....	54
4.2.3.2 QCM-D analysis	55
4.3 Results and Discussion	56
4.3.1 GPC	56
4.3.2 Zeta potential.....	57
4.3.3 QCM-D	59
4.4 Conclusions	63
4.5 References	64
Chapter 5: Pilot Scale Experiments	67
5.1 Introduction	67
5.1.1 Experimental design.....	68
5.1.2 Objectives.....	70
5.2 Methods and Experimental Design.....	71
5.2.1 Pilot column schematic and design.....	71
5.2.2 Influent water pretreatment.....	73
5.2.3 Seeding preparation and procedure.....	74
5.2.3.1 Seeding batch preparation and concentration determination	74
5.2.3.2 Seeding procedure	77
5.2.4 Sampling Plan	77
5.2.4.1 Filter run.....	77
5.2.4.2 Backwash	79
5.2.5 Analytical Methods	79
5.2.5.1 Microsphere Enumeration	79

5.2.5.2 Turbidity and particle counts.....	81
5.2.5.3 Free chlorine, pH, and conductivity.....	82
5.2.5.4 Major ions and metals	82
5.2.5.5 Total organic carbon (TOC).....	82
5.3.1 Influent Water Conditions.....	82
5.3.2 Microsphere influent concentration and log-removal.....	85
5.3.2.1 Influent surrogate concentration	85
5.3.2.2 Impact of flow rate on surrogate log-removal.....	87
5.3.2.3 Impact of influent conditions on surrogate log-removal	91
5.3.3 Statistical analysis of log-removal	95
5.3.3.1 ANOVA results.....	95
5.3.3.2 Interaction plots.....	96
5.3.3.3 Normal plot of effects.....	97
5.3.4 Deposition profile and rate coefficients	98
5.3.4.1 Deposition profiles.....	98
5.3.5 Correlation with turbidity and particle counts	105
5.3.6 Backwash microsphere concentrations	107
5.3.7 Mass balance, losses, and recovery	109
5.4 Summary and conclusions from pilot-scale experiments	111
5.4.1 Summary of main results	111
5.5 References	113
Chapter 6. Conclusions and future work.....	118
6.1 Major conclusions.....	118
6.2 Future work	119
References.....	121
Appendix A	132
Appendix B	136

List of Tables

Table 3.1 Particle concentrations for zeta potential analysis	35
Table 3.2 Percent recovery of microsphere surface modification with different biomolecules	36
Table 4.1 Number average molecular weight (Mn), weighted average molecular weight (Mw), and polydispersity index (PDI) of different polyelectrolytes	57
Table 5.1 Pilot scale experimental conditions	70
Table 5.2 Chemical pretreatment and filter operation parameters.....	74
Table 5.3 Sampling overview for each pilot filter run.....	78
Table 5.4 Ratio of microscopically determined microsphere counts to actual counts from manufacturer specifications.....	80
Table 5.5 Microsphere sample enumeration volumes and corresponding filter diameters for direct microscope counting	81
Table 5.6 Influent water quality parameters for direct and conventional filtration pilot experiments	83
Table 5.7 Water influent parameters with noteworthy differences between direct and conventional filtration influent.....	84
Table 5.8 Factor designations for two-way ANOVA	95
Table 5.9 ANOVA summary table	96
Table 5.10 T-E model attachment efficiency and single collector efficiency for direct and conventional filtration	102
Table 5.11 Percent loss (\pm SD) from seeding and backwash recovery for all experimental conditions.	110

Table 5.12 Anderson-Darling normality tests for log-removal data.....	134
Table 5.13 Contrast and effects table designations.....	135
Table 5.14a Total microsphere counts at different points of the experimental system for direct filtration pilot-column trials.....	137
Table 5.14b Total microsphere counts at different points of the experimental system for conventional filtration pilot-column trials	138

List of Figures

Figure 2.1 Casual agents of cryptosporidiosis and <i>Cryptosporidium</i> life cycle	9
Figure 2.2 Particle removal mechanisms in granular filtration.....	12
Figure 2.3 Structure of the electric double layer for a negatively charge cell, or colloid.	15
Figure 3.1 Unmodified carboxylate microsphere schematic representation.....	30
Figure 3.2 Schematic of conjugation of biomolecules to microsphere surface	31
Figure 3.3 Schematic representations of (a) AGP-modified microspheres, and (b) glycopolymers-modified microspheres.	32
Figure 3.4 Zeta potential (\pm SD) of microsphere particles with different biomolecule surface modifications in 1mM KCl.....	37
Figure 3.5 Visualization of microspheres by epifluorescent microscopy.....	38
Figure 3.6 Zeta potential (\pm SD) of viable and non-viable <i>C. parvum</i> oocysts. Non-viable oocysts are inactivated by UV irradiation.....	40
Figure 3.7 Zeta potential (\pm SD) for yeast particles cultivated at 1, 2, and 4-hour incubation at 37°C in PBS.....	41
Figure 3.8 Yeast hydrodynamic particle size (\pm SE) after cultivation at 1, 2, and 4-hour incubation periods, measured by DLS.....	42
Figure 3.9 <i>C. parvum</i> surrogate zeta potential comparison.	43
Figure 4.1 Structures of cationic polyelectrolytes (a) pDADMAC, (b) ECHA, and anionic polyelectrolyte (c) APAM.....	50
Figure 4.2 QCM-D principle; with (a) slow dissipation with a rigid film, and (b) fast dissipation with a “soft” (viscoelastic) film.....	52

Figure 4.3 Zeta potential of glycopolymer-modified microspheres under different concentrations of pDADMAC, with and without 5 mg/L alum.	58
Figure 4.4 Zeta potential of glycopolymer-modified microspheres under different concentrations of ECHA, with and without 5 mg/L alum.	59
Figure 4.5 Frequency shifts of 3 rd overtone for glycopolymer-modified microspheres adhered to SiO ₂ sensor surface.	60
Figure 4.6 Dissipation shifts of 3 rd overtone for glycopolymer-modified microspheres adhered to SiO ₂ sensor surface	61
Figure 4.7 Visualization of glycopolymer-modified microspheres adhered to SiO ₂ sensor surface	62
Figure 4.8 Slopes of frequency divided by dissipation at the end of the experiment.	63
Figure 5.1 Flow diagrams for direct filtration and conventional filtration	69
Figure 5.2 Pilot column photo.	72
Figure 5.3 Pilot column schematic with influent recirculation loop and inline instrumentation locations.	73
Figure 5.4 Pilot-scale influent surrogate concentrations.....	86
Figure 5.5 Pilot scale log-removals ± SD of glycopolymer-modified microspheres at 5.7 and 8.6 m/h for (a) direct filtration, and (b) conventional filtration	89
Figure 5.6 Pilot scale log-removals ± SD of glycopolymer-modified microspheres for conventional and direct filtration at (a) 8.6 m/h, and (b) 5.7 m/h.....	92
Figure 5.7 Interaction plots for log-removals +/- SE of pilot runs under different flow rates and filter operation conditions.....	97
Figure 5.8 Normal plot of effect for log-removal.	98

Figure 5.9. Deposition profile of microsphere removal in (a) direct filtration, and (b) conventional filtration under loading rate of 8.6 m/h, and 5.7 m/h. 99

Figure 5.10 Log₁₀-scale Deposition profile of microsphere removal in (a) direct filtration, and (b) conventional filtration under loading rate of 8.6 m/h, and 5.7 m/h.... 100

Figure 5.11 Deposition rate coefficients, K_d , as a function of filter media depth. Data shown are from (a) direct filtration, and (b) conventional filtration. 104

Figure 5.12 Average log removals \pm SD for glycopolymer-modified microspheres, turbidity, 3-5 μ m particles, 5-7 μ m particles, and 3-7 μ m particles 107

Figure 5.13 Log transformed backwash concentrations (\pm SD) for direct filtration pilot runs with filter loading rates of (a) 8.6 m/h, and (b) 5.7 m/h..... 108

Figure 5.14 Log transformed backwash concentrations (\pm SD) for conventional filtration pilot runs with filter loading rates of (a) 8.6 m/h, and (b) 5.7 m/h. 108

Figure 5.15 Observation order of log-removals versus model residuals 132

Figure 5.16 Fitted log-removal values versus model residuals..... 133

Figure 5.17 Normal probability plot for ANOVA of log-removals..... 134

List of Acronyms

AD	Anderson-Darling test for normality
AGP	α_1 -Acid glycoprotein
ANOVA	Analysis of variance
APAM	Anionic polyacrylamide
CFT	Colloidal filtration theory
DBP	Disinfection by-product
D	Dissipation
DI	Deionized water
DLS	Dynamic light scattering
DLVO	Derjaguin-Landau-Verwey-Overbeek theory
DMA	Dimethyl amine
ECHA	Epichlorohydrin amine
EDC	Carbodiimide crosslinker
F	Frequency
FITC	Fluorescein isothiocyanate
GPC	Gel permeation chromatography
IC	Ion chromatography
ICP-MS	Inductively coupled plasma mass spectrometry
IP	Isoelectric point
LT2ESWTR	Long Term 2 Enhanced Surface Water Treatment Rule
M_N	Number average molecular weight
M_W	Weighted average molecular weight
NOM	Natural organic matter
NG	Nelson-Ginn filtration model
NTU	Nephelometric Turbidity Unit
OD	Optical density
PAC	Powdered activated carbon
PBS	Phosphate-buffered saline
PDI	Polydispersity index
pDADMAC	Diallyldimethylammonium chloride

QCM-D	Quartz crystal microbalance with dissipation monitoring
RT	Rajagopalan-Tien filtration model
SD	Standard deviation
SDS	Sodium dodecyl sulphate
SE	Standard error
TE	Tufenkji-Elimelech correlation filtration model
TOC	Total organic carbon
USEPA	United States Environmental Protection Agency

Chapter 1. Introduction

1.1 *Cryptosporidium* public health risks

Drinking water treatment is of critical importance to maintain public health. In Canada, much of our drinking water supply is sourced from surface water. Ubiquitous in most surface waters are waterborne pathogens, such as *Giardia* and *Cryptosporidium*. In particular, *Cryptosporidium* spp. is a waterborne protozoan pathogen with a low infectious dose that can cause outbreaks of cryptosporidiosis, a gastrointestinal illness (Crittenden et al, 2005). Cryptosporidiosis presents most severely in young individuals, with symptoms including diarrhea, stomach cramps, and mild fever (Crittenden et al, 2005). Perhaps the most notable waterborne cryptosporidiosis outbreak occurred 1993 in Milwaukee, WI, where an estimated 403,000 residents became ill (MacKenzie et al, 1994). In Canada, an outbreak was observed in 2001 in North Battleford, Saskatchewan, affected 1907 individuals (Stirling et al 2001). More recently, an outbreak was observed in 2010 in Östersund, Sweden (Widerström et al, 2014).

Cryptosporidiosis incidents, not only limited to the previously noted events, have been mainly linked to inadequate removal of viable *Cryptosporidium* from drinking water, particularly during the oocysts stage, where *Cryptosporidium* is environmentally transmissible (Park et al, 2012; Metcalf and Eddy, 2003).

1.2 Needs for *Cryptosporidium* removal

Cryptosporidium oocysts are resistant to environmental modes of removal (e.g., soil and bank filtration), and transmission is fostered by the large number of oocysts produced by infected hosts (Chalmers, 2014). Presence of viable oocysts in drinking

water requires effective treatment and removal methods, which is critically important to ensure public health.

Since 1989, more attention has been given to *Cryptosporidium* due in part to the US Environmental Protection Agency's (EPA) Surface Water Treatment Rule (SWTR). Since the promulgation of the Long Term 2 Enhanced Surface Water Treatment Rule (LT2ESWTR) in 2006, utilities in the United States are required to monitor *Cryptosporidium* and achieve certain levels of inactivation or removal (typically 2 or 3-log) depending on raw water monitoring results (USEPA, 2005). The most recent federal guidelines provided by Health Canada require a minimum 3-log reduction and/or inactivation of *C. parvum* for utilities dedicated to drinking water treatment (Health Canada, 2012).

In Canada, direct filtration has become an established drinking water treatment method for surface water, particularly during winter conditions when water turbidity is typically low. Direct filtration involves coagulation and flocculation directly followed by filtration, without a settling process, unlike conventional treatment where settling occurs before filtration. Occasionally, during direct filtration operation in Edmonton AB, *Cryptosporidium* has been detected in effluent water from the granular filters (before any UV disinfection). This is significant, since effective filtration is required to maintain a multi-barrier approach for safe drinking water. Given this, the factors governing the removal of *Cryptosporidium* via direct filtration are not yet completely understood.

1.3 Monitoring of *Cryptosporidium*

The optimization of treatment processes is somewhat dependent on being able to monitor oocysts in drinking water. Evaluation and monitoring of *Cryptosporidium* log-reduction in water treatment poses a challenge due to difficulties associated with its concentration, identification, and enumeration. This involves sample concentration, particle elution, oocyst purification, fluorescence labeling, immunofluorescence microscopy, and further examination regarding the viability of oocysts. In addition, losses can occur within each step (LeChevallier et al, 1991). To reduce monitoring costs for utilities that require *Cryptosporidium* removal or inactivation, the LT2ESWTR allows for indicators that reliably quantify *Cryptosporidium* log removal (USEPA, 2005).

Traditionally, *C. parvum* has been considered and modeled as a colloidal particle (colloidal referring to suspended particles varying from 0.001 to 1.0 μm), and its removal has been correlated to turbidity removal (Emelko et al, 2005; Crittenden et al, 2005). This has proved problematic, as several studies have shown that turbidity provides only an approximate indicator of *Cryptosporidium* removal, and often overestimate oocysts removal (Swertfeger et al, 1999; Emelko, 2001; Huck et al, 2001). Since using viable *Cryptosporidium* oocysts to quantify and evaluate filtration processes at the pilot-scale is expensive and could pose public health risks, finding a reliable quantitative surrogate is important.

1.4 Need for reliable *Cryptosporidium* surrogates

Common examples of *Cryptosporidium* oocyst surrogates include algae, coliforms, *Bacillus subtilis* spores, yeasts, *E. coli*, and polystyrene microspheres (Emelko et al, 2005; USEPA 2005; Hagler, 2006; Chung, 2012). Polystyrene microspheres are not

ideal surrogates due to differences in surface properties (e.g., surface charge, isoelectric point) compared to viable *C. parvum* oocysts, resulting in different attachment and filtration characteristics (Pang et al, 2012). To more closely resemble oocyst surface characteristics, microspheres can be coated with biomolecules and then used to evaluate removal through granular filters. This has been done to some extent, but further investigation regarding the use of modified microspheres in pilot-scale filtration experiments is beneficial.

1.5 Overall study aims and thesis structure

The overarching goal of this thesis is to provide information that can be used to improve the overall operation of drinking water treatment, specifically with regards to *Cryptosporidium* removal in granular media filters. This was accomplished in three stages:

1. Develop and characterize effective *Cryptosporidium* surrogates to be used in filtration experiments.
2. Understand the impact of chemical pretreatment and polymers on the surface properties of *Cryptosporidium* surrogates and their interaction with solid surfaces.
3. Investigate the transport and removal of *Cryptosporidium* surrogates in pilot-scale granular media filters under both direct filtration and conventional filtration influent conditions at high and low flow rates.

This thesis is structured around these three stages. First, a brief literature review of *Cryptosporidium* removal in filtration is given (Chapter 2). The next three chapters (Chapters 3, 4, and 5) are experimental studies that address each of the above listed stages. Lastly, some brief conclusions and recommendations for future investigation are given (Chapter 6).

1.6 References

- Chalmers, R. M. Chapter Sixteen - *Cryptosporidium*. *Microbiology of Waterborne Diseases (Second Edition)* Academic Press, London. **2014**, 287-326.
- Chung, J. Development of fluorescently labelled *Cryptosporidium* oocysts surrogates to test the efficacy of sand filtration processes. PhD Dissertation, University of New South Wales, Australia **2012**
- Crittenden, J. C., Trussell, R. R., Hand, D. W., Howe, K. J., and Tchobanoglous, G. *MWH Water Treatment: Principles and Design: Principles and Design 2nd edition*. John Wiley & Sons, Danvers, MA. **2005**. pp 870-873.
- Emelko, M. B. Removal of *Cryptosporidium parvum* by granular media filtration, PhD Dissertation. The University of Waterloo. Waterloo, Canada. **2001**
- Emelko, M. B., Huck, P. M., and Coffey, B. M. A review of *Cryptosporidium* removal by granular media filtration. *American Water Works Association*, **2005**, 97(12), 101.
- Hagler, A.N. Yeasts as indicators of environmental quality. *In: Biodiversity and Ecophysiology of Yeasts* (eds. Rose, A.H., and Harrison, J.S.) **2006**, 515-532.

Health Canada. Guidelines for Canadian Drinking Water Quality—Summary Table **2012**

Water, Air and Climate Change Bureau, Healthy Environments and Consumer Safety Branch, Health Canada, Ottawa, Ontario

Huck, P. M., Emelko, M. B., Coffey, B. M., Maurizio, D. D. and O'Melia, C. R. Filter operation effects on pathogen passage. AWWA Research Foundation and American Water Works Association, Denver **2001**

LeChevallier, M. W., Norton, W. D., and Lee, R. G. *Giardia* and *Cryptosporidium* spp. in filtered drinking water supplies. *Applied Environmental Microbiology*. **1991**, 57(9), 2617-2621.

Mac Kenzie, W. R., Hoxie, N. J., Proctor, M. E., Gradus, M. S., Blair, K. A., Peterson, D. E., and Davis, J. P. A massive outbreak in Milwaukee of *Cryptosporidium* infection transmitted through the public water supply. *New England Journal of Medicine*, **1994** 331(3), 161-167.

Metcalf and Eddy Inc. Wastewater Engineering – Treatment and reuse. McGraw Hill, New York. **2003**.

Pang, L., Nowostawska, U., Weaver, L., Hoffman, G., Karmacharya, A., Skinner, A., and Karki, N. Biotin-and Glycoprotein-Coated Microspheres: Potential Surrogates for Studying Filtration of *Cryptosporidium parvum* in Porous Media. *Environmental Science and Technology*. **2012**, 46(21), 11779-11787.

Park, Y., Atwill, E. R., Hou, L., Packman, A. I., and Harter, T. Deposition of *Cryptosporidium parvum* oocysts in porous media: a synthesis of attachment efficiencies measured under varying environmental conditions. *Environmental Science and Technology*. **2012** 46(17), 9491-9500.

- Stirling, R., Aramini, J., Ellis, A., Lim, G., Meyers, R., Fleury, M., and Werker, D.
Waterborne Cryptosporidiosis Outbreak, North Battleford, Saskatchewan, April
2001.
- Swertfeger, J., Metz, D. H., DeMarco, J., Braghetta, A., and Jacangelo, J. G. Effect of
filter media on cyst and oocyst removal. *American Water Works Association
Journal*, **1999**, 91(9), 90-100.
- United States Environmental Protection Agency. Method 1623: *Cryptosporidium* and
Giardia in Water by Filtration/IMS/FA **2005**
- United States Environmental Protection Agency. National Primary Drinking Water
Regulations: Long Term 2 Enhanced Surface Water Treatment Rule. **2006**
[https://www.federalregister.gov/articles/2006/01/05/06-4/national-primary-
drinking-water-regulations-long-term-2-enhanced-surface-water-treatment-
rule#h-8](https://www.federalregister.gov/articles/2006/01/05/06-4/national-primary-drinking-water-regulations-long-term-2-enhanced-surface-water-treatment-rule#h-8) Retrieved January 27, 2015
- Widerström M, Schönning C, Lilja M, Lebbad M, Ljung T, and Allestam G. Large
outbreak of *Cryptosporidium hominis* infection transmitted through the public
water supply, Sweden. *Emerging Infectious Diseases*
http://wwwnc.cdc.gov/eid/article/20/4/12-1415_article. **2014** Retrieved October
20, 2014

Chapter 2. Literature Review

2.1 *Cryptosporidium* life cycle and infectivity

Cryptosporidiosis is recognized as a source of gastrointestinal disease in immunologically competent individuals, with the risk being highest in small children and the elderly (Fayer and Unger, 1986). Regarding the protection of public health from outbreaks of cryptosporidiosis, the main species that infect humans are *Cryptosporidium hominis* and *Cryptosporidium parvum* (Chung, 2012). These are single-celled protozoan pathogens that travel between hosts as oocysts, usually excreted in feces (Crittenden et al, 2005). The typical causal agents of cryptosporidiosis is shown in Figure 2.1, where pathogens are ingested by a host from a food or water source, the rapid life cycle is completed in 12-24 hours, and a high numbers of “thick-walled” oocysts are released via feces (Chung, 2012). Infections of cryptosporidiosis typically occur in the ileum section of the intestine, where ingested oocysts attach to the epithelial cells and quickly reproduce, resulting in gastrointestinal illness (Crittenden et al, 2005). The life cycle of individual oocysts is quite complex, and is shown in Figure 2.1.

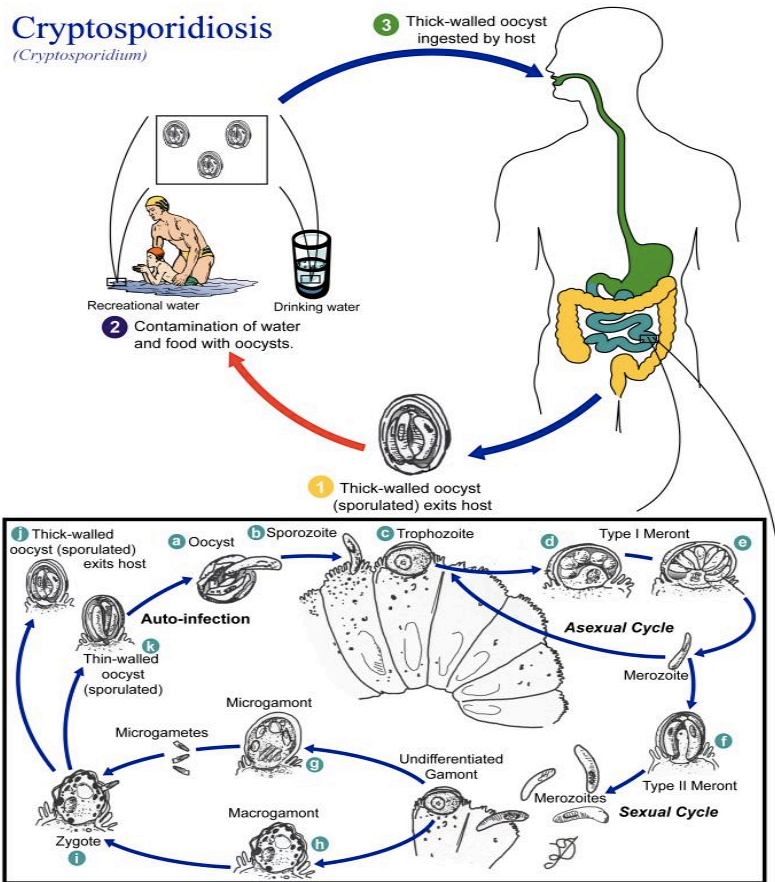


Figure 2.1 Causal agents of cryptosporidiosis and *Cryptosporidium* life cycle (CDC Public Health Image Library #3386, 2002)

Cryptosporidium has the ability to infect a wide range of warm blooded animals, which, given it's excellent survival, can result in relatively high environmental concentrations (Crittenden et al, 2005). This leads to the need for treatment of naturally occurring *Cryptosporidium* oocysts in drinking water. There are several methods used to treat drinking water, including both physical and chemical techniques as a part of the overall treatment process.

2.2 Drinking water treatment methods for *Cryptosporidium* removal

2.2.1 Chemical and UV treatment

Cryptosporidium oocysts are resistant to inactivation by many standard chemical disinfectants (Yang et al, 2013). Chlorine based disinfection (free and combined forms of chlorine) has been shown to be ineffective at concentrations typically applied to drinking water (2–6 mg/L; Rochelle et al, 2002). *Cryptosporidium* oocysts have been shown to be sensitive to ozone (Bukhari et al, 2000), but a substantial cost is associated with ozone treatment. UV disinfection offers excellent inactivation of *Cryptosporidium*, typically 3-log or better (Clancy et al, 2004; Hendricks, 2006). Although this does not provide continuous inactivation throughout a distribution system, it is important when employing a multi-barrier approach.

2.2.2 Physical treatment

Compared to the aforementioned chemical and UV methods, treatment of drinking water for *Cryptosporidium* has been demonstrated to be greatly dependent on filtration (Emelko et al, 2005). Physical treatment by granular filtration has been shown to be one of the most effective methods for removal (Chung, 2012). The combination of coagulation followed by filtration is relatively inexpensive, and is the most commonly used method of *Cryptosporidium* removal from drinking water (Emelko, 2003; Emelko and Huck 2005).

2.3 Review of removal mechanisms in granular filtration

2.3.1 Rapid filtration overview

Granular filtration has long been used in drinking water treatment to remove particles, with the two principle types being slow sand filtration and rapid filtration

(Pizzi, 2011). Rapid filtration is the prevailing method, which is distinguished from slow sand filtration by relatively coarser granular media a much faster flow rate (Crittenden et al, 2005). The basic features and process are given below (Crittenden et al, 2005):

1. A filter bed of granular media processed to a more uniform size compared to slow sand filtration
2. The use of coagulants to precondition influent water prior to filtration
3. Mechanical and hydraulic systems to remove accumulated solids from the filter bed (such as air scouring followed by backwashing)

2.3.2 Colloidal transport and removal mechanisms

There are several mechanisms that act on colloidal particles to remove them from bulk solution. These transport mechanisms were initially described in classical colloidal filtration theory (CFT), developed by Yao et al (1971). They are summarized below from Crittenden et al (2005).

- A. Hydrodynamic forces are caused by a nonuniform shear distribution in the filter bed. This streamlining and irregularity of flow patterns results in additional contact between particles and media grains.
- B. Diffusion occurs when particles depart from fluid streamlines due to Brownian motion, which can result in contact with media grains.
- C. Inertia leads particles to deviate from the streamline of fluid around media grains, and continue downwards to come into contact with a media grain.
- D. Interception is the result of particles remaining in the fluid streamlines that come into contact with filter media.

E. Sedimentation occurs when particles with density greater than water move away from fluid streamlines due to gravity.

The transport mechanisms of colloidal particles in filtration are represented below in Figure 2.2.

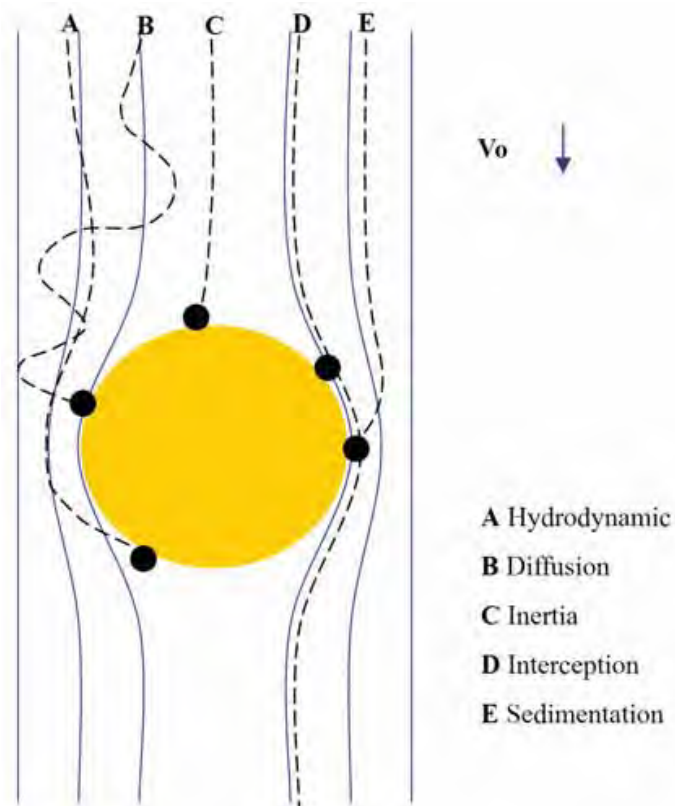


Figure 2.2 Particle removal mechanisms in granular filtration (adapted from Chung, 2012; Amirtharajah, 1988). Colloidal particles are represented by the small black circles. A single media grain is represented by the large yellow circle. Flow paths are represented by dashed lines.

The removal mechanisms shown in Figure 2.2 are particularly applicable in depth filtration, which is the removal of particles or flocs throughout the entire depth of the filter media (Hendricks, 2006). This occurs to particles or flocs that are smaller than media pore sizes by (1) the transport to filter media surfaces, and (2) attachment to filter media (Hendricks, 2006).

Opposed to depth filtration, and not shown in Figure 2.2, is mechanical straining. This occurs when particles with a diameter greater media pore sizes are removed from solutions. More formally, straining occurs when the ratio of particle diameter to the effective media grain size is 0.15 (Crittenden et al, 2005). In the case of typical silica sand filter media with an effective size of 0.35 mm, straining will occur for particles with a diameter greater than 52 μm , which is well outside the colloidal range (0.001 – 1.0 μm). Mechanical straining can cause an exponential increase in head-loss, which reduces effective filter run lengths (Hendricks, 2006). For depth filtration, head-loss increases linearly with time, which is more desirable in water treatment (Crittenden et al, 2005; Hendricks, 2006).

2.4 Review of colloidal filtration models

2.4.1 Review of colloidal filtration models

Several models have been proposed to describe the fundamental understanding of the filtration process. The basic fundamental model is the previously mentioned CFT model developed by Yao et al (1971). This is based on the accumulation of particles on a single collector (collector being defined as a single filter media granule), and has been noted to deviate from experimental data (Crittenden et al, 2005). Other proposed models include the Rajagopalan-Tien (referred to as RT) model (Rajagopalan and Tien, 1976), which largely considers Brownian diffusion and viscous resistance of water (Tufenkji and Elimelech, 2004; Crittenden et al, 2005). More recently, Tufenkji and Elimelech (2004) developed a new equation for predicting single collector efficiency (referred to as TE), which takes into account van der Waals forces and hydrodynamic forces. Additionally,

Nelson and Ginn (2011) developed a model (referred to as NG), which increases the range of CFT to include saturated subsurface environments, where groundwater velocity is very low compared to engineered flow conditions. A recent meta-analysis by Park et al (2012) compared these models across a broad range of systems (i.e. saturated porous media in subsurface, and filtration experiments), and found that *Cryptosporidium* oocyst attachment efficiency is more reliably estimated with the TE and NG models.

Generally, these models are used to explain the transport and attachment of particles to single media grains, or collectors. The parameters used for this are single collector efficiency (η), and attachment efficiency (α), which are described by the following equations (Crittenden et al, 2005):

$$\eta = \frac{\text{particles contacting collector}}{\text{particles approaching collector}}$$

$$\alpha = \frac{\text{particles adhering to collector}}{\text{particles contacting collector}}$$

The effectiveness of filtration of particles is largely dependent on particle stability, which is further discussed in section 2.4.2.

2.4.2 Particle stability and DLVO theory

Particle stability depends on a combination of repulsive forces (electrostatic force) and attractive forces (van der Waals force). The interaction of these two forces between particles is known as Derjaguin-Landau-Verwey-Overbeek (DLVO) theory (Crittenden et al, 2005). The aggregation of negatively charged particles (i.e. naturally occurring colloids, or *Cryptosporidium* oocysts) depends on overcoming the electrostatic repulsion maximum such that van der Waals forces dominate at short distances (Hayashi et al, 2001). This is largely reliant on the compression of the electric double layer, which

reduces the surface charge of particles and encourages aggregation (Crittenden et al, 2005). In practical terms, surface charge is measured by the electrophoretic mobility of particles, or zeta potential. A schematic of the double-layer structure and zeta potential is given below in Figure 2.3.

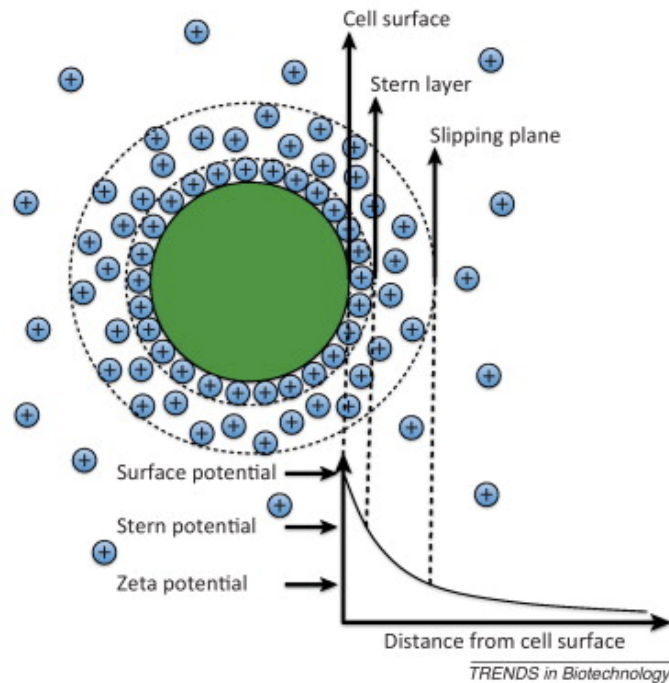


Figure 2.3 Structure of the electric double layer for a negatively charge cell, or colloid. Zeta potential is measured from the slipping plane, also known as the shear plane (adapted from Vandamme et al, 2013).

In the case of biological organisms, such as *Cryptosporidium*, DLVO theory has been used as both a qualitative and quantitative model to explain microbial behavior and adhesion (Hermansson, 1999; Hayashi et al, 2001); There is some disagreement in literature, where Boström et al (2001) suggest that DLVO theory is inconsistent based on dissolved ions and specific ion effects, which is more pronounced at high ionic strengths (i.e. above 0.01 M). At low ionic strengths (i.e. below 0.01 M), it is generally agreed that DLVO theory works well (Boström et al, 2001), which is supported experimentally

(Behrens et al, 2000). For the purposes of this thesis, DLVO theory is assumed to be valid as the applicable ionic strength ranges 0.001 to 0.01 M.

2.5 Role of pretreatment in removal

2.5.1 Coagulation and optimization for pathogen removal

To achieve particle destabilization by compression of the electrostatic double-layer, raw water is often chemically pretreated with coagulants and polymers to enhance the filtration effectiveness (Crittenden et al, 2005).

In general, for conventional treatment (i.e., coagulation/flocculation, sedimentation and filtration), coagulant addition aims to form larger particles, which are required for settling. This differs from direct filtration, where large particles and aggregates will block filter pores, which increases headloss and reduces the operational time for filter runs; however, if particles are too small they may not be completely removed (Crittenden et al, 2005). This presents a challenge, as optimal chemical pretreatment is required to maximize filter runs while maintaining effluent quality. Previous studies have investigated the optimization of pretreatment and flocculation time for direct filtration (Treweek 1979; Edzwald 1987; McCormick and King 1982; Huck et al 2000); but the impacts of coagulation and flocculation on direct filtration of *Cryptosporidium* are not fully addressed.

The importance of optimizing coagulation for protozoan pathogen removal has been well documented, where suboptimal chemical pretreatment resulted in reduced *Cryptosporidium* removal (Patania et al 1995; Arora et al, 2001; Chung 2012). More specifically, a study by Bustamante et al (2001) demonstrates that the removal of oocysts

with alum may occur during initial charge neutralization and is dependent on the bond strength at the oocysts-floc interface.

2.5.2 Polymers

In addition to metal coagulants like alum, the importance of polymers cannot be overstated. Organic polymers offer several advantages in water treatment, such as the lowering of required coagulant dose and reduced aluminum in treated water (Bolto and Gregory, 2007). Polymers are beneficial when dealing with slow-settling flocs in lower temperature waters, where floc toughness and settleability can be increased with appropriate polymer pretreatment (Bolto and Gregory, 2007).

Most often used in direct filtration processes are high charge density cationic polymers, for example, polydiallyldimethyl ammonium chloride (pDADMAC), and epichlorohydrin and dimethylamine (ECH/DMA; Bolto and Gregory, 2007). While high charge density cationic polymers are able to achieve charge neutralization, their main purpose is to incite interparticle bridging and adsorption (Crittenden et al, 2005). Interparticle bridging occurs where sections of a polymer adsorbed to a particle extend into the bulk solution and can become attached to vacant sites of other particles to form a “bridge” (McEwan, 1998). This is particularly important for direct filtration where influent water has a low particle concentration. Interparticle bridging followed by sedimentation (seen in Figure 2.2) during filtration is a main removal mechanism for particles, and the polymer dosage and type are important considerations such that small, tough flocs are formed inline prior to filtration (Crittenden et al, 2005; Bolto and Gregory, 2007). Further research is needed to investigate this in the context of *Cryptosporidium* removal. Additionally, initial chlorination and low water temperatures

may affect the surface properties of polymers, *Cryptosporidium* surface charge, and how they interact.

2.6 Review of *Cryptosporidium* detection and indicators

2.6.1 Overview of standard detection methods

To understand how oocysts are removed in water treatment, standardized detection methods need to be established. This often involves concentrating 10-100 L water by filtration, followed by particle elution, *Cryptosporidium* oocyst concentration and purification, fluorescence labeling, and examination by immunofluorescence microscopy. Further examination regarding the viability of oocysts is often required, and losses can occur within each step (LeChevalier et al, 1991). The most common methods follow this principle, with the most prevalent being US EPA Method 1623 (USEPA, 2005). Other methods include ISO Method 15553, and Microbiology of Drinking Water Part 14 (Chalmers, 2014).

2.6.2 *Cryptosporidium* indicators and surrogate

Traditionally, *Cryptosporidium* has been considered and modeled as a colloidal particle, and its removal has been correlated to particle removal measured as turbidity (Emelko et al, 2005). This has proved problematic, as several studies have shown that turbidity provides an approximate indicator of *Cryptosporidium* removal, and often overestimates oocysts removal (Swertfeger et al, 1999; Emelko, 2001; Huck et al, 2001).

Examples of *Cryptosporidium* oocyst surrogates include algae, coliforms,, *Bacillus subtilis* spores, and polystyrene microspheres (Emelko et al, 2005; Chung,

2012). Polystyrene microspheres have been of limited usefulness due to differences in surface properties (e.g., surface charge, isoelectric point) compared to viable *Cryptosporidium* oocysts, resulting in different attachment and filtration characteristics (Pang et al, 2012). *Saccharomyces cerevisiae* Type II, commonly called bakers yeast, has been considered as an indicator of environmental quality (Hagler, 2006), and has also been shown to have a resistance to conventional disinfection that is comparable to oocysts and coliforms (Haas et al, 1985). For this reason, and also because yeasts are simple and cost effective to cultivate, they offer much promise as *Cryptosporidium* surrogates.

2.7 Review of engineered polystyrene microspheres

2.7.1 Role of surface properties in filtration

Since surface properties are known to govern the removal characteristics of *Cryptosporidium* in granular filtration, the development of reliable surrogates is largely dependent on engineering similar surface properties, such as surface charge and isoelectric point (Emelko et al, 2005; Chung, 2012).

Previous studies indicate that *Cryptosporidium* oocysts are predominantly hydrophilic (Considine et al, 2002) and the charge responsible for this would lie at the edge of the oocyst cell membrane. Although there is some dispute regarding the precise biochemical makeup of *Cryptosporidium* cell wall, the negative charge of viable oocysts is generally thought to be from carboxyl groups from proteins (Dai and Hozalski, 2003). Other components of the cell wall include various carbohydrates and lipids (Chung, 2012). Such surface proteins have been shown to create an electrostatic repulsion

between *Cryptosporidium* oocysts and negatively charged quartz filter media, which can reduce their deposition rates in water filter media (Kuznar and Elimelech, 2005).

2.7.2 Polystyrene microsphere modification

To more closely resemble oocyst surface characteristics, polystyrene microspheres can be coated with biomolecules and then used to evaluate removal through granular filters. This has been done using a carbodiimide cross-linker to couple a glycoprotein and biotin to the surface of commercially available fluoresbrite carboxylate polystyrene microspheres (4.5 μm ; Pang et al, 2012). The modified microspheres provide a good match with viable *Cryptosporidium* oocysts (Pang et al, 2012), although there is a substantial cost associated with using glycoproteins.

No studies were identified where microspheres were coated with carbohydrates for use as *Cryptosporidium* surrogates. This is potentially a much more cost-effective method compared to glycoproteins, and one that this study seeks to address.

2.8 Areas for further study

The effectiveness and mechanisms of *Cryptosporidium* removal in granular media have been extensively studied, with several investigations regarding the transport and removal having been performed on a laboratory scale (Brush et al 1999; Harter et al, 2000; Hsu et al, 20001; Logan et al 2001; Dai and Hozalski, 2002; Tufenkji 2004; Tufenkji and Elimelech 2005; Kuznar and Elimelech 2006; Abudalo et al 2010; Pang et al 2012; Park et al 2012). Most experiments focus on the laboratory scale under well-controlled conditions. Clean sand or glass bead packed columns are often used. *Cryptosporidium* oocysts (viable and non-viable) or their surrogates are used in simple

electrolyte carrying solutions. Broadly, their results showed that flow rate, chemical pre-treatment, and media size/uniformity have the greatest effect on *Cryptosporidium* transport and removal.

When treating drinking water by rapid sand filtration under environmental conditions, the carrying solution is much more complicated. Bacteria, other suspended particles, total organic carbon (TOC), and temperature can all impact transport, but only limited studies have investigated their impacts. The deposition kinetics of *Cryptosporidium* can be affected by such complex carrying solutions, as oocysts can make initial contact on a collector surface, but are subsequently detached and carried away by other particles (Harter et al, 2000). The impact of temperature on direct filtration removal of *Cryptosporidium* is a very new research area and is very important to Canadian cities, as water temperatures are much lower in winter conditions.

As previously mentioned, there has been limited research where carbohydrates are used to modify microspheres. This study seeks to address this, and also investigate the efficacy of these modified microspheres as surrogates in filtration experiments.

2.9 References

- Abudalo, R. A., Ryan, J. N., Harvey, R. W., Metge, D. W., & Landkamer, L. Influence of organic matter on the transport of *Cryptosporidium parvum* oocysts in a ferric oxyhydroxide-coated quartz sand saturated porous medium. *Water Research*, **2010**. 44(4), 1104-1113.
- Amirtharajah, A. Some theoretical and conceptual views of filtration. *American Water Works Association*, **1988**. 36-46.

- Arora, H., Giovanni, G.D., and Lechevallier, M. Spent filter backwash contaminants and treatment strategies. *American Water Works Association*. **2001**, 93(5), 100-112
- Behrens, S. H., Christl, D. I., Emmerzael, R., Schurtenberger, P., and Borkovec, M. Charging and aggregation properties of carboxyl latex particles: Experiments versus DLVO theory. *Langmuir*, **2000** 16(6), 2566-2575.
- Bolto, B., and Gregory, J. Organic polyelectrolytes in water treatment. *Water Research*. **2007**, 41(11), 2301-2324.
- Boström, M., Williams, D. R. M., and Ninham, B. W. Specific ion effects: why DLVO theory fails for biology and colloid systems. *Physical Review Letters*, **2001** 87(16), 168103.
- Brush, C. F., Ghiorse, W. C., Anguish, L. J., Parlange, J. Y., & Grimes, H. G. Transport of *Cryptosporidium parvum* oocysts through saturated columns. *Journal of Environmental Quality*, **1999**. 28(3), 809-815.
- Bukhari, Z., Marshall, M. M., Korich, D. G., Fricker, C. R., Smith, H. V., Rosen, J., & Clancy, J. L. Comparison of *Cryptosporidium parvum* viability and infectivity assays following ozone treatment of oocysts. *Applied and Environmental Microbiology*, **2000**. 66(7), 2972-2980.
- Bustamante, H. A., Shanker, S. R., Pashley, R. M., and Karaman, M. E. Interaction between *Cryptosporidium* oocysts and water treatment coagulants. *Water Research*, **2001** 35(13), 3179-3189.
- Centers for Disease Control and Prevention. Public Health Image Library #3386.
CDC/Alexander J. da Silva, PhD, Melanie Moser. **2002**.

- Chalmers, R. M. Chapter Sixteen - Cryptosporidium. *Microbiology of Waterborne Diseases (Second Edition)* Academic Press, London. **2014**, 287-326.
- Chung, J. Development of fluorescently labelled *Cryptosporidium* oocysts surrogates to test the efficacy of sand filtration processes. PhD Dissertation, University of New South Wales, Australia **2012**
- Clancy, J. L., Marshall, M. M., Hargy, T. M., & Korich, D. G. Susceptibility of five strains of *Cryptosporidium parvum* oocysts to UV light. *Journal American Water Works Association*, **2004**, [84-93.
- Considine, R. F., Dixon, D. R. and Drummond, C. J. Oocysts of *Cryptosporidium parvum* and model sand surfaces in aqueous solutions: an atomic force microscope (AFM) study. *Water Research*. **2002**, 36 (14): 3421-3428.
- Crittenden, J. C., Trussell, R. R., Hand, D. W., Howe, K. J., and Tchobanoglous, G. *MWH Water Treatment: Principles and Design: Principles and Design 2nd edition*. John Wiley & Sons, Danvers, MA. **2005**. pp 870-873.
- Dai, X., and Hozalski, R. M. Evaluation of microspheres as surrogates for *Cryptosporidium parvum* oocysts in filtration experiments. *Environmental Science and Technology*. **2003**, 37(5), 1037-1042.
- Edzwald, James K., William C. Becker, and Steven J. Tambini. Organics, polymers, and performance in direct filtration. *Journal of Environmental Engineering* **1987**. 113, no. 1 167-185.
- Emelko, M. B. Removal of *Cryptosporidium parvum* by granular media filtration, PhD Dissertation. The University of Waterloo. Waterloo, Canada. **2001**

- Emelko, M. B. Removal of viable and inactivated *Cryptosporidium* by dual-and tri-media filtration. *Water Research*. **2003**, 37(12), 2998-3008.
- Emelko, M. B., Huck, P. M., and Coffey, B. M. A review of *Cryptosporidium* removal by granular media filtration. *American Water Works Association*, **2005**, 97(12), 101.
- Fayer, R., and Ungar, B. L. *Cryptosporidium* spp. and cryptosporidiosis. *Microbiological Reviews*, **1986**. 50(4), 458.
- Haas, C. N., Severin, B., Roy, D., Engelbrecht, R., Lalchandani, A., and Farooq, S. Field observations on the occurrence of new indicators of disinfection efficiency. *Water Research*. **1985**, 19(3), 323-329.
- Hagler, A.N. Yeasts as indicators of environmental quality. *In: Biodiversity and Ecophysiology of Yeasts* (eds. Rose, A.H., and Harrison, J.S.) **2006**, 515-532.
- Harter, T., Wagner, S., & Atwill, E. R. Colloid transport and filtration of *Cryptosporidium parvum* in sandy soils and aquifer sediments. *Environmental Science and Technology*, **2000**. 34(1), 62-70.
- Hayashi, H., Tsuneda, S., Hirata, A., and Sasaki, H. Soft particle analysis of bacterial cells and its interpretation of cell adhesion behaviors in terms of DLVO theory. *Colloids and Surfaces B: Biointerfaces*, **2001**. 22(2), 149-157.
- Hendricks, D.W. *Water Treatment Unit Processes: Physical and Chemical*. CRC Press. **2006**. pp 1020
- Hermansson, M. The DLVO theory in microbial adhesion. *Colloids and Surfaces B: Biointerfaces*, **1999**. 14(1), 105-119.

- Hsu, B. M., Huang, C., and Pan, J. R. Filtration behaviors of *Giardia* and *Cryptosporidium*—ionic strength and pH effects. *Water Research*, **2001**. 35(16), 3777-3782.
- Huck, P. M., Emelko, M. B., Coffey, B. M., Maurizio, D. D. and O'Melia, C. R. Filter operation effects on pathogen passage. AWWA Research Foundation and American Water Works Association, Denver **2001**
- Kuznar, Z. A., and Elimelech, M. Role of surface proteins in the deposition kinetics of *Cryptosporidium parvum* oocysts. *Langmuir*, **2005**. 21(2), 710-716.
- LeChevallier, M. W., Norton, W. D., and Lee, R. G. *Giardia* and *Cryptosporidium* spp. in filtered drinking water supplies. *Applied Environmental Microbiology*. **1991**, 57(9), 2617-2621.
- Logan, A. J., Stevik, T. K., Siegrist, R. L., and Rønn, R. M. Transport and fate of *Cryptosporidium parvum* oocysts in intermittent sand filters. *Water Research*, **2001**. 35(18), 4359-4369.
- McCormick, R. F., and King, P. H. Factors that affect use of direct filtration in treating surface waters. *Journal American Water Works Association*, **1982**. 234-242.
- McEwan, J.B. *Treatment processes for particle removal*. American Water Works Association. CRC Press. Denver, CO. **1998**. pp 85
- Nelson, K. E., and Ginn, T. R. New collector efficiency equation for colloid filtration in both natural and engineered flow conditions. *Water Resources Research*, **2011**. 47(5).
- Pang, L., Nowostawska, U., Weaver, L., Hoffman, G., Karmacharya, A., Skinner, A., and Karki, N. Biotin-and Glycoprotein-Coated Microspheres: Potential Surrogates for

- Studying Filtration of *Cryptosporidium parvum* in Porous Media. *Environmental Science and Technology*. **2012**, 46(21), 11779-11787.
- Park, Y., Atwill, E. R., Hou, L., Packman, A. I., & Harter, T.. Deposition of *Cryptosporidium parvum* oocysts in porous media: a synthesis of attachment efficiencies measured under varying environmental conditions. *Environmental Science and Technology*, **2012**. 46(17), 9491-9500.
- Patania, N. L. Jacangelo, J. G., Cummings, L., Wilczak, A., Riley, K. and Oppenheimer, J. Optimization of filtration for cyst removal. American Water Works Association Research Foundation, Denver **1995**
- Pizzi, N.G. *Water Treatment 4th edition*. American Water Works Association. Denver, CO. **2011**. pp 106
- Rajagopalan, R., and C. Tien. Trajectory analysis of deep-bed filtration with sphere-in-cell porous-media model. *AIChE*. **1976**. 22(3) 523-533
- Rochelle, P. A., Marshall, M. M., Mead, J. R., Johnson, A. M., Korich, D. G., Rosen, J. S., and De Leon, R. Comparison of in vitro cell culture and a mouse assay for measuring infectivity of *Cryptosporidium parvum*. *Applied and Environmental Microbiology*, **2002**. 68(8), 3809-3817.
- Swertfeger, J., Metz, D. H., DeMarco, J., Braghetta, A., and Jacangelo, J. G. Effect of filter media on cyst and oocyst removal. *American Water Works Association Journal*, **1999**, 91(9), 90-100.
- Treweek, Gordon P. Optimization of flocculation time prior to direct filtration. *Journal American Water Works Association* **1979**. 96-101.

- Tufenkji, N., and M. Elimelech. Correlation equation for predicting single-collector efficiency in physicochemical filtration in saturated porous media. *Environmental Science and Technology*. **2004**. 38(2), 529-536.
- Tufenkji, N. and Elimelech, M., Spatial distribution of *Cryptosporidium* oocysts in porous media: Evidence for dual mode deposition. *Environmental Science and Technology*. **2005**, 39, 3620-3629
- USEPA. Method 1623: *Cryptosporidium* and *Giardia* in Water by Filtration/IMS/FA **2005**
- Vandamme, D., Foubert, I., and Muylaert, K. Flocculation as a low-cost method for harvesting microalgae for bulk biomass production. *Trends in Biotechnology*, **2013**. 31(4), 233-239.
- Yao, K.M., Habibian, M.T., and O'Melia, C.R. Water and Waste Water Filtration: Concepts and Applications. *Environmental Science and Technology*. **1971**, 5(11), 1105-1112
- Yang, R., Murphy, C., Song, Y., Ng-Hublin, J., Estcourt, A., Hijjawi, N., Chalmers, R., Hadfield, S., Bath, A., Gordon, C., and Ryan, U. Specific and quantitative detection and identification of *Cryptosporidium hominis* and *C. parvum* in clinical and environmental samples. *Experimental Parasitology*, **2013**, 135(1), 142-147.

Chapter 3. Surrogate Development and Characterization

3.1 Introduction

The development and characterization of surrogates is the first step to understanding *Cryptosporidium* removal in direct filtration. Based on previous studies, both biological and non-biological surrogates were identified for this investigation: glycoprotein-modified polystyrene microspheres, glycopolymer-modified polystyrene microspheres, and fluorescently labeled yeast (Emelko et al, 2005; Chung, 2012; Pang et al, 2012; Hagler, 2006; Dai and Hozalski, 2003). The immediate focus was cost-effective surrogate development and characterization of surface properties compared to viable *Cryptosporidium* oocysts.

Since surface properties are known to govern the removal characteristics of *Cryptosporidium* in granular filtration. The development of reliable surrogates is largely dependent on engineering similar surface properties, such as surface charge and isoelectric point (Emelko et al, 2005; Chung, 2012).

Previous studies indicate that *Cryptosporidium* oocysts are predominantly hydrophilic (Considine, 2002), and the charge responsible for this would lie at the edge of the oocyst cell membrane. Although there is some dispute regarding the precise biochemical makeup of the *Cryptosporidium* cell wall, the negative charge of viable oocysts is generally thought to be from carboxyl groups from proteins (Dai and Hozalski, 2003). Other components of the cell wall include various carbohydrates and lipids (Chung, 2012).

To create surrogates that resemble the surface characteristics of viable *Cryptosporidium* oocysts, polystyrene microspheres of a diameter similar to *Cryptosporidium* were modified with a glycoprotein and a glycopolymer.

As a point of reference, naturally occurring viable *C. parvum* oocysts have a typical diameter of 4.5-5.5 μm (Pang et al, 2012; Harter et al, 2000), and zeta potential can range from -2 to -35 mV depending on age, isolates, strain, geological media, etc (Dai and Hozalski, 2003).

The objective of this section was to identify the most effective and economical surrogates for *Cryptosporidium* that will subsequently be used in pilot scale experiments to evaluate the removal of *Cryptosporidium* through granular filters.

3.2 Methods

3.2.1 Surrogate Development and Preparation

The particles examined were:

- a. Fluoresbrite carboxylate polystyrene microspheres (4.5 μm diameter)
 - Unmodified microspheres
 - Alpha-1-acid glycoprotein (AGP) modified microspheres
 - Glycopolymer-modified microspheres
- b. *Cryptosporidium parvum* oocysts
 - Viable oocysts
 - Non-viable oocysts (UV-irradiated)
- c. Yeast (*S. cerevisiae* Type II)
 - 1-hour incubation

- 2-hour incubation
- 4-hour incubation

3.2.1.1 Unmodified carboxylate polystyrene microspheres

Fluoresbrite YG carboxylate microspheres (4.50 μm) were purchased from Polysciences Inc. From the supplier data sheet, these particles were internally dyed with a yellow-green dye similar to fluorescein isothiocyanate (FITC, max excitation/emission = 441/486 nm); and are a monodisperse polystyrene microspheres with carboxylate groups on their surface (Polysciences Inc, 2015). The carboxyl groups can be used to covalently link functional groups. A small aliquot of particles was diluted to 5 mg/mL with DI water. From this solution, particles were further diluted with the appropriate background solution prior to zeta potential and dynamic light scattering (DLS) analysis. A schematic of unmodified microspheres is shown below.

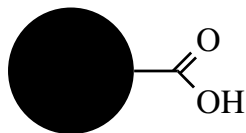


Figure 3.1. Unmodified carboxylate microsphere schematic representation

3.2.1.2 AGP-modified carboxylate microspheres

AGP was used to functionalize the surface of the unmodified microspheres. AGP from human plasma was purchased from Sigma-Aldrich. From the product information sheet, it is very water soluble (1000 mg/100 mL), the molecular weight is 33000 – 40800 g/mol, and the isoelectric point (IP) = 2.7. AGP from human plasma is a single chain of

183 amino acids, which can vary in exact composition (Fournier et al, 2000). A water-soluble carbodiimide cross-linker, EDC (1-ethyl-3-(3-dimethylaminopropyl) carbodiimide hydrochloride), was used to bind AGP to the surface of 4.5 μm fluoresbrite carboxylate polystyrene microspheres, similar to a study by Pang et al (2012). This procedure has been adapted from Bang Laboratories, Inc. and a schematic is shown below in Figure 3.2.

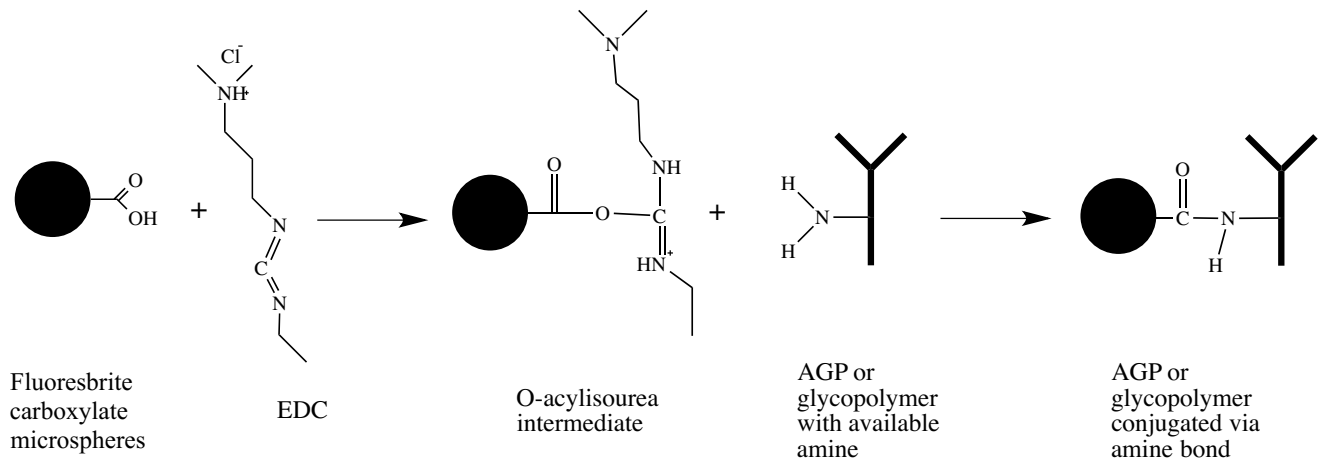


Figure 3.2 Schematic of conjugation of biomolecules to microsphere surface

3.2.1.3 Glycopolymer-modified microspheres

Glycopolymer-modified microspheres were made using the same procedure used for AGP-modified microspheres, with the only difference being the glycopolymer opposed to AGP. The glycopolymer itself was synthesized at the University of Alberta.

The form of the functionalized microspheres is shown below in Figure 3.3

modification procedure. The signal from the flow cytometer was gated using forward light scatter (a function of particle size), and a fluorescence detector optimized for FITC (filtered at 530 nm, which is a function of fluorescent intensity). For each sample, the number of microspheres were counted over a 15s time interval and the corresponding sample concentration found.

3.2.1.4 *Viable C. parvum*

Viable C. parvum oocysts were obtained from Hyperion Research Ltd. (Medicine Hat, AB) and shed on August 23, 2014. Received suspensions of approximately 10^7 oocysts in 10 mL PBS were received in a fecal slurry, passed through mice. Further purification was performed at the University of Alberta using differential centrifugation (Zilberman et al, 2009). 3.0 mL of the fecal slurry was floated on 30 mL of 1.0 M sucrose and centrifuged at 500x g for 10 minutes at room temperature. Two distinct layers were formed. The top layer and the phase boundary between the two layers were suctioned by pipette and poured into another 50 mL tube, which was then centrifuged at 700x g for 10 minutes. The resulting pellet was washed twice and resuspended in DI water.

The purified solution was enumerated with a hemocytometer. The purified viable *C. parvum* concentration was 5×10^5 oocysts per mL.

3.2.1.5 *Non-viable C. parvum*

Non-viable *C. parvum* oocysts were obtained from Hyperion Research Ltd. (Medicine Hat, AB) and shed on August 23, 2014. Cultivated oocysts were inactivated at Hyperion Research laboratories using UV irradiation. Specific UV dose and fluence rate

parameters were not provided. Suspensions of approximately 10^7 oocysts in 10 mL PBS were received in a fecal slurry, passed through mice. Non-viable *C. parvum* oocysts were purified using the same protocol as described for viable *C. parvum* oocysts. A 20 μ L aliquot of the purified solution was stained with Tryptan blue and enumerated using a hemocytometer. Purified non-viable *C. parvum* concentration was 4×10^5 oocysts per mL.

3.2.1.5 Yeast at 1-, 2-, and 4-hour incubation

The cultivation of yeast (*S. cerevisiae* Type II, or Bakers yeast) is simple and cost effective. Previous investigations have demonstrated that a small amount (approximately 0.1 g dry yeast), incubated for 1 hour at 37°C in sterile PBS yields 10^8 - 10^9 cells, determined by optical density (OD), where an OD of 1 corresponds to 3×10^7 yeast particles per mL (Bergman, 2001). Yeast was grown as previously described, with incubation times of 1, 2, and 4 hours. Serial dilutions were performed with DI water to appropriate concentrations of approximately 10^6 cells/mL. The yeast suspension was then washed twice with DI water by centrifugation at 4000x g. Once washed, yeast was pelleted and resuspended in appropriate KCl background solution for analysis.

3.2.2 Zeta potential and particle size measurement methods

3.2.2.1 Zeta Potential

Established parameters used to characterize surrogates include surface charge (evaluated as zeta potential), isoelectric point, and particle size. Zeta potential was measured by microelectrophoresis over pH range from 3 to 10 in a background solution of 1mM (90Plus Zeta, Brookhaven Instruments Corporation, Holtsville, NY). Measurements were done in a controlled environment using background solutions of 1

mM KCl. The pH of background solutions was adjusted using 10mM NaOH and 10mM HCl to the desired values of pH 3-10. Particle suspensions were prepared in the filtered background solution of interest and the electrophoretic mobility was measured at 22°C. To maintain personnel safety, all open *C. parvum* oocysts suspensions were prepared in biosafety cabinet. Samples were prepared for analysis by centrifuging 0.5 mL aliquots in 2 mL centrifuge tubes and resuspending in the appropriate background solution. Samples were kept sealed until analysis was performed. Suspension concentrations used for zeta potential measurement are listed below in Table 3.1.

Table 3.1 Particle concentrations for zeta potential analysis

Particle	Concentration (particles per mL)
Unmodified carboxylate microspheres	2×10^6
AGP-modified microspheres	1.5×10^5
Glycopolymer-modified microspheres	1.5×10^5
Viable <i>C. parvum</i> oocysts	7.2×10^4
Non-viable <i>C. parvum</i> oocysts	8.5×10^4
Yeast (after 1 hour incubation)	1.5×10^6
Yeast (after 2 hour incubation)	3×10^6
Yeast (after 4 hour incubation)	2×10^6

3.2.2.2 Particle Size

DLS was used to measure particle size and suspension polydispersity of yeast suspensions (90Plus Zeta, Brookhaven Instruments Corporation, Holtsville, NY). DLS works by shining a laser at a particle suspension and observing the scattered light (Johal, 2011). When measurements of scattered light are made in quick succession, the rate of diffusion of particles can be calculated, which can be directly related to the hydrodynamic radius, or particle size, using the Boltzmann constant (Johal, 2011).

Particle size of modified and unmodified microspheres was confirmed visually by epifluorescence microscopy (Microscope Axio Imager.M2, Carl Zeiss, Germany) with a wide-field fluorescence microscope excitation light source (X-ite 120Q, Lumen Dynamic, ON, Canada). Suspension concentration for viable and non-viable *C. parvum* oocysts was 7×10^4 and 8×10^4 oocysts/mL, respectively. These solutions did not exhibit a high enough DLS signal intensity, thus the size was visually approximated to be 4 μm using a hemocytometer.

3.3 Results and Discussion

3.3.1 Fluoresbrite carboxylate polystyrene microspheres

3.3.1.1 Microsphere modification zeta potential results

The effectiveness of the microsphere modification process, in terms of particle numbers, is shown below in Table 3.2. Using unmodified microspheres as a point of reference, the percent recovery for each modification process was very high, which suggests negligible loss in the modification process. The variation observed, particularly where recovery was above 100%, may be attributed to random error associated with diluting the highly concentrated unmodified microspheres suspension (25 mg/mL) to the sample concentration (1.0 mg/mL).

Table 3.2 Percent recovery of microsphere surface modification with different biomolecules (n=5)

	<u>Percent Recovery \pm Standard Dev.</u>
Unmodified microspheres	--
AGP-modified microspheres	97.5 ± 1.1
Glycopolymer-modified microspheres	107.7 ± 2.0

Figure 3.4 shows that AGP- and glycopolymer-modified microspheres exhibit a considerably more positive zeta potential than unmodified microspheres. This is particularly evident at the pH range from 5 to 10, where both AGP- and glycopolymer-modified microspheres have zeta potentials \approx -20 to -30 mV, with the AGP modification resulting in a slightly more positive charge than the glycopolymer modification. This is contrasted by unmodified microspheres with zeta potential \approx -95 mV over the same pH range (pH 5-10). At lower pH (pH <5), the IP of all microsphere treatments was reached, where IP \approx 3.3 for both AGP-modified and unmodified microspheres. The glycopolymer modification resulted in an IP=4.7.

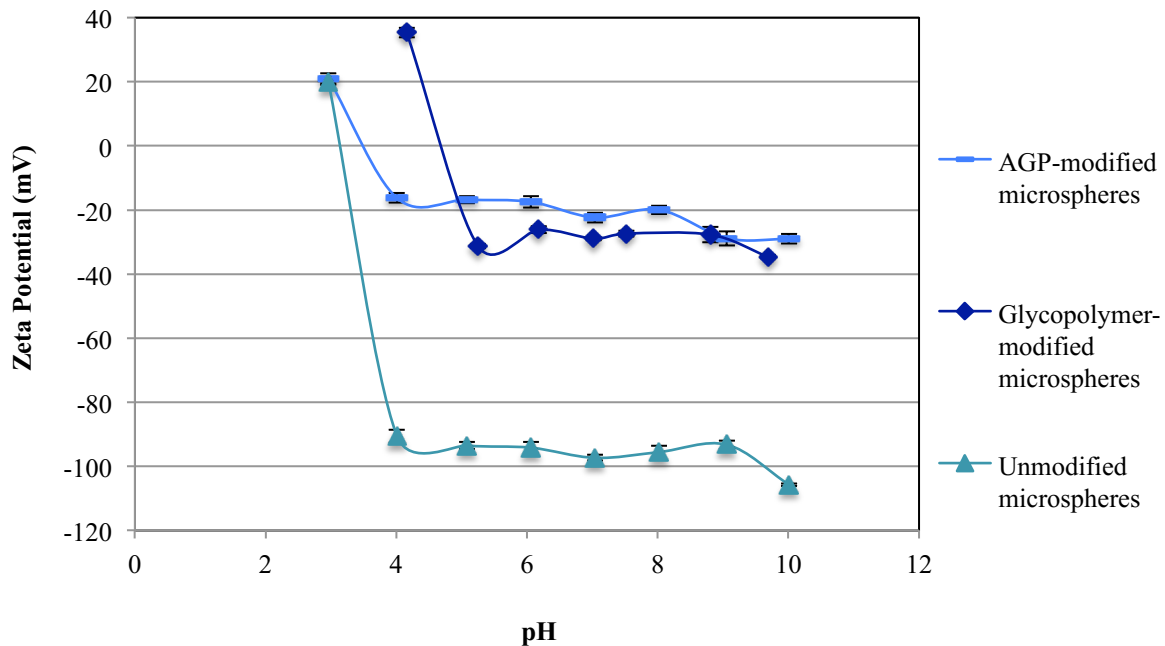


Figure 3.4 Zeta potential of microsphere particles with different biomolecule surface modifications in 1mM KCl. Average and one standard deviation of 5 measurements are shown.

The results in Figure 3.4 demonstrates that both AGP and glycopolymer surface modifications are effective at reducing the zeta potential magnitude of unmodified microspheres. Previous studies of AGP-coupled microspheres show excellent long-term

stability due to their covalent coupling, as little change was observed in zeta potential and IP over time (Pang et al, 2009). The long-term stability of biomolecule coupling, as measured by zeta potential, was not tested in this study. Because both glycopolymer and AGP were covalently linked to the microsphere surface, it can be reasoned that they will exhibit long-term stability.

Since the zeta potential is similar for both modifications in pH range of interest (pH 7-9), it can be concluded that the most cost effective option is best. In this case, the glycopolymer-modification represents a significant cost savings since commercially available AGP is ten times the cost of synthesized glycopolymer.

3.3.1.2 Microsphere size

In order to confirm the size of microspheres directly (in addition to DLS), visual inspections were performed by epifluorescent microscopy at 200x zoom. Two photographs showing microspheres and their measured diameters are shown below in Figure 3.5. The visual results agree with the manufacturer specifications of 4.5 μ m diameter with coefficient of variation = 7%.

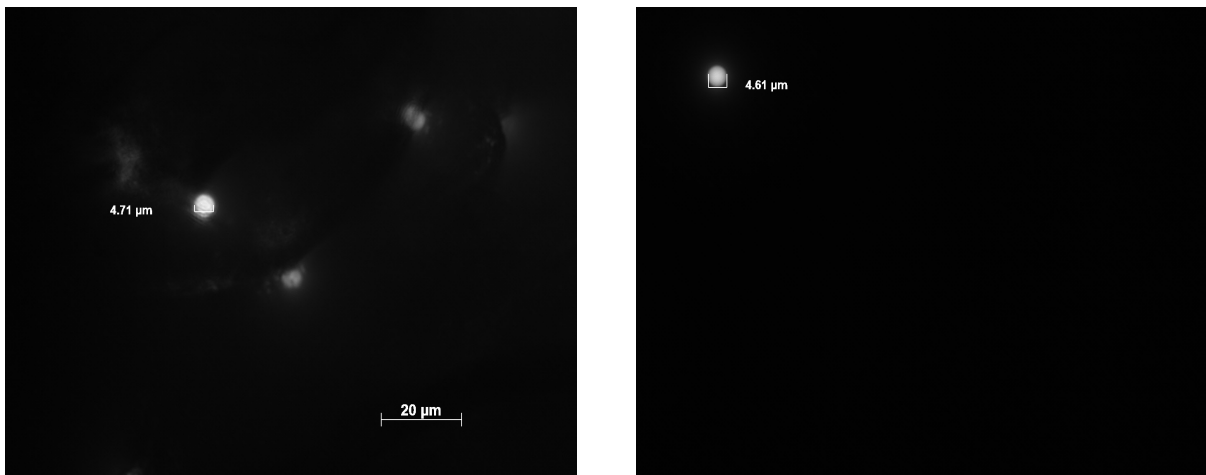


Figure 3.5 Visualization of microspheres by epifluorescent microscopy.

3.3.2 *C. parvum* oocysts

3.3.2.1 *C. parvum* oocyst size and zeta potential (viable and non-viable)

Figure 3.6 shows zeta potential of both viable and non-viable *C. parvum* oocysts. Viable oocysts show a slightly less negative zeta potential (≈ -19 mV) at pH 7-9 compared to the non-viable oocysts (≈ -30 mV). These values fall into a reasonable range of what can be expected for naturally occurring viable oocysts, which can have a zeta potential from -2 to -35 mV (Dai and Hozalski, 2003). The IP observed for both viable and non-viable oocysts was approximately 3, which agrees with values observed in the literature where $IP \approx 2.5-3$ (Pang et al, 2012; Abudalo, 2005). The non-viable oocysts showed a more negative zeta potential, which is most likely due to difference in age or isolates. Although it has been reported that certain methods inactivation can impact the surface properties of *Cryptosporidium* oocysts, primarily chemical inactivation with formalin and heating (Abadulo et al, 2005), this has not been widely observed for inactivation by UV irradiation.

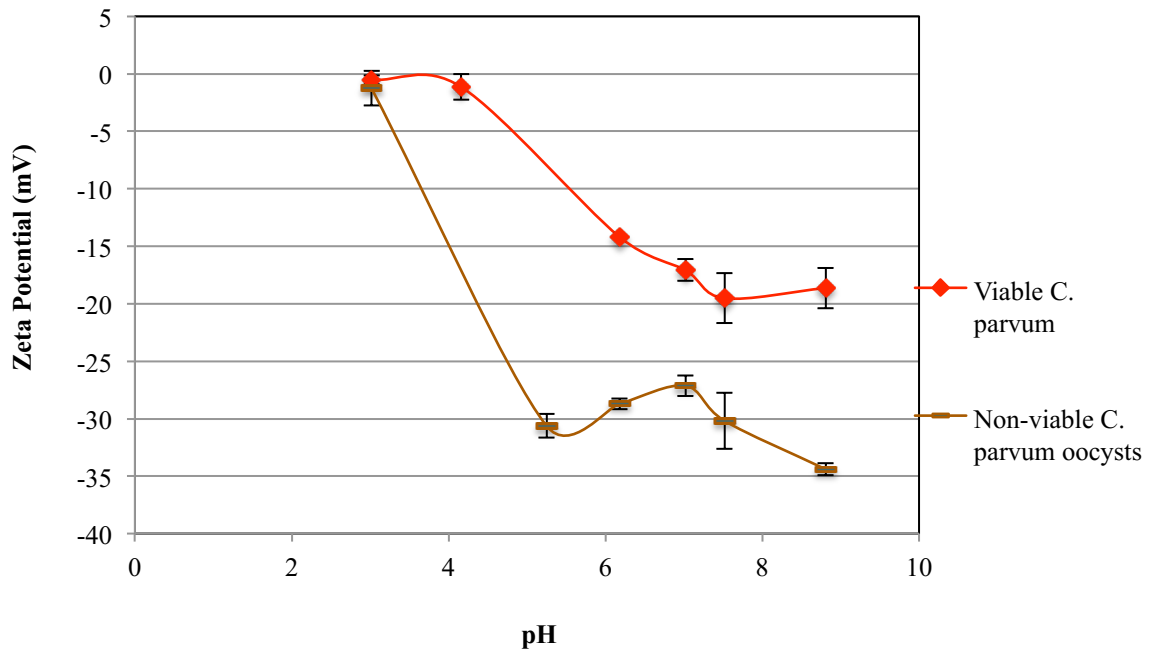


Figure 3.6 Zeta potential of viable and non-viable *C. parvum* oocysts. Non-viable oocysts are inactivated by UV irradiation. Average and one standard deviation of 5 measurements are shown.

3.3.3 Yeast

3.3.3.1 Yeast zeta potential (1, 2, and 4-hour incubation)

Zeta potential of yeast at 1, 2, and 4-hour incubation times is shown Figure 3.7. An $IP \approx 3$ was observed for all incubation times. At pH above 5, all yeast zeta potential range from -15 to -32 mV. Generally, the zeta potential trended towards being more negatively charged with longer incubation time. The 1-hour incubation time yielded yeast particles with similar zeta potential to viable *C. parvum*, or within the reported range of viable *C. parvum* oocysts. Yeast is cost-effective and very simple to cultivate, which makes it an attractive option for use as a *Cryptosporidium* surrogates in pilot-scale experiments.

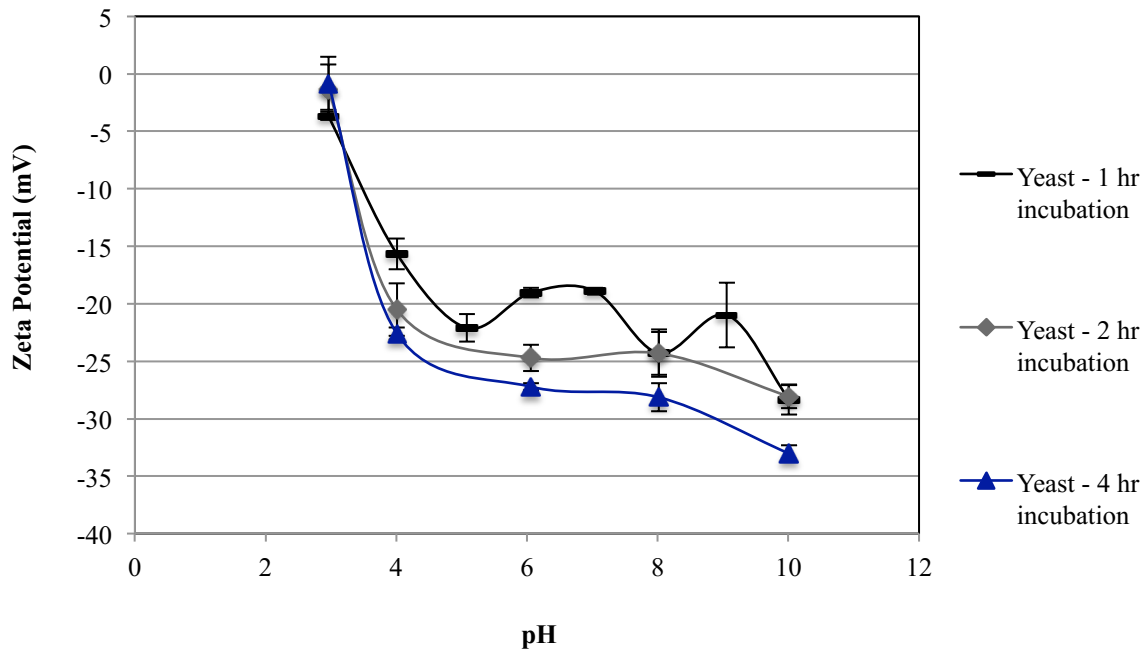


Figure 3.7 Zeta potential for yeast particles cultivated at 1, 2, and 4-hour incubation at 37°C in PBS. Average and one standard deviation of 5 measurements are shown.

3.3.3.2 Yeast particle size

Figure 3.8 shows the size of yeast, measured as hydrodynamic radius by DLS, changes very little with longer incubation periods. Cultivated yeast has a hydrodynamic radius ranging from 4.5-5.0 μm for all incubation times. This falls into the reported size range of 4.5-5.5 μm for naturally occurring *Cryptosporidium* oocysts (Pang et al, 2012; Harter et al, 2000).

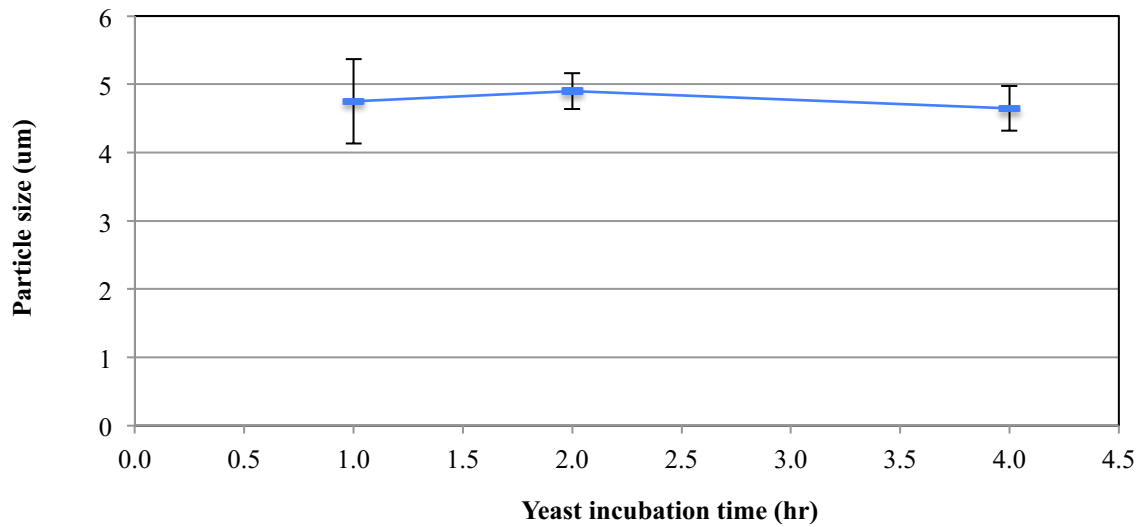


Figure 3.8 Yeast hydrodynamic particle size after cultivation at 1, 2, and 4-hour incubation periods, measured by DLS. Average and standard error of 4 measurements are shown.

Based on the gathered data, there are several attractive features for using yeast as *Cryptosporidium* surrogates. Namely low cost, and similar surface charge and size compared to naturally occurring *Cryptosporidium* oocysts. Despite these advantages, there are challenges posed by enumeration techniques, which may appreciably increase the cost involved. Even with using a relatively fast and simple enumeration method, such as flow cytometry, an additional step after cultivation is required to fluorescently label yeast. This is done to distinguish the yeast particles of interest from any particles present that are present and may exhibit autofluorescence. Also, for the purposes of pilot scale column experiments, yeast particles need to be concentrated on a filter, such as an Envirochek sampling capsule, and recovered with an eluent. Using Envirochek sampling capsules would increase the cost by two to three times compared to modified microspheres (which are enumerated by microscopy), and there are also fewer sampling points available.

3.3.4 Comparison of potential surrogates

The particles with the most promise as *Cryptosporidium* surrogates are shown below in Figure 3.9, where comparisons of zeta potential can be made to viable *C. parvum* (shown in red). All investigated surrogates fall in the documented range of *C. parvum* zeta potential (-2 to -35 mV). Considering the common pH range of surface water, between 6 and 9, the zeta potential appears to be quite stable for all surrogates. Closest to viable *C. parvum* zeta potential are yeast and AGP-modified microspheres, at approximately -20 mV at pH 8. Glycopolymer-modified microspheres more closely resemble non-viable oocyst zeta potential, approximately -28 mV at pH 8.

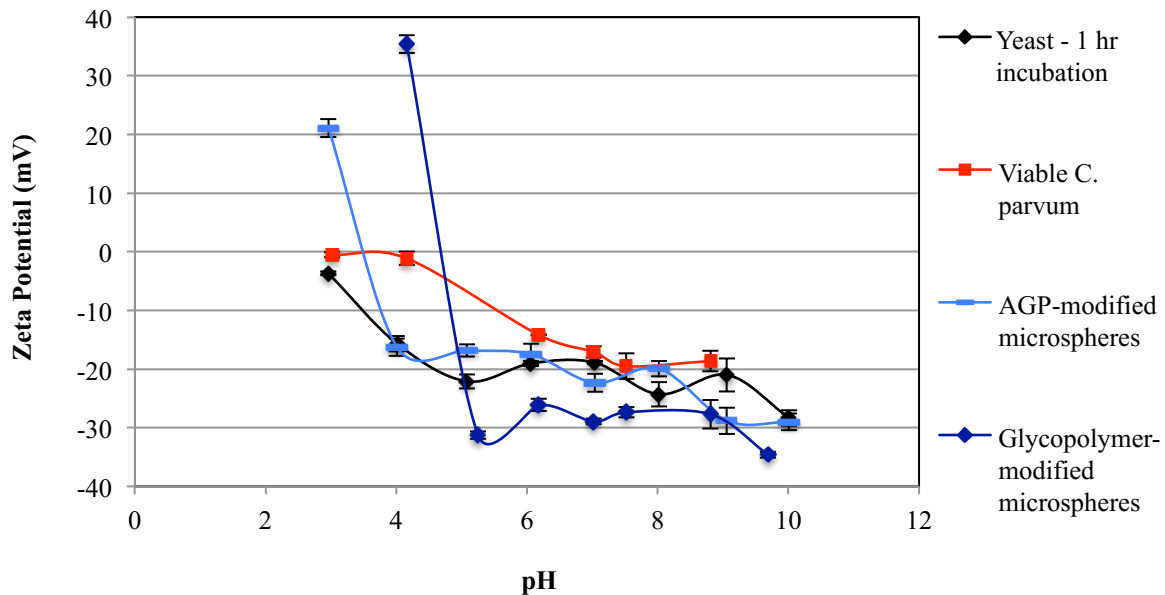


Figure 3.9 *C. parvum* surrogate zeta potential comparison. Not shown are unmodified microspheres. Average and one standard deviation of 5 measurements are shown.

3.4 Conclusions

Based on criteria of particle size and surface charge, it can be concluded that the following particles can act as appropriate *Cryptosporidium* surrogates. It should be noted

that yeast incubation times of 2- and 4-hours were omitted as the same results were obtained with the shortest incubation time.

- AGP-modified microspheres,
- Glycopolymer-modified microspheres,
- Yeast (1-hr) surrogates

As previously stated, the objective of this section was to identify the most effective and economical surrogates for *Cryptosporidium* to be used in pilot scale filtration experiments. As the size and surface charge are similar between the particles listed above, additional criteria need to be considered. Primarily, the cost associated with development, enumeration protocols, and the effectiveness in filtration experiments are considered.

- Yeast poses several benefits. It is by far the most inexpensive particle to obtain, very few materials are needed, and the cultivation is not-labour intensive. One disadvantage is the potential for variation in the growth of yeast. This could also be viewed from a different perspective, as yeast can represent the variation in naturally occurring oocysts and also behave the way a biological particle would in a granular filter. Enumeration poses additional costs and time, as fluorescent labeling is required and particles need to be concentrated on a filter prior to analysis on flow cytometry or microscopy. Despite these apparent disadvantages, yeast offers great potential and should be strongly considered in future trials for evaluating filtration performance and optimization, both on a pilot-scale and full-scale.
- AGP-modified microspheres offer more consistency in size and surface charge compared to yeast, which is an important factor in controlled experiments. The

enumeration is straightforward, which can be done visually by microscopy or flow cytometry without the need for concentrating and eluting samples prior to analysis. The major drawback to AGP-modified microspheres is the cost associated with purchasing the protein. Although this protein is similar to what has been found in the cell wall of *Cryptosporidium* oocysts (Chung, 2012), similar surface charge results were obtained at a fraction of the cost.

- Glycopolymer-modified microspheres have all the same benefits as AGP-modified microspheres, but cost significantly less to produce. The glycopolymer carbohydrate can be synthesized easily and inexpensively, and the conjugation procedure is the same for each type of microsphere.

Based on the results discussed, the glycopolymer-modified microspheres were selected to use in further pilot-scale filtration tests and chemical pretreatment and optimization experiments. It is presumed that these particles will behave similarly to viable *Cryptosporidium* oocysts in the way they interact with coagulants and coagulant aids, and also in their transport and removal in dual-media filters.

3.5 References

Abudalo, R. A., Bogatsu, Y. G., Ryan, J. N., Harvey, R. W., Metge, D. W., & Elimelech, M. Effect of ferric oxyhydroxide grain coatings on the transport of bacteriophage PRD1 and *Cryptosporidium parvum* oocysts in saturated porous media. *Environmental Science and Technology*, **2005** 39(17), 6412-6419.

- Bangs Laboratories Inc. TechNote 205 – Covalent Coupling; Fishers, IN, Rev #5. **2013**.
Vol KT/MM-03/2002, p. 6
- Bergman, L.W. Chapter 2: Growth and Maintenance of Yeast. *In: Two-Hybrid Systems Methods and Protocols* (ed. MacDonald, P.N.) **2001**, 9-10
- Considine, R. F., Dixon, D. R. and Drummond, C. J. Oocysts of *Cryptosporidium parvum* and model sand surfaces in aqueous solutions: an atomic force microscope (AFM) study. *Water Research*. **2002**, 36 (14): 3421-3428.
- Chung, J. Development of fluorescently labelled *Cryptosporidium* oocysts surrogates to test the efficacy of sand filtration processes. PhD Dissertation, University of New South Wales, Australia **2012**
- Dai, X., and Hozalski, R. M. Evaluation of microspheres as surrogates for *Cryptosporidium parvum* oocysts in filtration experiments. *Environmental Science and Technology*. **2003**, 37(5), 1037-1042.
- Emelko, M. B., Huck, P. M., and Coffey, B. M. A review of *Cryptosporidium* removal by granular media filtration. *American Water Works Association*, **2005**, 97(12), 101.
- Fournier, T., Medjoubi-N, N., and Porquet, D. Alpha-1-acid glycoprotein. *Biochimica et Biophysica Acta (BBA)-Protein Structure and Molecular Enzymology*. **2000**, 1482(1), 157-171.
- Hagler, A.N. Yeasts as indicators of environmental quality. *In: Biodiversity and Ecophysiology of Yeasts* (eds. Rose, A.H., and Harrison, J.S.) **2006**, 515-532.
- Harter, T., Wagner, S., and Atwill, E. R. Colloid transport and filtration of *Cryptosporidium parvum* in sandy soils and aquifer sediments. *Environmental Science and Technology*, **2000**, 34(1), 62-70.

- Johal, M. S. *Understanding nanomaterials*. **2011**. CRC Press. pp. 195-196
- Pang, L., Nowostawska, U., Ryan, J. N., Williamson, W. M., Walshe, G., and Hunter, K. A. Modifying the surface charge of pathogen-sized microspheres for studying pathogen transport in groundwater. *Journal of Environmental Quality*, **2009** 38(6), 2210-2217.
- Pang, L., Nowostawska, U., Weaver, L., Hoffman, G., Karmacharya, A., Skinner, A., and Karki, N. Biotin-and Glycoprotein-Coated Microspheres: Potential Surrogates for Studying Filtration of *Cryptosporidium parvum* in Porous Media. *Environmental Science and Technology*. **2012**, 46(21), 11779-11787.
- Polysciences Fluoresbrite YG Carboxylate Microspheres 4.50µm. Polysciences Inc. Warrington, PA. **2015**. <http://www.polysciences.com/default/fluoresbrite-yg-carboxylate-microspheres-450-m>
- Sigma-Aldrich. Alpha-1-Acid Glycoprotein Product Information. Saint Louis, MO. ALF/RXR 9/02. http://www.sigmaaldrich.com/content/dam/sigmaaldrich/docs/Sigma/Product_Information_Sheet/2/g9885pis.pdf
- Zilberman, A., Zimmels, Y., Starosvetsky, J., Zuckerman, U., and Armon, R. A two-phase separation method for recovery of *Cryptosporidium* oocysts from soil samples. *Water, Air, and Soil Pollution*, **2009**. 203(1-4), 325-334.

Chapter 4. Chemical pretreatment and polyelectrolyte optimization

4.1 Introduction

4.1.1 Background

Chemical pretreatment is an important step in the overall drinking water treatment process. For surface waters that contain colloidal particles, coagulants are used to destabilize suspended particles, which then enhances the filtration process (Crittenden et al, 2005). This is typically achieved using hydrated aluminum sulphate, or alum ($\text{Al}_2(\text{SO}_4)_3 \cdot 14\text{H}_2\text{O}$). Polyelectrolyte coagulant aids are also commonly used to augment the coagulation and flocculation process. The importance of pretreatment for the removal of *Cryptosporidium* has been previously established in Chapter 2, where suboptimal pretreatment has resulted in reduced removal (Patania et al 1995; Arora et al, 2001; Bustamante et al, 2001, Chung 2012). There have been limited studies on the relationship between treatment performance and polyelectrolyte structure (Bolto and Gregory, 2007).

In order to more fully understand how to improve *Cryptosporidium* removal, chemical pretreatment was investigated, with specific concern given to polyelectrolyte type and dosage. This was done using the glycopolymer-modified microspheres as *Cryptosporidium* surrogates, which were previously characterized in Chapter 3. Several techniques were used, including zeta potential and a procedure developed for quartz crystal microbalance with dissipation monitoring (QCM-D). A brief summary of polyelectrolyte types and QCM-D are given below.

4.1.3 Polyelectrolyte characteristics

Polyelectrolytes used in water treatment are typically synthetic long-chain molecules that are water-soluble and have a structure designed to provide distinctive physico-chemical properties (Zhu et al, 1995; Bolto and Gregory, 2007). Polyelectrolytes are broadly categorized by their ionic nature: given as cationic, anionic, or non-ionic. The most important characteristics of polyelectrolytes are molecular weight and charge density (Bolto and Gregory, 2007), with higher molecular weight, linear polyelectrolytes being most effective for particle bridging (Ghosh et al, 1985). Charge density can influence bridging effectiveness, and there is also difficulty in adsorbing to particles with the same charge (Bolto and Gregory, 2007).

Anionic polyelectrolytes contain several negatively charged sites most often due to carboxyl groups, and can be in both the low and high molecular weight range. Conversely, cationic polyelectrolytes usually have a prevalence of amino groups and relatively low molecular weight range (Zhu et al, 1995). Cationic polyelectrolytes are used the most often due to their high charge density, which can result in better natural organic matter (NOM) removal and the formation of smaller flocs (Matilainen et al 2010). Anionic polyelectrolytes are used for forming larger, easily settleable flocs (Matilainen et al 2010), and are better suited for conventional treatment where sedimentation is involved.

For this study, three commercially available polyelectrolytes were used: Magnafloc LT-7996, Magnafloc LT-7981, and Magnafloc LT-27AG, which are described in detail below (all information obtained from BASF Corporation product sheets). Monomers of each are shown in Figure 4.1.

- a) Magnafloc LT-7996 is a cationic diallyldimethylammonium chloride (pDADMAC) homopolymer with high molecular weight and high charge density.
- b) Magnafloc LT-7981 is a cationic epichlorohydrin amine (ECHA) with high low molecular weight and high charge density.
- c) Magnafloc LT-27AG is an anionic polyacrylamide (APAM) with a high molecular weight and medium charge density.

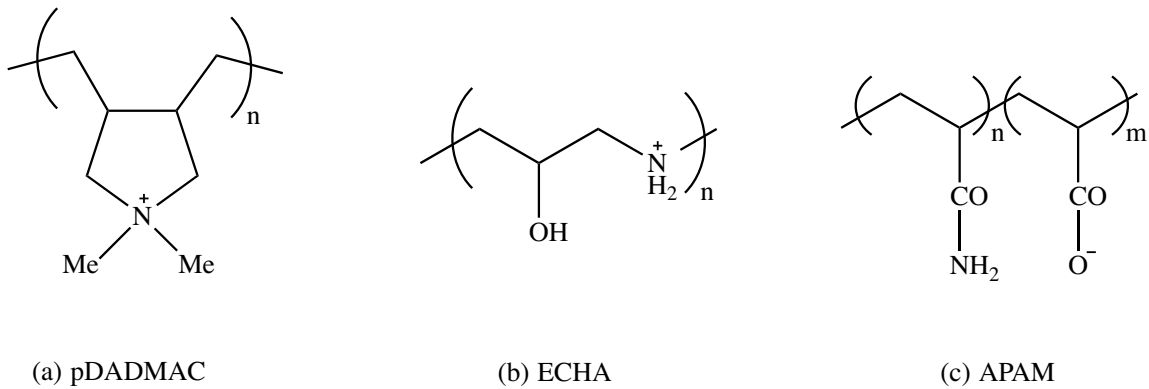


Figure 4.1 Structures of cationic polyelectrolytes (a) pDADMAC, (b) ECHA, and (c) APAM.

For the sake of clarity, the polyelectrolytes will hereafter be referred to by their chemical structures and not their commercial names.

4.1.3 QCM-D background

Quartz crystal microbalance (QCM) has been a powerful tool for gravimetric analysis, particularly for the measurement of mass and thickness of materials as small as a few nanograms (Johal, 2011). This technology operates on the piezoelectric principle, where an electric field can be induced by a physical stress in certain types of crystals.

This was developed in the late 1800's by Jacques and Pierre Curie, who later expanded this principle to the converse, or reverse, piezoelectric effect, whereby a piezoelectric crystal can be physically changed by applying a voltage (Johal, 2011).

In 1959, Sauerbrey developed the proportional relationship between mass deposited on piezoelectric quartz crystals and resulting resonant frequency shift, which is described by the Sauerbrey equation:

$$\Delta m = \frac{-C \cdot \Delta f}{n}$$

where Δm and Δf are mass frequency, n is the overtone number of the crystal ($n=1,3,5,7,9,11$), and C is a constant depending on the specific quartz crystal (Sauerbrey, 1959; Johal et al, 2011). For this experiment, 5 MHz quartz crystals were used, where $C = 17.7 \text{ ng Hz}^{-1} \text{ cm}^{-2}$ (Biolin Scientific, 2014).

Using this principle, a quartz crystal will oscillate at specific resonant frequencies in response to an applied AC voltage. QCM can detect very small changes in the resonant frequency in real time as a result of molecules adhering to the quartz crystal sensor surface. The Sauerbrey equation was not developed for solid-liquid interfaces, and generally underestimates the mass adsorbed due to viscoelastic properties (Johal, 2011). This has led to QCM with additional dissipation monitoring.

Dissipation monitoring provides information regarding the type of material adhering to a surface, such as thickness, density, and viscoelasticity (Johal, 2011).

Dissipation is formally defined as:

$$D = \frac{E_{lost}}{2n E_{stored}}$$

where E_{lost} is the energy lost (or dissipated) during one oscillation cycle, and E_{stored} is the total energy stored in the quartz crystal oscillator (Biolin Scientific, 2014). A “soft” film will not completely couple to the oscillation of the quartz crystal, and the crystal’s energy is effectively dissipated; conversely, a “rigid” film will oscillate with the crystal and energy will not be quickly dissipated (Johal, 2011; Biolin Scientific, 2014). This is represented below in Figure 4.2.

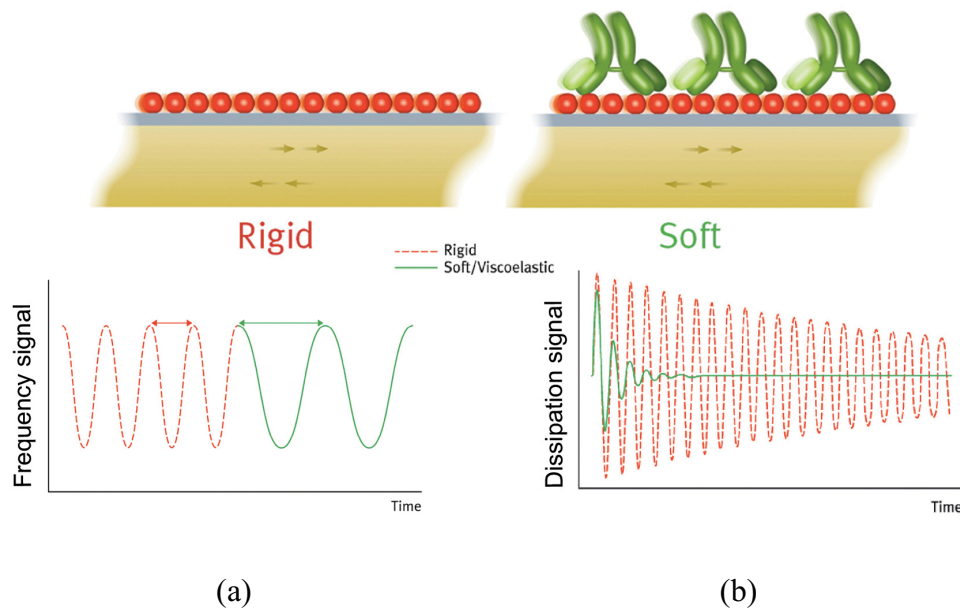


Figure 4.2 QCM-D principle; with (a) slow dissipation with a rigid film, and (b) fast dissipation with a “soft” (viscoelastic) film (Biolin Scientific, 2014)

Using a quartz crystal coated in SiO_2 , the adhesion of cells (or microspheres in this case) to the sensor surface can be investigated. Cell-surface interactions have been previously assessed using QCM-D (Poitras and Tufenkji, 2009; Marcus et al, 2012; Wang et al, 2014). This can provide insight into the processes by which cells approach, deposit, and attach to different surfaces. These processes can involve hydrodynamic and physical-chemical interactions (Torkzaban et al, 2007).

With regards to *Cryptosporidium*, there has been previous work done using QCM-D as a biosensor for the presence and quantification of oocysts in water samples (Poitras et al, 2009). There are some potential applications regarding the removal of *Cryptosporidium* in granular media filters. Since silica (SiO₂) sand is a widely used type of filter media and QCM-D sensors can be coated with SiO₂, the attachment of oocysts to SiO₂ surfaces can be investigated under varying carrying solutions.

This study seeks to address the attachment of *Cryptosporidium* oocysts to SiO₂ in the presence of different polyelectrolyte coagulant aids, using glycopolymer-modified microspheres as surrogates.

4.2 Methods and materials

4.2.1 Gel permeation chromatography

Gel permeation chromatography (GPC) was used to characterize the polyelectrolytes in terms of number average molecular weight (M_n), weighted average molecular weight (M_w), and polydispersity index (PDI). This analysis was performed by Yinan Wang (University of Alberta Chemical and Materials Engineering Department).

4.2.2 Zeta potential

Zeta potential measurements were used to understand the impact of polyelectrolyte concentration on the surface charge of *Cryptosporidium* surrogates. In order more closely represent real-world conditions, two conditions were tested: with 5 mg/L alum and without alum.

Glycopolymer-modified microsphere suspensions were prepared with a particle concentration of 5×10^5 particles/mL. The background solution of 1 mM KCL was adjusted to pH 8 and filtered prior to use. Cationic polyelectrolyte solutions of 100 mg/L were prepared by serial dilution from the manufacturer stock (active content concentration is 414000mg/L for ECHA; 207000mg/L for pDADMAC). A range of polyelectrolyte concentrations (0 to 2.0 mg/L) were added to microsphere suspensions and homogenized prior to analysis. For the experimental condition with 5 mg/L alum, aliquots from a freshly prepared solution of diluted liquid alum (48%) were added to each particle suspension.

Zeta potential of each sample was then measured by microelectrophoresis over (90Plus Zeta, Brookhaven Instruments Corporation, Holtsville, NY); all measurements were done at 22°C. APAM was not considered in the zeta potential analysis as it was not considered for use in direct filtration column trials, and a very low surface tension resulted in difficulty obtaining accurate concentrations from serial dilution of the stock.

4.2.3 QCM-D

The premise of this experiment is to coat glycopolymer-modified microsphere *C. parvum* surrogates with a polyelectrolyte coagulant aid, and then inject the particles to SiO₂ QCM sensors. As previously mentioned, these sensors were chosen to model the attachment of surrogates to silica sand, a common type of filter media. The QCM-D methods were adapted from a previous study by Caruso and Mohwald (1999).

4.2.3.1 Glycopolymer-modified microsphere preparation for QCM-D

The polyelectrolyte layer was deposited to the surface of glycopolymer-modified microspheres surrogates by adding approximately 5×10^5 microspheres to a 1.25 mL aliquot of a 1.0 mg/L filtered aqueous polyelectrolyte solution. This suspension was occasionally stirred, allowing 20 min for dispersion and polyelectrolyte adsorption. Excess polyelectrolyte was removed by two repeated wash/redispersion cycles using centrifugation (13500g, 15 min). Washing was done using DI water. Polyelectrolyte-coated microspheres were then resuspended and diluted to 10 mL in a filtered solution of 1 mM KCl at pH 8. A 0.5 mL aliquot of each solution was enumerated by flow cytometry. Cationic polyelectrolyte solutions (i.e. glycopolymer-modified microspheres with ECH and pDADMAC coatings) were diluted to the same microsphere concentration ($10^5/\text{mL}$). APAM and control samples were not further diluted due to a limited remaining concentration.

4.2.3.2 QCM-D analysis

SiO₂ sensors, QCM-D modules, and tubing was cleaned prior to use by flowing 2% sodium dodecyl sulphate (SDS) followed by ultrapure water through all components. SiO₂ sensors were further rinsed with ultrapure water, dried with N₂ gas, and cleaned with UV radiation for 10 minutes.

Once cleaning was completed, sensors were placed in QCM-D modules and filtered background solution of 1mM KCl at pH 8 was injected at 150 $\mu\text{L}/\text{min}$ until frequency (F) and dissipation (D) values were stable (approximately 10 minutes). The polyelectrolyte-coated glycopolymer-modified microsphere suspensions were then injected at 50 $\mu\text{L}/\text{min}$ until F and D were stable, or until no particle suspension remained

(160 minutes). The sensors were then rinsed with background solution at 150 $\mu\text{L}/\text{min}$ to remove loosely bound particles. The adhered particles on each sensor were visualized using epifluorescence microscopy (Microscope Axio Imager.M2, Carl Zeiss, Germany) with a light source (X-cite 120Q, Lumen Dynamic, ON, Canada).

It should be noted that the described methods for analysis by QCM-D required a substantial amount of trial and error. Several attempts were made at coating SiO_2 sensors with ECHA, pDADMAC, and APAM, and then injecting glycopolymer-modified microspheres to measure the deposition. This was not successful or reproducible due to difficulty with the polyelectrolyte coating, unclean and old sensors, and residual microspheres remaining in the tubing.

4.3 Results and Discussion

4.3.1 GPC

The characteristics of the two cationic polyelectrolytes were similar to the manufacturer specifications, molecular weight listed by BASF as “high” and “medium” for pDADMAC and ECHA, respectively. GPC analysis results in Table 4.1 show that pDADMAC has approximately twice the molecular weight of ECHA (585,700 and 245,900 g/mol , respectively). The anionic polyelectrolyte results were different than expected, with APAM molecular weight being very low from the GPC. The manufacturer (BASF Corporation) lists APAM molecular weight as being “very high”. Since this anionic commercially available polyelectrolyte is known to have a very high molecular weight, it can be concluded that error was likely involved in the APAM analysis.

The exceptionally high PDI for each cationic polyelectrolyte (32.86 for ECHA, 36.85 for pDADMAC) suggests that the molecule chains exist in broad size range and are non-uniform. APAM appears to exist in a more uniform dispersion, but the aforementioned error in analysis may invalidate this result.

Table 4.1 Number average molecular weight (M_n), weighted average molecular weight (M_w), and polydispersity index (PDI) of different polyelectrolytes

	M_n (g/mol)	M_w (g/mol)	PDI
ECHA (cationic)	7,500	245,900	32.86
pDADMAC (cationic)	15,900	585,700	36.85
APAM (anionic)	11,600	20,900	1.36

M_n - number average molecular weight; total weight of all polymer molecules divided by number of polymer molecules

M_w - weighted average molecular weight

PDI - M_w / M_n

4.3.2 Zeta potential

There appears to be a charge reversal of glycopolymer-modified microspheres in the presence of each cationic polyelectrolyte. This is observed in Figure 4.3 and Figure 4.4, where charge reversal occurs at concentrations of approximately 0.15 mg/L for each pDADMAC and ECHA. This is the polyelectrolyte concentration where the isoelectric point of glycopolymer-modified microspheres is reached (i.e. zeta potential = 0 mV). Interesting to note that the addition of 5 mg/L alum results in a charge reversal without the presence of polyelectrolyte, which is likely due to the high concentration of positively charged aluminum in solution, and the effect of increasing ionic strength compressing the double-layer associated with the microspheres in suspension.

These results agree with the classic experiments of Black et al (1966), where charge reversal of kalonite clay suspensions occurred at cationic polyelectrolyte

concentrations of approximately 0.25 mg/L; and the amount of polymer adsorbed to particles is constant with dosages higher than 0.7 mg/L (Black et al, 1966; Crittenden et al, 2005).

These results would seem to suggest that cationic polyelectrolytes can be introduced in very low concentrations (0.15 mg/L) to achieve the desired result of a neutral electrophoretic mobility (zeta potential = 0); or not added at all when alum is used. This observation should be taken with reservation, as it should be considered that a main objective for using cationic polyelectrolytes, particularly in direct filtration, is to encourage interparticle bridging and the formation of smaller, tougher flocs (Bolto and Gregory, 2007). These experiments were performed under well-controlled, clean conditions that do not accurately represent the complexity of natural source water. Addition of polyelectrolytes is still necessary, with the selection and dosage determined empirically (Crittenden et al, 2005).

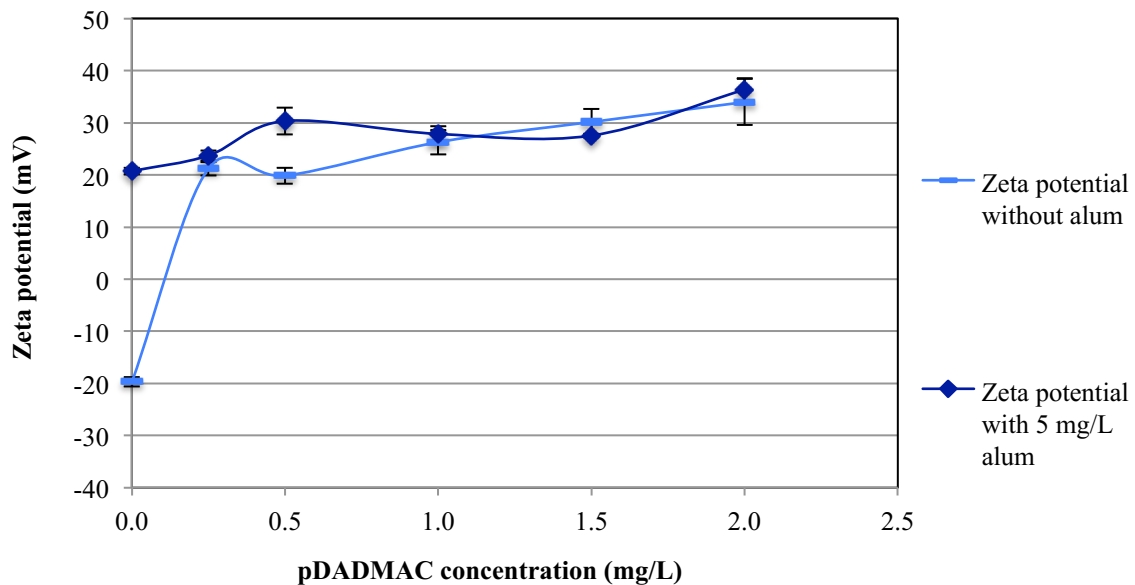


Figure 4.3 Zeta potential of glycopolymer-modified microspheres under different concentrations of pDADMAC, with and without 5 mg/L alum. Average and one standard deviation of 5 measurements are shown.

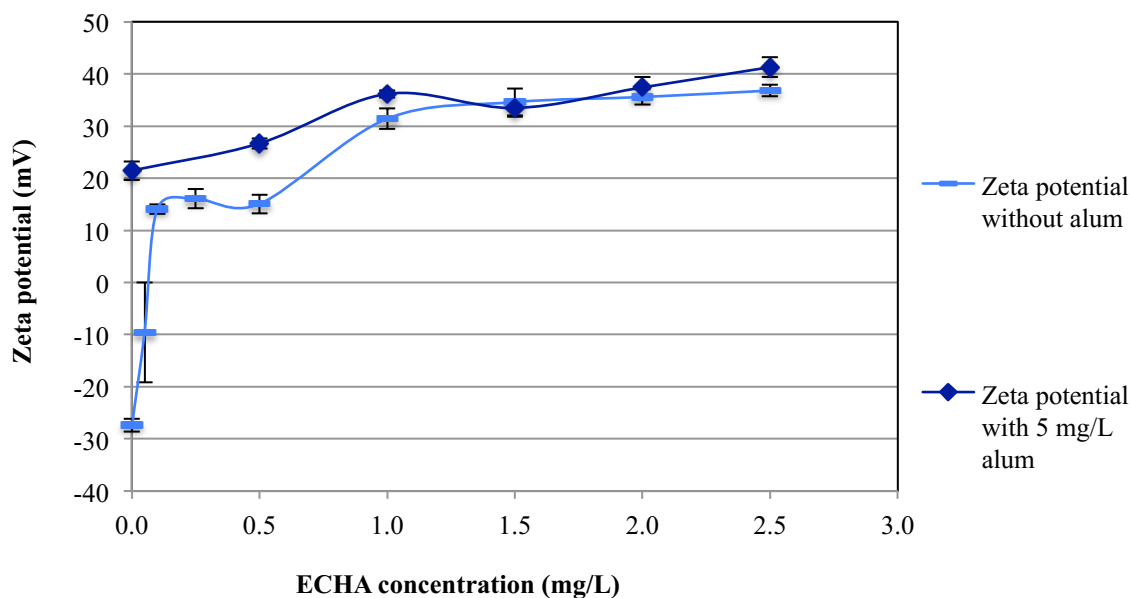


Figure 4.4 Zeta potential of glycopolymer-modified microspheres under different concentrations of ECHA, with and without 5 mg/L alum. Average and one standard deviation of 5 measurements are shown.

4.3.3 QCM-D

The frequency and dissipation shifts of SiO_2 sensors induced by the adhesion of glycopolymer-modified microspheres with various polyelectrolyte coatings (pDADMAC, ECHA, APAM, and no coating) are shown in Figure 4.5 and Figure 4.6. Negative frequency shifts are indicative of mass being adsorbed onto the sensor surface. This can be observed for each cationic polyelectrolyte treatment (pDADMAC and ECHA), and the control treatment, even after washing with background solution. Frequency shifts became more negative after washing for the cationic treatments, which is likely a result of the increased wash flow rate (i.e. greater shear force) carrying microspheres that may have accumulated in the tubing and flow module.

The anionic polyelectrolyte treatment (APAM) appears to have an immediate deposition of microspheres on sensor surface. These microspheres are likely very weakly adsorbed to the surface, as the anionic coating will not interact strongly with the negative SiO₂ surface. The marked increase in frequency when sensors are washed suggests that the stronger shear forces of the washing solution remove the weakly adsorbed microspheres.

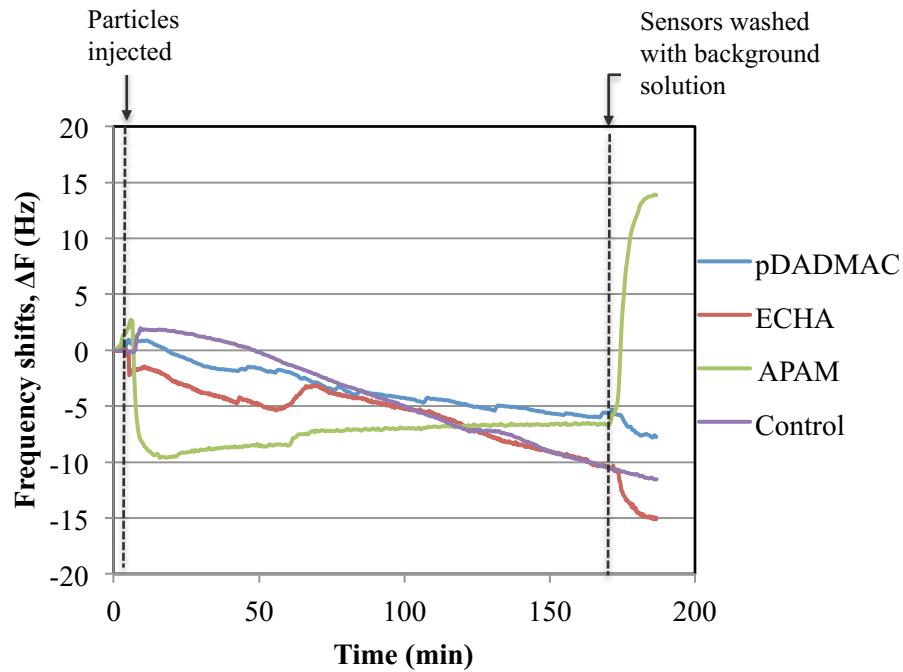


Figure 4.5 Frequency shifts of 3rd overtone for glycopolymer-modified microspheres adhered to SiO₂ sensor surface with (a) pDADMAC, (b) ECHA, (c) APAM coatings, and (d) control (microspheres with no coating).

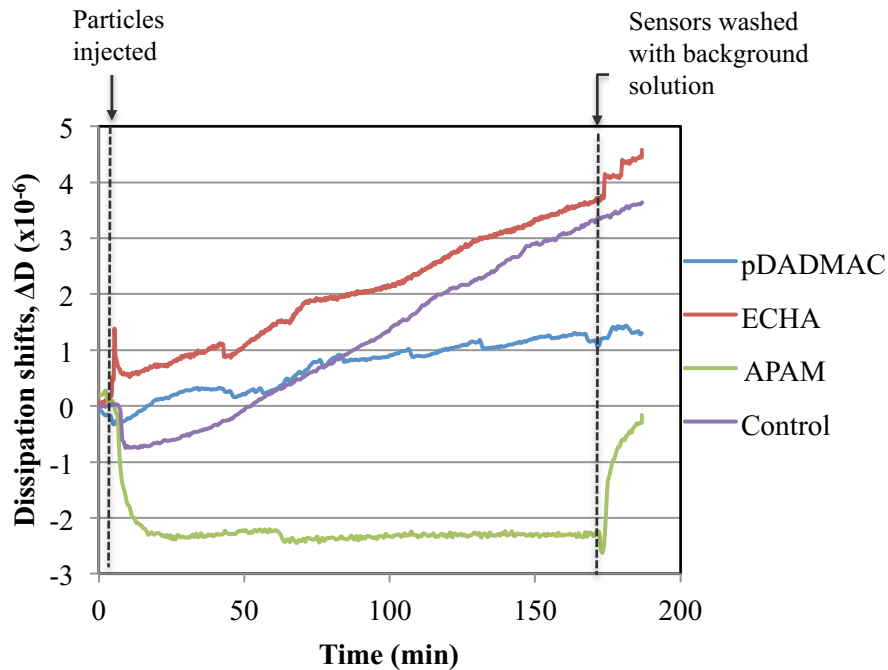
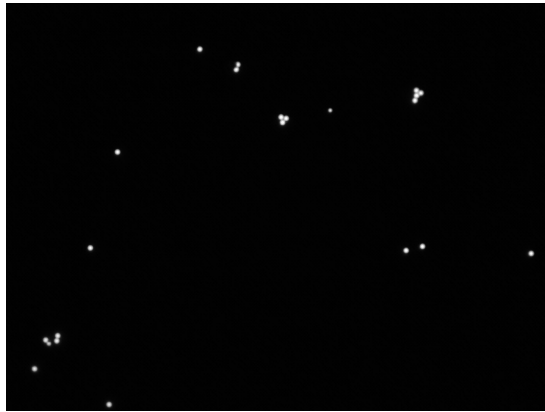


Figure 4.6 Dissipation shifts of 3rd overtone for glycopolymer-modified microspheres adhered to SiO₂ sensor surface with (a) pDADMAC, (b) ECHA, (c) APAM coatings, and (d) control (microspheres with no coating)

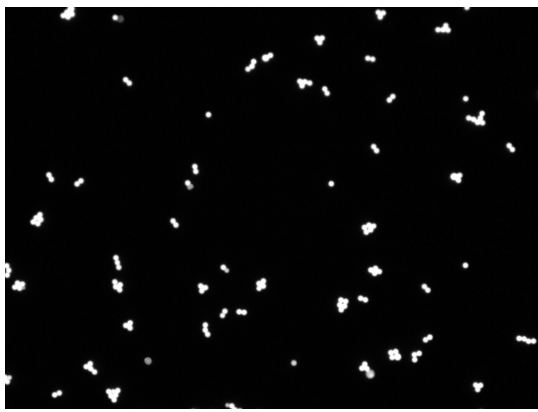
ECHA seems to be a more effective option for pretreatment compared to pDADMAC, which can also be seen in photographs of sensor surfaces in Figure 4.7. Based on frequency shifts, no chemical pretreatment (i.e. control treatment) also appears to be as effective as ECHA. It should also be considered that the methods used reasonably high concentrations of polyelectrolytes, which would likely result in secondary adsorption of polyelectrolyte chains to the microsphere surface and stabilize the particles. This stabilization may help to explain the low amount of aggregation in cationic treatments compared to APAM and control treatments (seen in Figure 4.7).



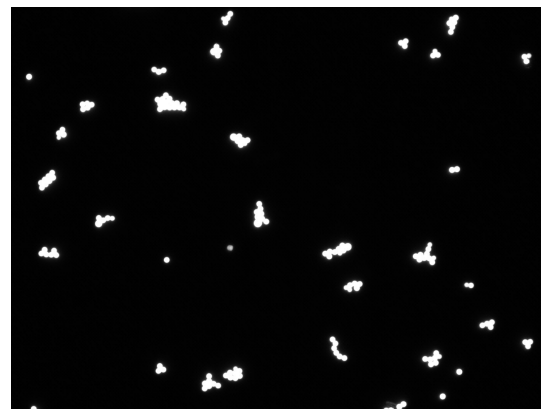
(a) pDADMAC



(b) ECHA



(c) APAM



(d) Control

Figure 4.7 Visualization of glycopolymer-modified microspheres adhered to SiO_2 sensor surface under different polyelectrolyte coatings, using epifluorescent microscopy

Figure 4.8 plots $\Delta F/\Delta D$ of each overtone at the end of the experiment after washing. This is beneficial comparison, as the ratio cancels out the density of deposited microspheres and nonuniformity of overtones. The ratio becomes inherent to the characteristics of the specific microsphere treatment deposited onto a particular surface (Marcus et al, 2012). In this case, the higher magnitude of $\Delta F/\Delta D$ resulting from low dissipation confirms the rigid nature of the microspheres. Moderate increases and positive $\Delta F/\Delta D$ point to an elastic connection being formed, where the rigid nature of microspheres helps to release water from the interface between the microsphere surface

and SiO₂ (Marcus et al, 2012). This could be problematic for the use of glycopolymer-modified microspheres as *Cryptosporidium* surrogates, as rigid polystyrene spheres may not behave similarly to non-rigid biological cells in real-world filtration.

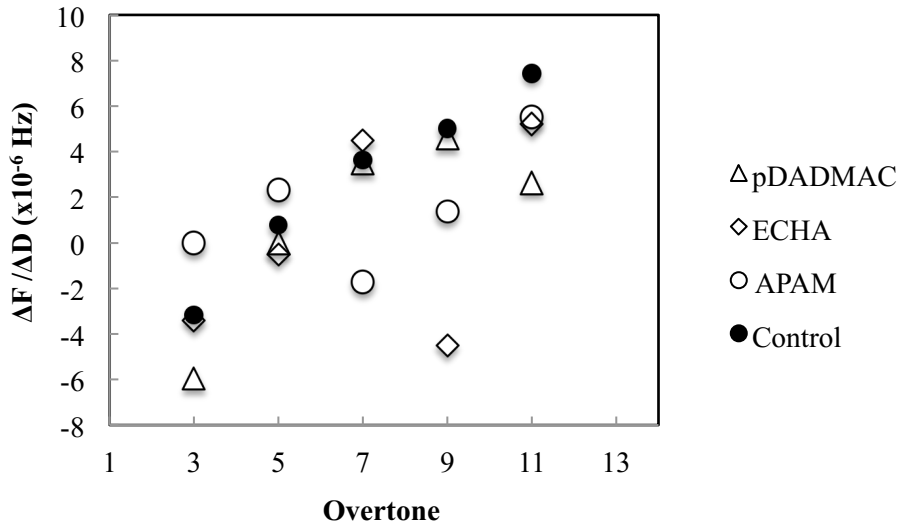


Figure 4.8 Slopes of frequency divided by dissipation at the end of the experiment. Dissipation values close to zero (i.e. +/- 0.01) were approximated to be zero such that $\Delta F/\Delta D$ is not at an extreme value.

4.4 Conclusions

The investigation of chemical pretreatment show that ECHA is likely the best option of the three polyelectrolytes investigated. Based on the zeta potential analysis, it can achieve charge reversal of glycopolymer-modified microspheres at very low concentrations (0.15 mg/L), which is due to its high charge density, noted as being 100% (Bolto and Gregory, 2007). QCM-D investigations also support this, as ECHA resulted in better attachment to SiO₂ surfaces than pDADMAC.

Possibly the most important conclusion that can be drawn from this section is that the well-controlled experiments may not accurately represent real-world conditions. Certain interpretations can be made from the data with regards to optimizing chemical

pretreatment, but the “clean” conditions tested do not take into account the additional complexities of raw water prior to treatment. Other factors such as elevated turbidity, natural organic matter, and water temperature will have an impact on how water is chemically pretreated, and therefore how the pretreatment impacts the removal of *Cryptosporidium* oocysts. There is potential that the methods used can be further developed to model attachment (and attachment kinetics) of biological organisms to filter media, particularly with QCM-D.

4.5 References

- Arora, H., Giovanni, G.D., and Lechevallier, M. Spent filter backwash contaminants and treatment strategies. *American Water Works Association*. **2001**, 93(5), 100-112
- Biolin Scientific. QCM-D Technology. **2014**. <http://www.biolinscientific.com/q-sense/technologies/> Accessed May 25, 2015
- Black, A. P., Birkner, F. B., and Morgan, J. J. The effect of polymer adsorption on the electrokinetic stability of dilute clay suspensions. *Journal of Colloid and Interface Science*, **1966**. 21(6), 626-648.
- Bustamante, H. A., Shanker, S. R., Pashley, R. M., and Karaman, M. E. Interaction between *Cryptosporidium* oocysts and water treatment coagulants. *Water Research*, **2001** 35(13), 3179-3189
- Caruso, F., and Möhwald, H. Preparation and characterization of ordered nanoparticle and polymer composite multilayers on colloids. *Langmuir*, **1999**. 15(23), 8276-8281.
- Chung, J. Development of fluorescently labelled *Cryptosporidium* oocysts surrogates to

- test the efficacy of sand filtration processes. PhD Dissertation, University of New South Wales, Australia **2012**
- Ghosh, M. M., Cox, C. D., and Prakash, T. M.. Polyelectrolyte selection for water treatment. *Journal American Water Works Association*, **1985** 67-73.
- Johal, M. S. *Understanding nanomaterials*. **2011**. CRC Press. pp. 105-108
- Marcus, I. M., Herzberg, M., Walker, S. L., and Freger, V. Pseudomonas aeruginosa attachment on QCM-D sensors: the role of cell and surface hydrophobicities. *Langmuir*, **2012** 28(15), 6396-6402.
- Matilainen, A., Vepsäläinen, M., and Sillanpää, M. Natural organic matter removal by coagulation during drinking water treatment: A review. *Advances in Colloid and Interface Science*, **2010**. 159(2), 189-197.
- Patania, N. L. Jacangelo, J. G., Cummings, L., Wilczak, A., Riley, K. and Oppenheimer, J. Optimization of filtration for cyst removal. *AWWA Research Foundation and American Water Works Association*, Denver CO, **1995**
- Poitras, C. and Tufenkji, N.. A QCM-D-based biosensor for E. coli O157: H7 highlighting the relevance of the dissipation slope as a transduction signal. *Biosensors and Bioelectronics*, **2009**. 24(7), 2137-2142.
- Poitras, C., Fatisson, J., and Tufenkji, N. Real-time microgravimetric quantification of *Cryptosporidium parvum* in the presence of potential interferents. *Water Research*, **2009** 43(10), 2631-2638.
- Sauerbrey, G. Use of vibrating quartz for thin film weighing and microweighing. *Z. Phys*, **1959**. 155(2), 206-222.

- Torkzaban, S., Bradford, S. A., and Walker, S. L. Resolving the coupled effects of hydrodynamics and DLVO forces on colloid attachment in porous media. *Langmuir*, **2007**. 23(19), 9652-9660.
- Wang, Y., Narain, R., and Liu, Y. Study of Bacterial Adhesion on Different Glycopolymer Surfaces by Quartz Crystal Microbalance with Dissipation. *Langmuir*, **2014**. 30(25), 7377-7387.
- Zhu, H., Smith, D.W., Zhou, H., and Stanley, S.J. Selection of polymers as filter aid for E.L. Smith Water Treatment Plant Softened Water. *Environmental Engineering Technical Report*. University of Alberta. Edmonton, AB, Canada. **1995**

Chapter 5: Pilot Scale Experiments

5.1 Introduction

Due to environmental persistence and resistivity to established chemical disinfection by chlorination, the preferred methods for removing *Cryptosporidium* oocysts from drinking water is through physical means, such as coagulation and flocculation followed by granular filtration (Chung, 2012). The basic process of filtration for drinking water treatment involves a filter bed of granular media, use of coagulants to chemically pretreat raw water, and backwashing the filter bed to remove accumulated solids (Crittenden et al, 2005). Common types of filter media are sand, coal, and anthracite, which are processed to a fairly uniform size distribution (Chung, 2012). Particles adhere to filter media and are removed throughout the entire filter bed by depth filtration (Crittenden et al, 2005). Proper chemical pretreatment is necessary for this removal to occur, and coagulants such as alum and cationic/anionic polymers are added to properly destabilize particles (Crittenden et al, 2005). There are several operational parameters associated with both the chemical pretreatment and granular media. Such parameters include: coagulant type and dosage, polymer type and dosage, filter media type, size, depth, and flow rate (Crittenden et al, 2005; Patania et al, 1995).

Several studies have noted the need to understand the impact of different operational parameters on *Cryptosporidium* oocyst removal (Abadulo et al, 2005; Emelko et al, 2005; Gitis, 2008). Since the need for *Cryptosporidium* surrogates has been established in previous chapters, and glycopolymer-modified microspheres have been developed and identified as potentially effective *C. parvum* surrogates, this chapter will

focus on pilot-scale filtration experiments using glycopolymer-modified microspheres as *C. parvum* surrogates.

In order to gain a better understanding of how *Cryptosporidium* is transported and removed in filtration, it is important to translate the previously described bench-scale experiments (where the impact of polymer coagulation aids was investigated) to a real-world application. Since there are substantial logistical challenges involved with performing experiments on full-scale water treatment operations, a pilot-scale design is used.

With existing pilot-scale columns, a wide range of data from influent, effluent, deposition profiles, and backwash can be gathered. To understand how *Cryptosporidium* is transported and removed in filtration, the impact of two different influent pretreatment conditions under high and low flow rates was investigated. The experimental design and specific objectives are outlined further in section 5.1.1 and 5.1.2.

5.1.1 Experimental design

Experiments for this study were conducted at E.L. Smith Water Treatment Plant, operated by EPCOR, located in Edmonton, AB. Pilot filter runs were conducted during two different operational modes: direct filtration and conventional filtration.

Direct filtration represents the water influent conditions for winter months, where no clarification is occurs. Low doses of alum (5 mg/L), and cationic filter polymer were (2 mg/L ECHA) added inline. Rapid mixing, coagulation, and flocculation are accomplished inline prior to filtration.

Conventional filtration represents influent water conditions in summer months. Higher alum dose (~50-60 mg/L), anionic polymer (APAM), and powdered activated carbon (PAC) are added. PAC use is seasonal, often during spring runoff to treat taste and odours. Following pretreatment, water undergoes declining rate flocculation and sedimentation in a clarifier prior to filtration.

In general, the post-clarifier water in conventional filtration has lower turbidity and particle counts as compared to the direct filtration conditions. Process diagrams are shown below in Figure 5.1.

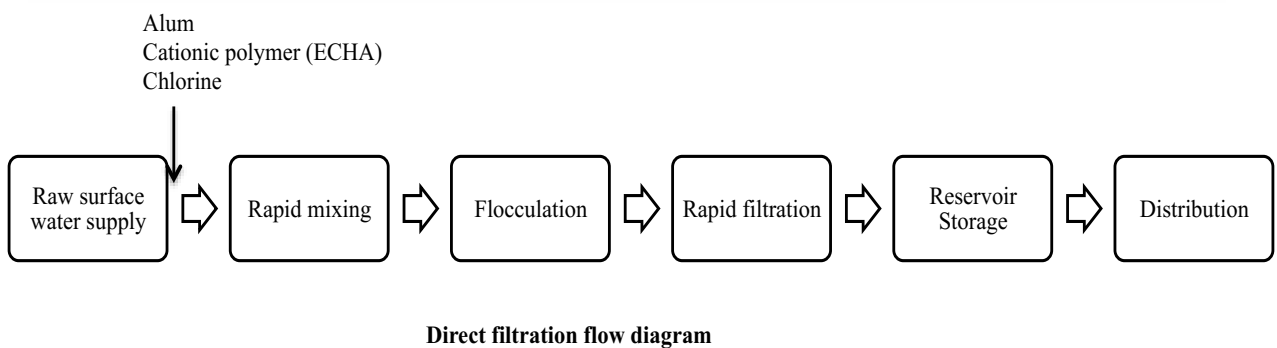
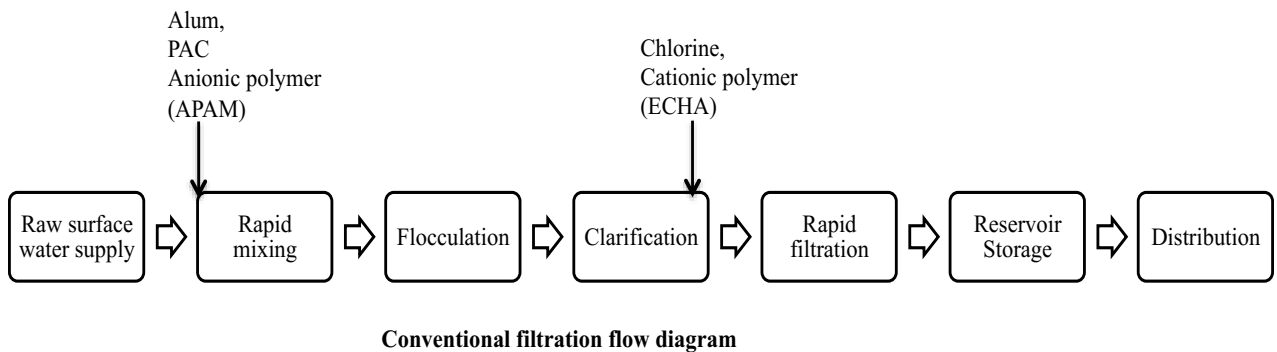


Figure 5.1 Flow diagrams for direct filtration and conventional filtration

The experiment was designed to compare the transport and removal of *Cryptosporidium* oocysts surrogates under direct filtration and conventional filtration conditions with high and low filter loading rates. Four pilot column experiments were conducted in duplicate, for a total of 8 columns runs. A separate control column with the same media specifications was run at the same time, and not dosed with surrogates. The conditions investigated are shown below in Table 5.1.

Table 5.1 Pilot scale experimental conditions

	Pilot Column Operation	Filter loading rate (m/hour)
Run 1	Direct Filtration	High (8.6)
Run 2	Direct Filtration	Low (5.7)
Run 3	Conventional Filtration	High (8.6)
Run 4	Conventional Filtration	Low (5.7)

5.1.2 Objectives

The overarching objective was to provide information that can be used to improve the overall operation of drinking water treatment, specifically with regards to *C. parvum* removal. The sampling points and the experimental design were selected to meet the more specific objectives listed below:

1. Investigate the impact of flow rate and influent water conditions on the log-removal of *Cryptosporidium* surrogates.
2. Develop a deposition profile and find deposition rate coefficients at different influent conditions and loading rates.
3. Correlate the measured influent and effluent parameters (particle counts, turbidity) with the removal of surrogates.

4. Conduct a mass balance of surrogates to understand the losses and recovery for the experimental system.

5.2 Methods and Experimental Design

5.2.1 Pilot column schematic and design

At the pilot plant, six identical 3-meter columns were constructed, one of which is pictured in Figure 5.2. The insides of the columns used for pilot trials were coated with sand to minimize wall effects and preferential flow regimes. This greatly enhanced filter performance and extended the length of filter runs such that they represented full-scale conditions more so than non-sand coated columns. The two sand-coated columns were filled with media layers of sand and anthracite. Seven sampling ports were set at equal depths and covered with a fine mesh to obtain depth profiles of surrogate removal.

Two sand-coated columns were used for surrogate dosing experiments. An additional column was filled with media at the same specifications as the experimental columns and used a control for the monitoring of pressure, flow, and effluent water quality.



Figure 5.2 Pilot column photo. The influent recycle line is not connected. Side sampling ports and media depths are shown.

Influent water originated from a common splitter box, which ensured constant influent conditions among all filter trains. On-line instrumentation was used to measure flow rate, turbidity, and particle counts in influent and effluent water. Conductivity, pH and free chlorine were measured by online instrumentation for the influent only. A separate batch tank for surrogates was connected to the appropriate column in each train. To minimize settling and maintain constant surrogate concentrations in the influent, a recycle line was used to pump influent water from slightly above the anthracite layer to the top of the water column. A sampling line was placed on the recycle line with a three-way splitter to measure influent concentration of surrogates. A filtration system schematic for this is shown below in Figure 5.3. Surrogates were seeded from a covered 1-L Wheaton bottle located beside each filter using a peristaltic pump. A mixing plate was used to ensure that surrogate suspensions were agitated throughout the entire seeding period.

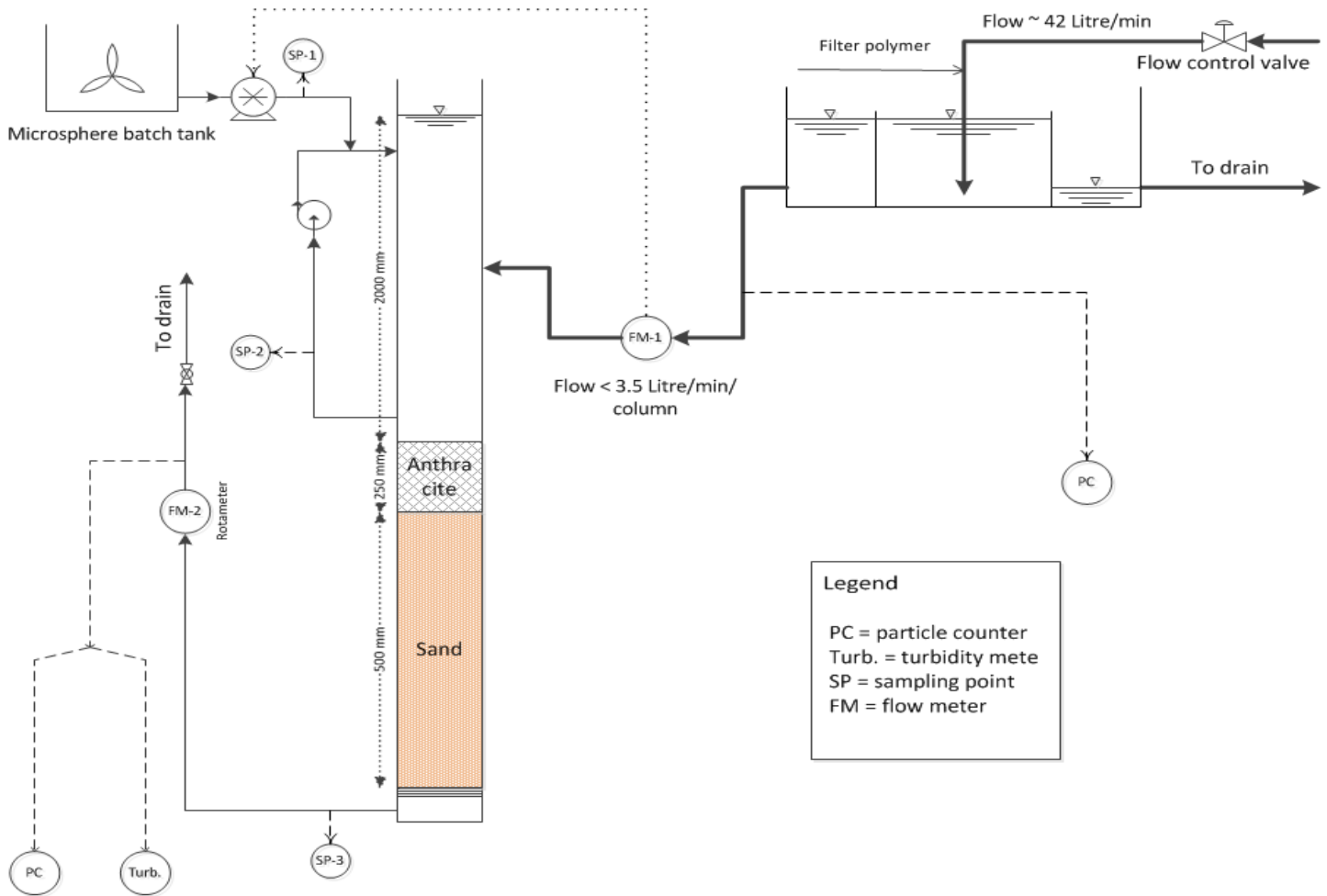


Figure 5.3 Pilot column schematic with influent recirculation loop and inline instrumentation locations. Media depths are approximate.

5.2.2 Influent water pretreatment

Influent water for pilot-scale experiments was taken from full-scale plant operation pre-filter water. For direct filtration, rapid mixing is done with a low dose of alum and filter polymer. An additional 1.5 mg/L of filter polymer is added to the already present 0.5 mg/L, to a total of 2.0 mg/L. Although higher than a typical polymer dose, this concentration was required based on preliminary pilot-scale filter experiments such that filter run times were similar to full-scale operation. Coagulation and flocculation

were achieved inline after the rapid mix, and there was no sedimentation. Particulate matter was removed directly by filtration.

Conventional filtration influent water has been chemically pre-treated with higher doses of alum, primary polymer, and filter polymer. It undergoes coagulation by rapid mixing, flocculation, and sedimentation prior to use at the pilot plant. A summary of pertinent chemical pretreatment and operational parameters is given in Table 5.2. Where applicable, values are provided for each filter loading rate condition.

Table 5.2 Chemical pretreatment and filter operation parameters

	Direct Filtration	Conventional Filtration
Chemical Pretreatment (mg/L)		
Alum dose	5.0	65.8 ¹ , 52.0 ²
Filter polymer	2.0	0.1
Primary polymer	--	0.27 - 0.30
PAC	--	19.8 ¹ , 6.0 ²
Free chlorine	1.8 ¹ , 0.54 ²	2.25 ¹ , 0.98 ²
Media Depth (mm)		
Anthracite		205
Sand		600
Effective Media size (mm)		
Anthracite		0.8 - 0.9
Sand		0.35
Media uniformity		
Anthracite		<1.5
Sand		<1.5

1 – Dose is specific to loading rate of 8.6 m/h

2 – Dose is specific to loading rate of 5.7 m/h

5.2.3 Seeding preparation and procedure

5.2.3.1 Seeding batch preparation and concentration determination

The seeding batch concentration required for each flow rate was determined in four steps: (1) Estimating total log removal, (2) calculating required microsphere dose,

(3) finding the dosing time for a given filtration rate, and (4) calculate the seeding batch concentration.

(1) Estimate total log removal

Note that these are conservative estimations that were used for calculation purposes. The actual observed log-removals are discussed later.

- Estimated removal by filtration = 2-log
- Estimated losses due to seeding recirculation, sampling loop tubing, tubing, etc = 2 - log
- Total estimated removal = 4-log

(2) Dose calculations

If the limit of quantification is 100 microspheres/L, then the desired concentration in the effluent is 100 microspheres/L. This was a conservative assumption based on preliminary flow cytometry and direct microscopy studies, which are more fully addressed in section 5.2.5.1. Influent dose calculation is as follows:

- Influent dose = limit of quantification x estimated log removal
- Influent dose = 100 microspheres/L x 10^4 = 10^6 microspheres/L

(3) Estimated dosing time for 8.6 m/h flow rate

In order to normalize between different flow rates, the volume of displaced water above filter media was used. For columns with internal diameter of 16.3 cm, a flow rate of 8.6 m/h corresponds to 3 L/min

- 1 volume of displaced water = 46 L
- Dosing time for 3 volumes of displaced water = $3 \times 46 \text{ L} / 3 \text{ Lmin}^{-1} = 46$ min

(4) Seeding batch pump calculation

The peristaltic pumps used have two rotor apparatuses that are both set at the same speed. The larger rotor is used for the recirculation loop (with 3 mm inner diameter tubing), and the smaller for the seeding batch (with 1.6 mm inner diameter tubing). To maintain a recirculation flow rate of 200 mL/min, the pump operates at 90% of the maximum speed. This results in a seeding loop flow rate of 22 mL/min.

$$\begin{aligned} \text{Seeding batch concentration} &= \frac{\text{required number of microspheres}}{\text{required seeding batch volume}} \\ &= \frac{(\text{influent concentration}) \times (\text{volume displaced water}) \times (\# \text{ of water displacements})}{(\text{time for 1 displacement of water}) \times (\# \text{ of water displacements}) \times (\text{pump flow rate})} \\ &= \frac{(10^6 \text{ microspheres/L}) \times (46 \text{ L per displacement}) \times (3 \text{ displacements})}{(15.3 \text{ min}) \times (46 \text{ L per displacement}) \times \left(22 \frac{\text{mL}}{\text{min}}\right) \times \left(\frac{1 \text{ L}}{1000 \text{ mL}}\right)} \end{aligned}$$

- Seeding batch concentration (for filtration flow rate of 8.6 m/h) = 1.36×10^8 microspheres/L.

For a filtration rate of 5.7 m/h, the recirculation rate and dose rate will remain the same (200mL/min and 22 mL/min, respectively). The number of microspheres will remain the same (1.38×10^6 microspheres/L), and a higher seeding batch volume of 1.5 L is required. This results in a seeding batch concentration of 9.2×10^7 microspheres/L.

5.2.3.2 Seeding procedure

Seeding suspensions were prepared the day prior to pilot runs with a 5 mg/mL solution of glycopolymer-modified microspheres. Seeding suspensions were covered in aluminum foil and kept at 4°C until use, with 1 mL of each seeding batch used for enumeration.

A constant microsphere concentration in the influent water was maintained with the previously mentioned recirculation loop. The seeding batch was introduced into the recirculation loop using a peristaltic pump and a three-way valve. The seeding batch was dosed directly into the top of the water column in each filter (see Figure 5.2). The surrogate suspension was placed on a magnetic stir plate and constantly agitated over the duration of dosing.

5.2.4 Sampling Plan

5.2.4.1 Filter run

Surrogates were dosed to a targeted influent concentration of approximately 10^6 /L following filter ripening (effluent turbidity was below 0.10 NTU). Since the actual volume of water above filter media does not change, but the loading does, the sampling

times were normalized to the number of displaced water columns above the filter media. By doing this, comparisons between loading rates were done more easily, and surrogate seeding procedure assumptions and calculations could be verified.

Samples were collected for the duration of 5 displaced water columns for direct filtration, and 6 displaced water columns for conventional filtration. Table 5.3 shows an example of the sampling regime that was performed for a loading rate of 8.6 m/h. The number of displaced water columns and sampling times are noted.

Table 5.3 Sampling overview for a pilot filter run at 8.6 m/h

	Sampling time (min from start of surrogate dosing)	Influent	Effluent	Side ports
Pre-surrogate dose (control)	--	X	X	--
Displaced water column 1	7.5	X	X	--
	15	X	X	X
Displaced water column 2	22.5	X	X	--
	30	X	X	X
Displaced water column 3	37.5	X	X	--
	45	X	X	X
Displaced water column 4	60	X	X	--
Displaced water column 5	75	X	X	X
Displaced water column 6*	90	X	X	--

* - Samples were only collected for conventional filtration runs

Influent samples and side port samples were collected in 50 mL sterile polypropylene centrifuge tubes. Effluent samples were collected in 1-L amber Wheaton bottles. To minimize the impact on flow rate and to reduce any preferential flow patterns within the filter media, the sampling flow rate was kept very low (approximately 25 mL/min). Only one side-port sample was collected at a time as to minimize the impact on flow rate. All sample bottles were pre-labeled and covered after being collected to reduce

the amount of fluorescent quenching. All sample bottles were stored at 4°C in a walk-in storage refrigerator at the University of Alberta.

5.2.4.2 Backwash

Pilot-column filter runs typically lasted 10-16 hours. The backwashing procedure involves a 10-minute air scour, followed by backwashing at rates of 14-18 L/min. The backwash sampling line is located on the backwash overflow. Samples were taken at times of 0, 1, 2, 3, 5, and 10 minutes during the backwash. It should be noted that 0-minute samples were not collected for direct filtration. After analysis of direct filtration backwash samples, the conventional filtration backwash sample plan was expanded to include 0-minute samples.

5.2.5 Analytical Methods

5.2.5.1 Microsphere Enumeration

Fluorescent polystyrene microspheres were analyzed and enumerated using an epifluorescence microscope (Axio Imager.M2, Carl Zeiss, Germany) with a wide-field fluorescence microscope excitation light source (X-ite 120Q, Lumen Dynamic, ON, Canada). The microscope was also equipped with a camera to visualize and record images. For enumeration purposes, a 10X objective lens was combined with the 10X eyepiece to provide a 100X total magnification. Sample aliquots were measured with a graduated cylinder, and then quantitatively deposited onto 0.45 µm nitrocellulose filters under vacuum. 25 image fields of each filter were taken. No background fluorescence was observed, as microspheres were bright enough that the camera needed to compensate for overexposure. This resulted in only the extremely bright microspheres being seen.

Particles on each image were counted using ImageJ. A program was written to convert jpg images into 8-bit binary format, background removed and then resulting microspheres counted. Manual spot checks were performed (accuracy of image counting software is approximately +/- 1 microspheres if the counts per image is over 25). Microsphere counts were normalized to the field of view area (0.61 mm), and then multiplied by the entire surface area of the filter to find the total microspheres for a given sample volume. Two different filter diameters were used, 25mm was used for low concentration samples, and 47mm was used for more concentrated samples.

This method was first validated on a bench scale with known microsphere concentrations of $10^3/L$ and $10^6/L$. The concentration was determined by manufacturer specifications and serial dilutions from the original manufacturer specified stock concentration of stock of $5 \times 10^8/mL$. Each test was performed in duplicate. Results indicate that at low concentrations ($10^3/L$) there is a slight overestimation. Results at higher concentrations are more reliable. Overall, this method is shown to be relatively simple and effective, although somewhat labour intensive.

Table 5.4 Ratio of microscopically determined microsphere counts to actual counts from manufacturer specifications. Filter seeding batch runs are given as the ratio of microscopically determined concentration to the targeted concentration for seeding.

			Ratio of microscopic count to actual count	Standard deviation (n=2)
Method validation	$10^3/L$	--	1.29	0.22
	$10^6/L$	--	1.06	0.26
Filter run seeding batch	Direct Filtration ¹	8.6 m/h	1.37	--
	Direct Filtration	5.7 m/h	0.91	0.03
	Conventional Filtration	8.6 m/h	0.87	0.04
	Conventional Filtration	5.7 m/h	1.25	0.07

1- Seeding batch for direct filtration at 8.6 m/h prepared as one batch and split into two vessels. The original batch was enumerated and as such no SD can be determined from the single sample.

Sample volumes and filter diameters for the pilot-scale experiments are shown below in

Table 5.5.

Table 5.5 Microsphere sample enumeration volumes and corresponding filter diameters for direct microscope counting

		Sample volume (mL)	Filter diameter (mm)
Influent	--	50	47
Effluent	--	200	25
Seeding batch	--	1	47
	<u>Depth (cm)</u>		
	10	50	47
Side Ports	20.5	50	47
	31	50	47
	42	50	25
	53	50	25
	64	50	25
	<u>Time (min)</u>		
	0	5	47
Backwash	1	10	47
	2	20	47
	3	50	47
	5	50	25
	10	50	25

5.2.5.2 Turbidity and particle counts

Online turbidity meters were used to measure influent and effluent turbidity and particle counts. In addition to total particle counts, particle counts in certain size ranges

were also measured. The ranges measured are: 2-3 μm , 3-5 μm , 5-7 μm , 7-10 μm , 10-15 μm , 15-20 μm , 2-20 μm , and >20 μm .

5.2.5.3 Free chlorine, pH, and conductivity

Free chlorine was measured as the combination of HOCl and OCl⁻ in the filter influent using a polarographic method. Similarly, pH and conductivity are both measured inline with pH and conductivity probes.

5.2.5.4 Major ions and metals

Ion chromatography (IC) was used to measure the major anions in solution. Influent cations and metals were filtered, diluted with nitric acid, and analyzed by ICP-MS (Elan 9000, Perkin Elmer, Waltham, MA).

5.2.5.5 Total organic carbon (TOC)

TOC provides an indication of the carbon molecules bound in organic compounds. Samples were taken from the pilot-column influent reservoir and measured at the University of Alberta. No microspheres were present in these samples.

4.3 Results and Discussion

5.3.1 Influent Water Conditions

Comparing between direct and conventional filtration influent, less particulate matter was observed in direct filtration. Flocculation and sedimentation removes much of the particulate matter in conventional filtration, which reduces turbidity and particle counts compared to direct filtration. TOC, conductivity and pH are similar for both influents. Ionic strength is approximated using a modification of the Russell prefactor developed by Zeng et al (2011), where conductivity ($\mu\text{S}/\text{cm}$) is related to ionic strength

(M) by a factor of 1.27×10^{-6} . This provides an indication of the total amount of dissolved ions in solution, which were very similar for both influent conditions. Moreover, concentrations of both monovalent and divalent species were similar. These results and a broader summary of conditions for direct and conventional filtration influent is are given in Table 5.6. Water quality parameters of pH, total particle counts, and conductivity values are averaged over the duration of pilot column experiments.

Table 5.6 Filter influent water quality parameters for direct and conventional filtration pilot experiments

		Direct Filtration	Conventional Filtration
Water quality			
	pH	7.9	7.0
	Turbidity (NTU)	3.53 ¹ , 3.27 ²	0.73 ¹ , 0.58 ²
	Total particle counts (no/mL)	22810	9700
	TOC (mg/L)	1.49	2.18
	Conductivity (µS/cm)	373	380
	Ionic strength (mM)	0.474	0.483
Metals (mg/L)			
	Boron	2.96	1.35
	Sodium	11.5	10.1
	Magnesium	17.2	14.8
	Aluminum	0.215	0.111
	Silicon	7.25	6.25
	Phosphorous	0.299	0.272
	Potassium	1.59	2.37
	Calcium	126	116
	Iron	0.933	0.872
	Strontium	0.884	0.801

1 – Turbidity for direct and conventional filter influent at a loading rate 8.6 m/h

2 – Turbidity for direct and conventional filter influent at a loading rate 5.7 m/h

In addition to increased particle counts and turbidity for direct filtration influent water, the chemical pretreatment also distinctly different, as previously shown in Table

5.2. The alum dose in direct filtration is known; conversely, much of the alum added in conventional filtration forms $\text{Al}(\text{OH})_3$ precipitate during flocculation and is removed during clarification. The concentration remaining in pre-filter water is not known. Similarly, PAC addition in conventional filtration occurs in the rapid mix before clarification. A portion of the PAC may be removed via sedimentation, but there is a portion left in the influent, which is subsequently removed by filtration. The actual concentration PAC in conventional filtration influent water is not known.

Zeta potential was measured directly from influent samples. The positive value for direct filtration is likely due to increased filter polymer dosage, as the polymer is ECHA (MagnaFloc LT7981) with a high charge density (Bolto and Gregory, 2007). The negative zeta potential for conventional filtration can be attributed to the presence of PAC, which has a negative electrophoretic mobility (Lau et al, 2005).

The main differences in the influent water conditions are summarized below in Table 5.7. This includes measured parameters from raw river water and chemical pretreatment.

Table 5.7 Water influent parameters with noteworthy differences between direct and conventional filtration influent.

	Direct Filtration	Conventional Filtration
Turbidity (NTU)	3.53 ¹ , 3.27 ²	0.73 ¹ , 0.58 ²
Total particle counts (no./mL)	22810	9700
Alum dose (mg/L)	5	65.8 ¹ , 52.0 ²
PAC dose (mg/L)	--	19.8 ¹ , 6.0 ²
Filter polymer (mg/L)	2	0.1
Zeta potential (mV)	3.9	-2.13 ¹ , -14.3 ²

1 – Dose is specific to loading rate of 8.6 m/h

2 – Dose is specific to loading rate of 5.7 m/h

5.3.2 Microsphere influent concentration and log-removal

5.3.2.1 Influent surrogate concentration

The influent concentration of glycopolymer-modified microsphere surrogates is shown below in Figure 5.4. Surrogates were dosed until three displaced water columns passed through the filter, at which time the seeding batch was empty, Water above the filter media was constantly recirculated over the duration of the experiment (during and after seeding). For both direct and conventional filtration, the data shown are comprised of duplicate runs from each of 5.7 and 8.6 m/h, for a total of 4 measurements for each data point. In each case, the influent concentration can be seen to increase sharply from the start of dosing until 1 displaced water column, and then a gradual increase until the end of the dosing period, at which time no new surrogates are seeded and the residual surrogate concentration decreases. For direct filtration, the measured influent concentration ranged from $5.8 \times 10^4/L$ to $1.2 \times 10^6/L$. Conventional filtration has a considerably lower influent concentration, which is due to a limited amount of the original glycopolymer-modified microsphere stock. This was done to hold the seeding batch concentration constant across both flow rate conditions under conventional filtration. The measured influent concentration range of conventional filtration was $6.1 \times 10^4/L$ to $6.4 \times 10^5/L$.

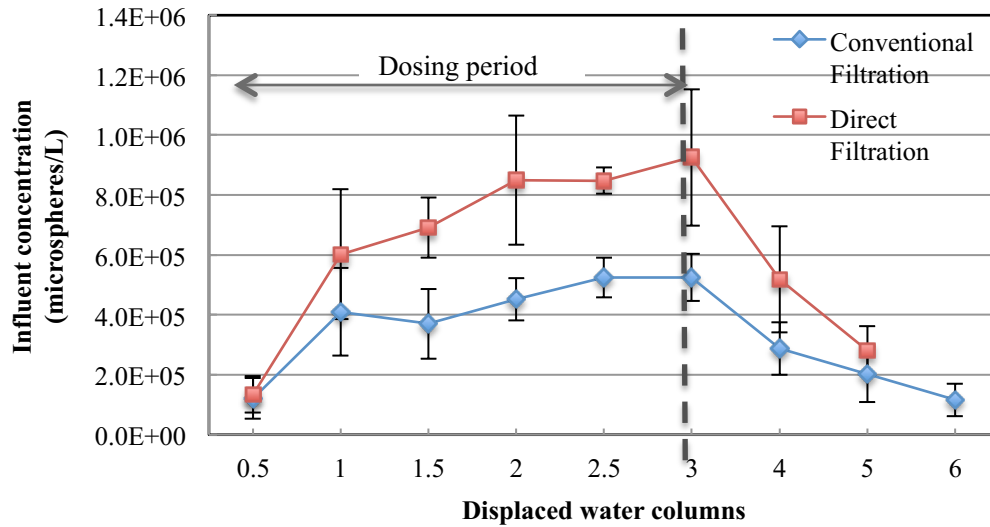


Figure 5.4 Pilot-scale influent surrogate concentrations. Average glycopolymer-modified microsphere concentration \pm SD (n=4). Data are normalized to the number displaced water columns for both direct filtration and conventional filtration. Surrogates were dosed from 0 to 3 displaced water columns..

The decrease in concentration from 3 displaced water columns confirms that the seeding plan was effective and proceeded as expected. The previously described dosing calculations resulted in the proper seeding time, as the influent concentration dropped after the dosing period was completed. It can be safely assumed that recirculation loop resulted in mixing of the influent water column (recirculation flow rate is approximately 200 mL/min). The shortest time for seeding the influent was 45 minutes, which is comparable to similar experiments (Emelko, 2003). Recirculation encouraged the slow decline of influent microspheres, which resulted in removal being observed over a longer period of time, as compared to a single slug dosage without recirculation.

A range of influent concentrations was observed, with almost an order of magnitude difference in direct filtration runs ($10^5 - 10^6/L$). Although somewhat limited, this enables additional understanding of the impact of initial concentration on log-removal. Bearing in mind that the influent concentration change was within one log unit,

the present investigation found that influent concentration did not have an appreciable impact on log-removals. The interpretation of this result is somewhat limited due to the high influent concentration and small amount of concentration change; which points to a need for further exploration. In particular, a study by Assavasilavasukul et al (2008) investigating the effect of *C. parvum* concentrations on the log-removal in conventional filtration demonstrated that oocyst removal is dependent on influent concentration, with higher removals observed for higher influent concentration. This was done over a much broader range on influent concentrations, and the log-removals they observed in the higher influent concentrations ($10^5 - 10^6/L$) generally agree with the results of this study (2-4 log, approximately). Trials with lower microsphere concentrations should be performed to more closely resemble naturally occurring oocysts concentrations where typical concentrations in surface waters are $<0.0001-3$ oocysts/L, and 0.34 oocysts/L in Alberta (Assavasilavasukul et al, 2008; LeChavelier et al, 1991).

5.3.2.2 Impact of flow rate on surrogate log-removal

The impact of flow rate on surrogate removal under direct filtration conditions can be seen in Figure 5.5a. The data shown are log-removals from the start of surrogate dosing, and measured over a range displaced water columns above filter media. Influent and effluent sample pairs were matched by the sampling time. Log-removals are similar for both 5.7 and 8.6 m/h flow rates, with log-removal at 5.7 m/h being slightly higher for the duration of the experiment. A paired-sample t-test was conducted to compare the log-removals at 5.7 and 8.6 m/h. There was a significant difference observed ($t(7) = -4.09$,

$p < 0.0046$); average log-removals (\pm SD) over the duration of the experiment are 1.73 ± 0.15 and 1.46 ± 0.18 for 5.7 and 8.6 m/h, respectively.

The impact of flow rate on surrogate log-removal under conventional filtration conditions can be seen in Figure 4.5b. Similarly to the results of direct filtration experiments, low flow rate resulted in higher log-removals compared to high flow rate. Between flow rates, the magnitude of log-removal was much larger at 5.7 m/h than 8.6 m/h, with average log-removals (\pm SD) over the duration of the experiment being 3.08 ± 0.39 and 2.06 ± 0.18 for 5.7 and 8.6 m/h, respectively. A paired-sample t-test was conducted to compare the log-removals, which showed a significant difference observed ($t(8) = -9.21, p < 0.0001$).

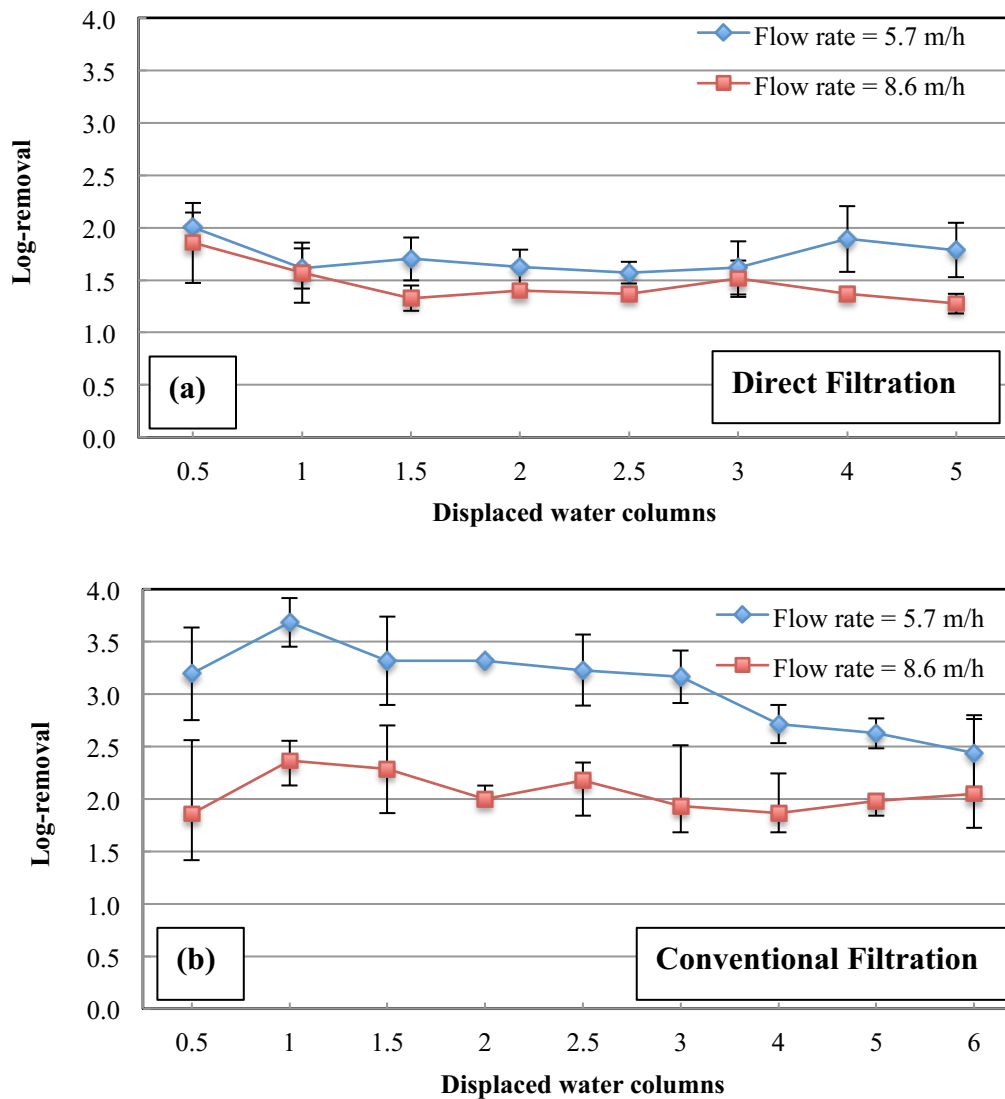


Figure 5.5 Average pilot scale log-removals \pm SD of glycopolymer-modified microspheres for replicate filter runs at 5.7 and 8.6 m/h for (a) direct filtration, and (b) conventional filtration

With both types of influent conditions, it can be seen that decreasing flow rate results in better log-removal. This is most likely due to physical influences in the filter. It has been demonstrated that a combination of physical factors govern particle removal in filters, which include media grain size, flow rate, surface characteristics of particles, specifically zeta potential and hydrophobicity (Dai and Hozalski, 2003).

Under direct filtration influent conditions, the chemical environment for both 8.6 and 5.7 m/h filter runs was consistent, with the main difference being slightly higher turbidity in the 8.6 m/h filter run, 3.53 NTU compared to 3.27 NTU for 5.7 m/h (see Table 5.6). Considering the similarity of chemical conditions, the higher log-removal for lower flow rate can be mainly attributed to lowered hydraulic shear, which agrees with the literature (Crittenden et al, 2005). From Figure 5.5a, increased hydraulic shear from higher flow rates results in slightly lower attachment, as there is less contact of the water streamline with filter media. Higher flow rates may also promote the detachment of particles (Emelko et al, 2005).

For conventional filtration, the difference between log-removals at high and low flow rates is much more noticeable. Similar to direct filtration, higher log-removal at lower flow rate can be attributed to increased transport of microspheres to the surface of filter media, and subsequent attachment. The noticeable difference between high and low flow rates could suggest that preferential flow pathways and hydraulic shearing are a more predominant mechanism in the attachment (and potentially detachment) of microspheres in conditions with lower turbidity and particle counts (i.e. conventional filtration compared to direct filtration).

Preferential flow pathways, and hydraulic shearing to a lesser extent, may not solely explain the difference seen in conventional filtration. Referring to Table 5.6, the chemical conditions of the influent are not entirely consistent. This was largely unavoidable as the filter trials were performed at the start of runoff with a very limited time frame. The largest difference in chemistry between the high and low flow rate conditions is the dose of PAC, with 19.8 mg/L PAC in high flow rate trial and 6.0 mg/L

PAC in the low flow rate trial (both doses occurred prior to flocculation and sedimentation). Although PAC is often used to treat water for odour and colour (Crittenden et al, 2005), in this experiment the size of PAC particles may have led to increased microsphere log-removal. PAC particles typically have a diameter of 24 μm (Lau et al, 2005). This is much larger than the microspheres (4.5 μm) or *Cryptosporidium* (3-6 μm), and as such the dominant removal mechanism is likely sedimentation or straining (Amirtharajah, 1988). For an influent with destabilized (or even partially destabilized) particles, the presence of PAC could lead to increased aggregation and attachment of microspheres to filter media by sedimentation.

5.3.2.3 Impact of influent conditions on surrogate log-removal

To offer a different comparison, the data from Figure 5.5 are switched, such that the influent conditions are compared at the same flow rate. For a flow rate of 8.6 m/h, Figure 5.6a shows a higher log-removal for conventional filtration (2.06 ± 0.18) compared to direct filtration (1.46 ± 0.18). This observed difference was statistically significant, $t(25) = -6.58$, $p < 0.0001$). A similar result is observed in Figure 5.6b, where conventional filtration log-removal (3.08 ± 0.39) is significantly higher than compared to direct filtration (1.73 ± 0.15) at a flow rate of 5.7 m/h ($t(25) = -11.54$, $p < 0.0001$).

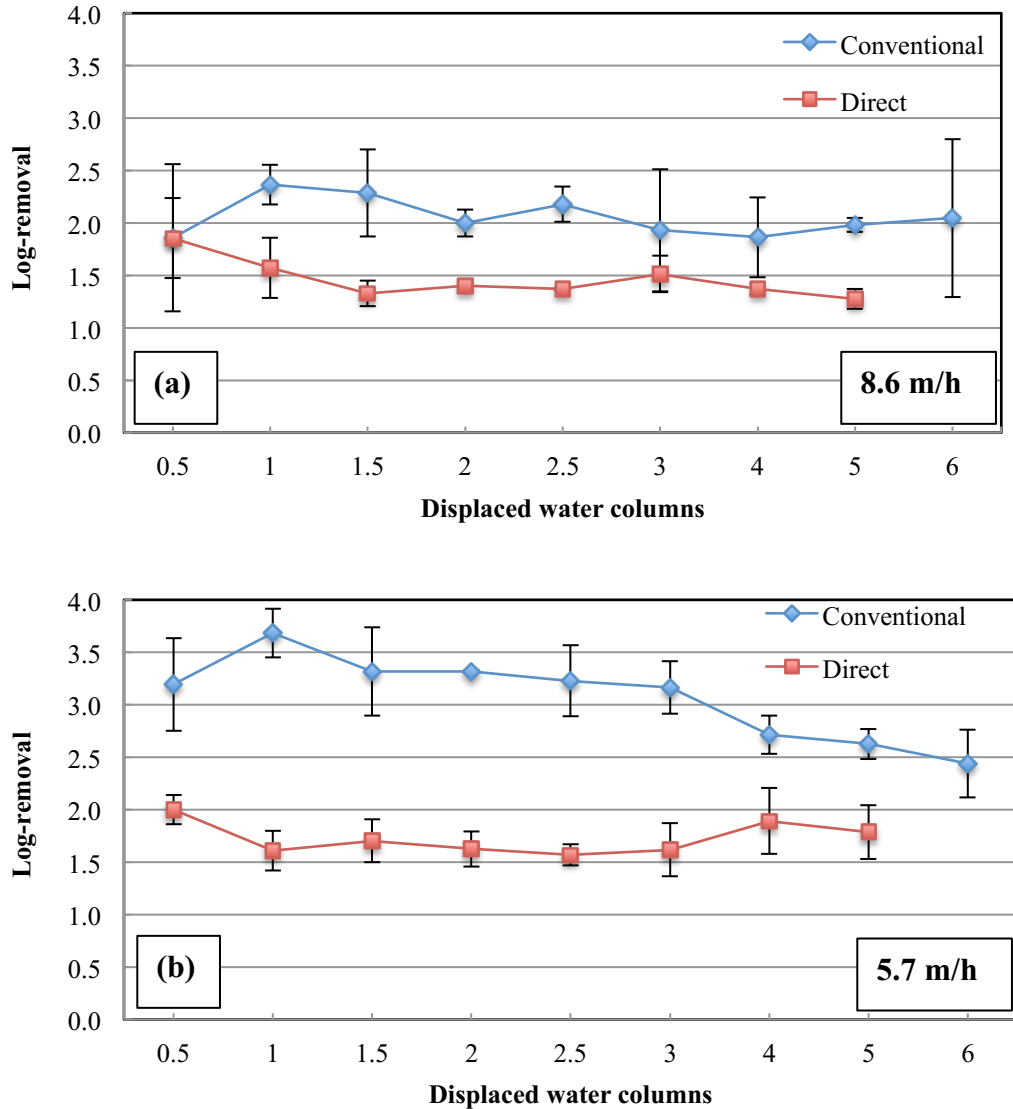


Figure 5.6 Average pilot scale log-removals \pm SD of glycopolymer-modified microspheres for replicate filter runs under conventional and direct filtration at (a) 8.6 m/h, and (b) 5.7 m/h

The impact of influent conditions on log-removal of microspheres seen in Figure 5.6 is noticeably greater than that of flow rate. The presence of increased turbidity and particle counts in the influent of direct filtration is likely the reason for this. In water filtration, removal is governed by diffusion and sedimentation removal mechanisms (Crittenden, 2005; Emelko, 2005). Although somewhat overpredictive in terms of oocyst removal (Tufenkji and Elimelech, 2005; Park et al, 2012), classical colloidal filtration

theory (CFT) is illustrative of the processes leading to deposition on media grains (Yao et al, 1971). In CFT, diffusion is the predominant removal mechanism for particles $<1 \mu\text{m}$, as particle size approaches the size of water molecules; and sedimentation is predominant for particles $5\text{-}25\mu\text{m}$, due to the force of gravity and the settling velocity (Amirtharajah, 1988). As a minimum transport efficiency is reached for $1\text{-}2\mu\text{m}$ particles, and both oocysts and microspheres are close to this size ($3\text{-}6\mu\text{m}$; Yao et al, 1971; Amirtharajah, 1988), the removal depends on the surface properties of these particles and their interaction with media grains (Emelko, 2005).

For this study, higher turbidity and particle counts in direct filtration may have led to the decreased removal compared to conventional filtration. The net forces between microspheres and particles/turbidity in the bulk solution need to be considered in the context of flow conditions and chemical pretreatment. The net forces in this case are considered to be the combination of the attractive van der Waals forces, repulsive electrostatic forces (or DLVO theory), steric interactions, and hydrophobic interactions (Crittenden et al, 2005).

Lower log-removal in direct filtration suggests that the net forces between microspheres and bulk solution particles/turbidity are more attractive than in conventional filtration. This may have resulted in reduced transport to filter media, lowered attachment, and the subsequently lower observed log-removals in direct filtration. This is also supported by the positive zeta potential measured in the influent (3.9 mV , Table 5.6), which is a function of chemical pretreatment, as zeta potential of glycopolymer-modified microspheres at pH 8 in a similar ionic strength is approximately -28mV . Although the reduced energy barrier can increase microsphere attachment to

media, this may have led to increased attachment to turbidity and particles in the bulk solution; additionally the occupation of favourable adhesion sites on filter media by colloidal particles may have reduced microsphere attachment. Furthermore, as there are substantially more suspended particles and turbidity in direct filtration influent, the magnitude of the interaction between microspheres and the bulk solution could lead to further decreased attachment. Additionally, the previously discussed impact of PAC in conventional treatment influent may also result in better log-removals.

Detachment of microspheres should also be considered. For a deposited microsphere to become detached from filter media, forces shearing the microsphere from the media must be greater than the adhesive forces holding the microsphere (Crittenden et al, 2005; Chung, 2012). The effect of this is most likely more prominent in the high flow rate condition of 8.6 m/h. The magnitude in the log-removal difference between direct and conventional filtration is lessened compared to 5.7 m/h.

To summarize the results from Figure 5.5 and Figure 5.6:

- Due to increased hydraulic shearing, higher flow rate has a negative impact on log-removal of surrogates.
- Conventional filtration resulted in higher log-removals than direct filtration at both high and low flow rate conditions, likely due to decreased turbidity and particle counts in the conventional filtration influent, and the presence of PAC.

- All trials conducted resulted in statistically significant differences in log-removal when comparing between flow rate conditions and filter influent conditions.

5.3.3 Statistical analysis of log-removal

5.3.3.1 ANOVA results

To more fully understand the impact of filter influent conditions and flow rate, the interaction between these factors, and the magnitude of the effects, a 2x2 ANOVA was performed on the log-removal response for flow rate and filter operation conditions. For the purposes of this analysis, influent conditions are considered as the combination of turbidity, particle counts, and chemical pretreatment, which are the parameters that differ most between conventional and direct filtration. In general, direct filtration has higher influent turbidity, higher particles counts, higher polymer dose, and no PAC compared to conventional filtration (refer to Table 5.2 and Table 5.3 for exact influent parameters). The factors and levels used in the 2x2 ANOVA are listed below in Table 5.8.

Table 5.8 Factor designations for two-way ANOVA

Factor	Levels	Values
Influent conditions	2	Direct filtration
		Conventional filtration
Flow rate	2	5.7 m/h
		8.6 m/h

The assumptions for a 2x2 ANOVA were met for independence and normality. Homoscedasticity was not met between two data sets (direct filtration at 8.6 m/h, and conventional filtration at 5.7 m/h). This may impact the interpretation of the interaction term in the ANOVA results. Data transformations (square-root and log transformations)

did not impact the significance of results, where all p-values were well below 0.05. Since it has been established that the ANOVA is quite robust to moderate departures from the assumption of equal variance (Elliot and Woodward, 2007), the non-transformed data are shown. Assumptions and data transformations are discussed further in Appendix A.

The 2x2 ANOVA results in Table 5.9 show that the main effects (influent condition and flow rate), and interaction have a statistically significant impact on log-removal of surrogates ($p < 0.0001$ for both main effects and interaction terms).

Table 5.9 ANOVA summary table

Source	df	SS	MS	F-Value	P-Value
Influent conditions	1	17.01	17.01	158.6	<0.0001
Flow rate	1	7.64	7.64	71.2	<0.0001
Interaction (influent conditions x flow rate)	1	2.07	2.07	19.3	<0.0001
Error	64	6.87	0.11		
Total	67	34.09			

5.3.3.2 Interaction plots

The interaction plots for influent condition and flow rate are shown in Figure 5.7. The results clearly demonstrate that influent conditions have the largest effect on log-removal. Conventional filtration resulted in higher log-removals at both flow rates, with the impact being more pronounced at 5.7 m/h. The impact of flow rate also be observed, where decreased flow rate results in higher log-removals for each type of influent condition, especially conventional filtration. Although the interaction of influent conditions and flow rate has a statistically significant impact on log-removal, it is not as clearly observed in the interaction plots as the main effects.

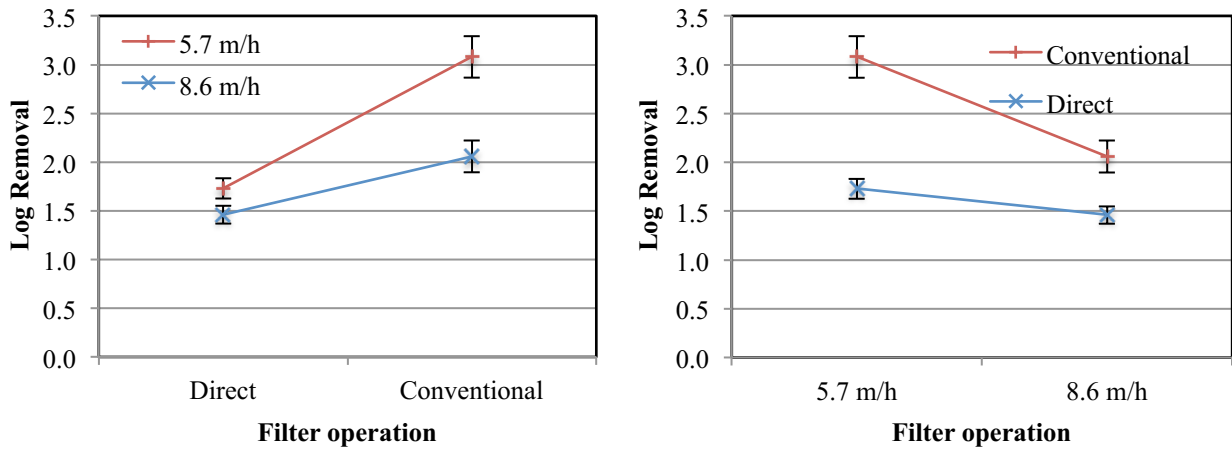


Figure 5.7 Interaction plots for log-removals \pm SE of pilot runs under different flow rates and filter operation conditions (n=16 for direct; n=18 for conventional)

5.3.3.3 Normal plot of effects

As the p-values for main effects and interaction were all well below 0.05, the value of effects was plotted against the n-score. Since interaction plots in Figure 5.7 provide a visual indication of the effects, a normal plot was constructed to provide an indicator of the magnitude for each main effect and interaction. Figure 5.8 shows negative effect of influent conditions and flow rate on log-removal. Results demonstrate that low turbidity and particle counts impact log-removal more so than the other conditions considered.

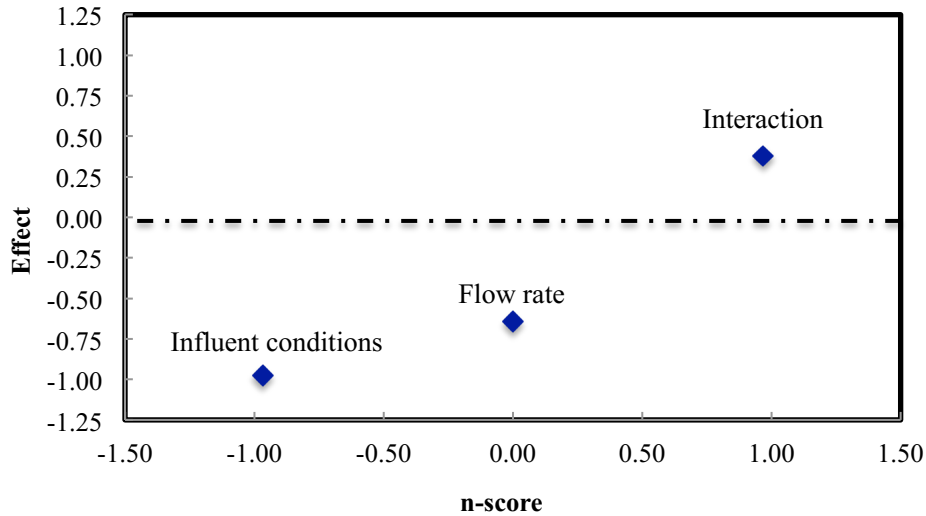


Figure 5.8 Normal plot of effect for log-removal.

5.3.4 Deposition profile and rate coefficients

5.3.4.1 Deposition profiles

Side ports were used to develop a deposition profile of removal in the granular media. No discernable trend was observed for the change of the depth profile over the course of the filter run, data from all samples were used to develop the deposition profiles. The data are shown in two ways, first as relative microsphere concentration with respect to filter media depth, shown in Figure 5.9. Displaying data in this way more clearly show the overall removal in the column, particularly in the anthracite layer.

The same data are then shown on a log-scale in Figure 5.10, where the impact of flow rate on the deposition profile and the depth filtration is more easily observed than without a log-scale in Figure 5.9. Microsphere concentrations are relative to the influent concentration, and denote the microspheres that are not attached the filter media and are still in the bulk solution.

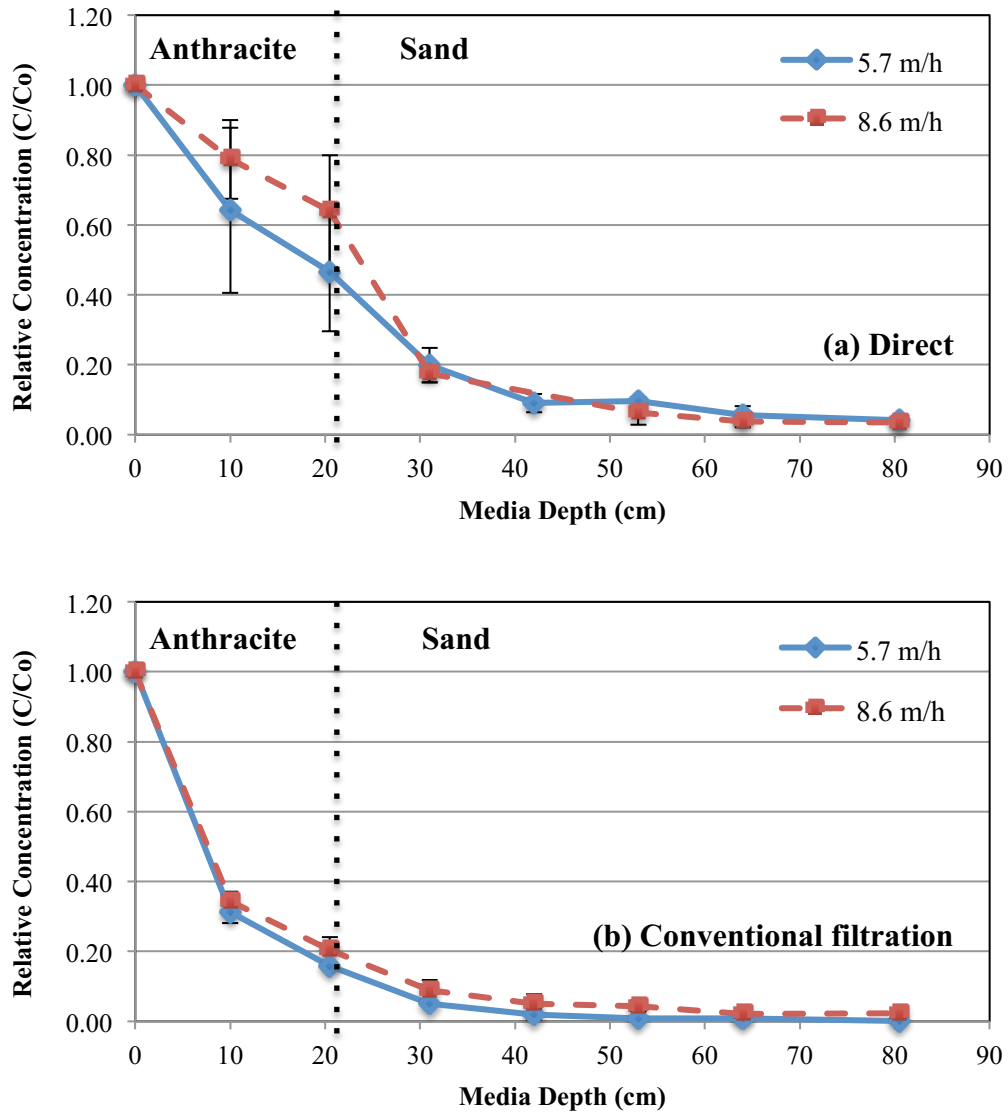


Figure 5.9. Deposition profile of microsphere removal in (a) direct filtration, and (b) conventional filtration under loading rate of 8.6 m/h, and 5.7 m/h. Relative concentration (\pm SD, $n=2$) of microspheres removed by filter media is plotted against media depth.

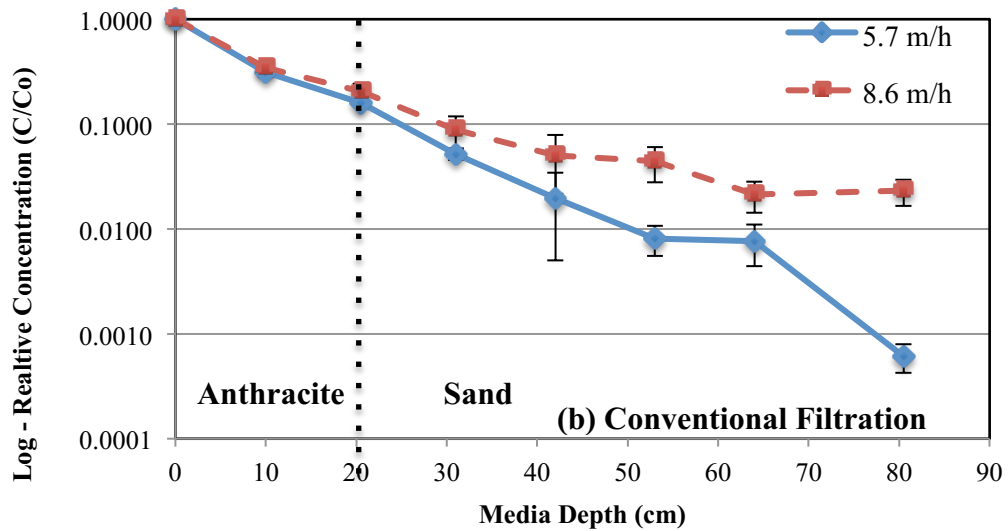
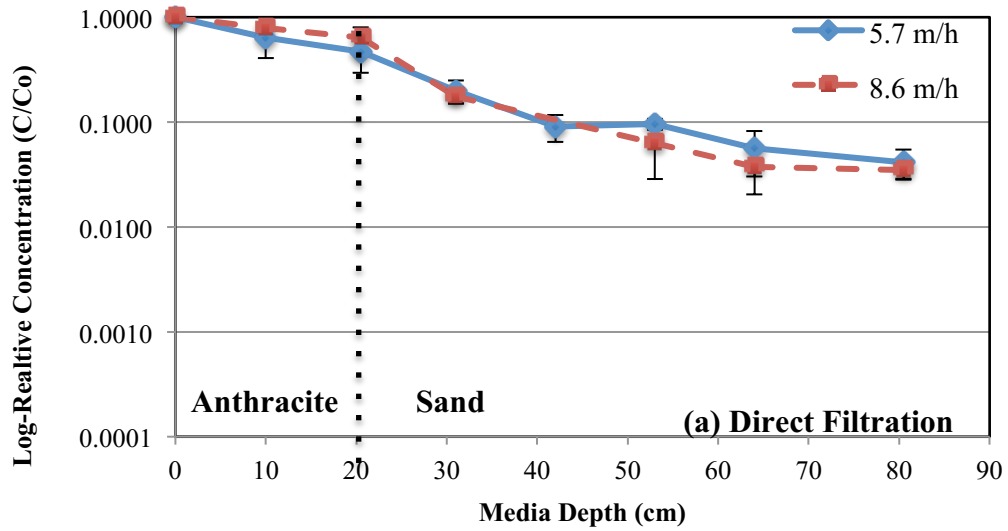


Figure 5.10 Log₁₀-scale Deposition profile of microsphere removal in (a) direct filtration, and (b) conventional filtration under loading rate of 8.6 m/h, and 5.7 m/h. Relative concentration (\pm SD, n=2) of microspheres removed by filter media is plotted against media depth.

For direct filtration, Figure 5.9a shows that approximately 50% of microspheres are removed in the anthracite layer, with the remaining ~99% removed in the sand. Conventional filtration achieves much better log-removal in the anthracite layer, shown in Figure 5.9b, with the approximately 80% of microspheres removed.

Displaying data on a log scale is more descriptive of the total log-removal and the depth removal, particularly in the sand layer where few microspheres remain in bulk solution. Figure 5.10 clearly shows better overall log-removal for conventional filtration. Notably, Figure 5.10b indicates that cleaner influent conditions in conventional filtration result in more depth filtration compared to direct filtration conditions, as more removal is achieved further into the filter column. Flow rate appears to have more of an impact for conventional filtration, where increased depth filtration is achieved with lower flow rate (Figure 5.10b). This difference between flow rate conditions was not observed for direct filtration (Figure 5.10a).

This suggests that influent conditions with higher turbidity and particle counts are less susceptible to perturbations of increased or decreased flow rate (i.e. direct filtration in Figure 5.10a). Conversely, while relatively cleaner influent conditions of conventional filtration lead to better attachment and log-removal, a higher hydraulic shear from a higher flow rate of 8.6 m/h may reduce microsphere transport to filter media, particularly deeper in the filter bed past 30 cm. Increased depth removal at lower flow rate of 5.7 m/h suggests that increased transport and removal occurs as compared to 8.6 m/h, with removal mechanisms likely due to sedimentation and interception (Figure 5.10b).

5.3.4.2 Deposition rate coefficients

To gain a more complete picture of the microsphere deposition in the filter, the deposition rate coefficients were calculated. A recent study by Park et al (2012) compared the applicable filtration models: Rajagopalan-Tien (RT), Tufenkji-Elimelech (TE), and Nelson-Ginn (NG). It was found that *C. parvum* oocyst attachment efficiency is more reliably estimated with the TE and NG models (Park et al, 2012).

Considering this, for the purposes of the present study, the TE correlation model is used. The values for attachment efficiency (α) and single collector efficiency (η) are given below in Table 5.10 for different depths in the filter. The calculated values of α for anthracite are given as 1.0, at depths of 10 and 20.5 cm. In the sand layer, it can be observed that attachment efficiency is generally higher for conventional filtration compared to direct filtration.

The single collector efficiency is generally higher for conventional filtration in both sand and anthracite layers. The difference is more pronounced for anthracite, where direct filtration η ranges 0.0038-0.0044 compared to 0.0108-0.0144 for conventional.

Table 5.10 T-E model attachment efficiency and single collector efficiency for direct and conventional filtration. Values presented as averages of both high and low flow rates.

Depth (cm)	Attachment efficiency (α)		Single collector efficiency (η)	
	Direct	Conventional	Direct	Conventional
0	--	--	--	--
10	<i>1.0*</i>	<i>1.0*</i>	<i>0.0044</i>	<i>0.0144</i>
20.5	<i>1.0*</i>	<i>1.0*</i>	<i>0.0038</i>	<i>0.0108</i>
31	0.69	1.0*	0.0022	0.0036
42	0.71	1.06	0.0024	0.0034
53	0.63	0.95	0.0020	0.0031
64	0.62	0.88	0.0020	0.0028
80.5	0.54	0.89	0.0017	0.0029

Note – italicized values refer to anthracite; non-italicized refer to sand

* - TE equation resulted in α greater than 1; attachment efficiency is assumed to be 1.0

The data suggest that anthracite is a slightly more efficient collector than sand, and has an appreciably better attachment efficiency, which implies that all the particles that contact each anthracite collector adhere to it. A few considerations can be made from this.

First, since anthracite is the top layer, influent conditions likely impact α and η values more so than sand. This is likely a function of lower turbidity and particles in the influent of conventional filtration influent, and also the presence of PAC, which has been previously discussed.

With sand being located below anthracite, it may be affected less by influent conditions since over 50% of microspheres are removed in the anthracite layer. This can also be seen by the magnitude in the change of α and η as the media changes from anthracite to sand after 20.5 cm.

The values of α and η can be used to find the deposition rate coefficients, which are plotted in Figure 5.11. This helps to explain how flow rate and influent conditions impact the rate at which microspheres are deposited on each media type. The results for both direct and conventional filtration are shown, with conventional filtration generally having higher deposition rates. General trends also show that flow rate has a positive impact on deposition rates, with 8.6 m/h flow rate resulting in higher rate coefficients than 5.7 m/h. There also appears to be a slight decreasing trend in deposition rate coefficients with increased column length.

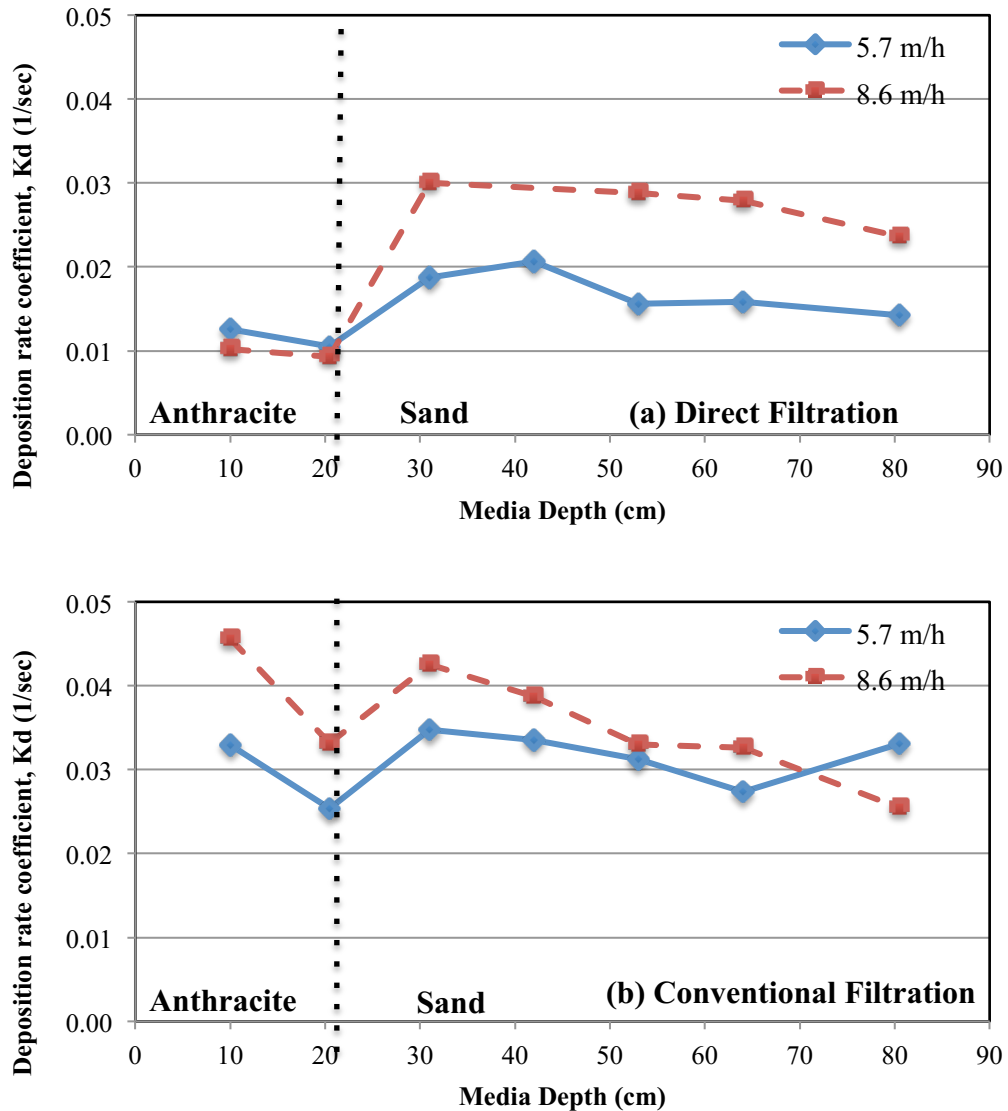


Figure 5.11 Deposition rate coefficients, K_d , as a function of filter media depth. Data shown are from (a) direct filtration, and (b) conventional filtration.

For direct filtration, the difference in K_d of sand and anthracite helps to explain the observed log-removals and the deposition profiles, where microspheres are removed more effectively by sand. More interesting are the results of conventional filtration, where a steep decline in K_d is observed for the anthracite layer, and increase again for sand. The likely cause for this is due to removal mechanisms that are fundamental to

filtration under “unfavourable” conditions, namely straining (Li et al, 2004). The influent solutions for both direct and conventional filtration can be considered “unfavourable”, as each had very low ionic strength (approximately 0.48mM for each, Table 5.6), which reduces the transport of particles to filter media grains. Evidence of this for conventional filtration is further demonstrated by the presence of PAC and possibly residual alum and APAM from the initial coagulation. This may have encouraged additional flocculation of particles and subsequent straining or sedimentation in the anthracite layer.

It is interesting to note that while “unfavourable” conditions may have existed in direct filtration (due to increased turbidity), this may not have resulted in straining in the anthracite layer. The similarity of K_d values deeper into the sand layer in direct and conventional filtration at both flow rate conditions suggests that straining is not a prevalent removal mechanism; interception and sedimentation are likely the prevalent mechanisms. Removal by diffusion due to Brownian motion is not expected to have any impact, as this mechanism mainly affects particles $<1\mu\text{m}$ (yao et al, 1971), and microspheres are much larger ($4.5\mu\text{m}$).

5.3.5 Correlation with turbidity and particle counts

As previously mentioned in Chapter 2, *Cryptosporidium* has traditionally been considered and modeled as a colloidal particle, and its removal has been correlated to particle removal measured as turbidity (Emelko et al, 2005). Several studies have shown that turbidity provides an approximate indicator of *Cryptosporidium* removal, and can often overestimate oocyst removal (Swertfeger et al, 1999; Emelko, 2001; Huck et al, 2001). Although a rigorous analysis is not performed in this study, a simple comparison

is illustrative of the variation that can exist when correlating oocysts surrogate removal to turbidity and particle counts.

A benefit of online instrumentation used is that the particle counters are able to separate counts per mL into different particle size ranges, which helps to narrow the particle count parameter into a range inclusive of naturally occurring oocysts size (3-6 μm). Figure 5.12 shows averaged log-removals over the experimental duration for glycopolymer-modified microspheres, particle counts, and turbidity. The values for particle counts and turbidity were obtained from a control pilot-column that was run at the same time with the same influent, but not seeded with microspheres.

The microsphere log-removal appears to line up with turbidity reasonably well for direct filtration at 5.7 m/h, but is also much greater for conventional filtration at 5.7 m/h. Particle counts have reasonably consistent log-removals, but are clearly higher than microsphere log-removal for every filter trial with the exception of conventional filtration at 5.7 m/h.

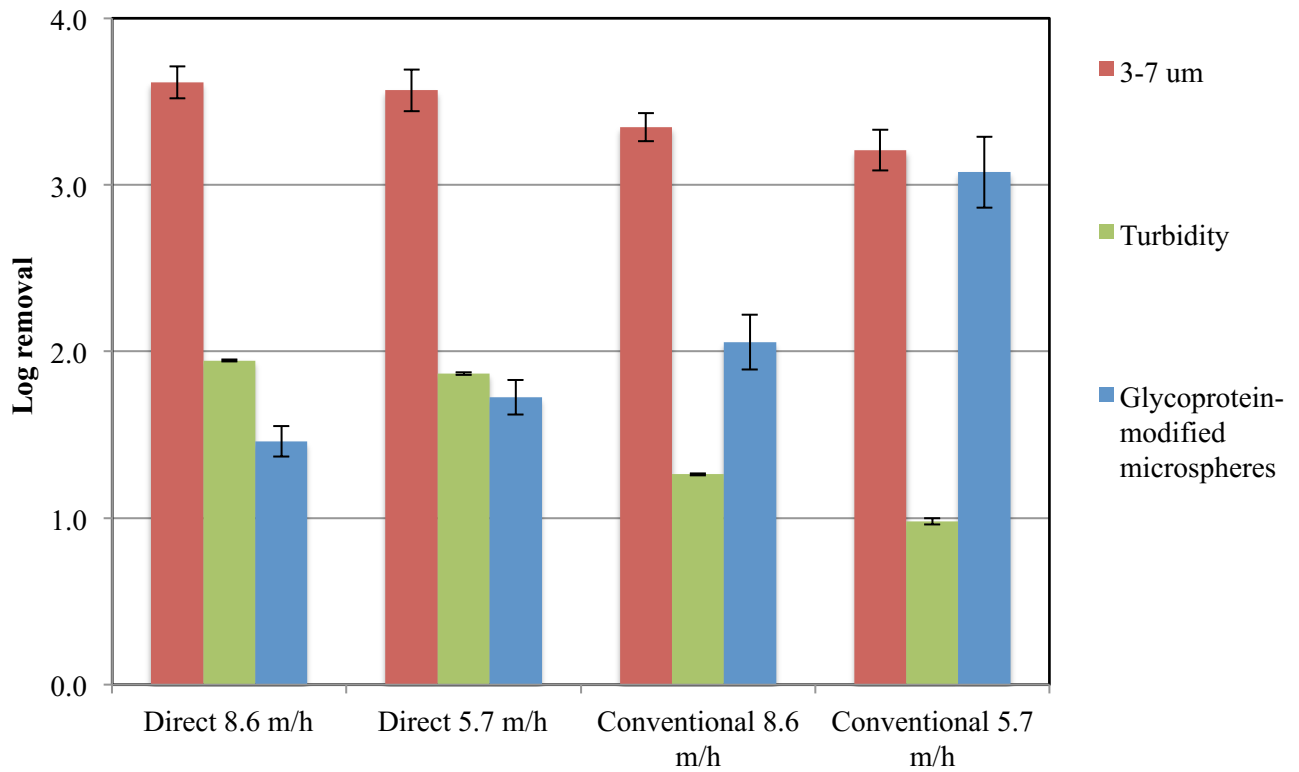


Figure 5.12 Average log removals \pm SD for glycopolymer-modified microspheres, turbidity, and 3-7 μ m particles. Results are shown for direct filtration at 5.7 and 8.6 m/h (n=16); and conventional filtration at 5.7 and 8.6 m/h (n=18).

This variability seen in Figure 5.12 suggests that influent turbidity, particle counts, and microsphere behave differently in filters and may not be subject to the same removal mechanisms. Notwithstanding a more comprehensive analysis of the data, this brief comparison agrees with previous findings that suggest turbidity and particle count removal may not be suitable surrogates for quantifying *Cryptosporidium* oocyst removal (LeChavelier et al, 1991; Patania et al, 1995).

5.3.6 Backwash microsphere concentrations

Backwashing occurred after the filter run reached particle breakthrough. A 10-minute air scour was followed by backwashing. The microsphere concentrations in backwash samples strongly follow a log-linear trend over time, seen in Figure 5.13 and Figure 5.14. This shows the bulk of microspheres accumulated in filter media are detached and removed by backwash in the first 3 minutes of backwashing. Visually, a slug of accumulated turbidity and PAC (in the case of conventional filtration) was noted during the first minute of backwash.

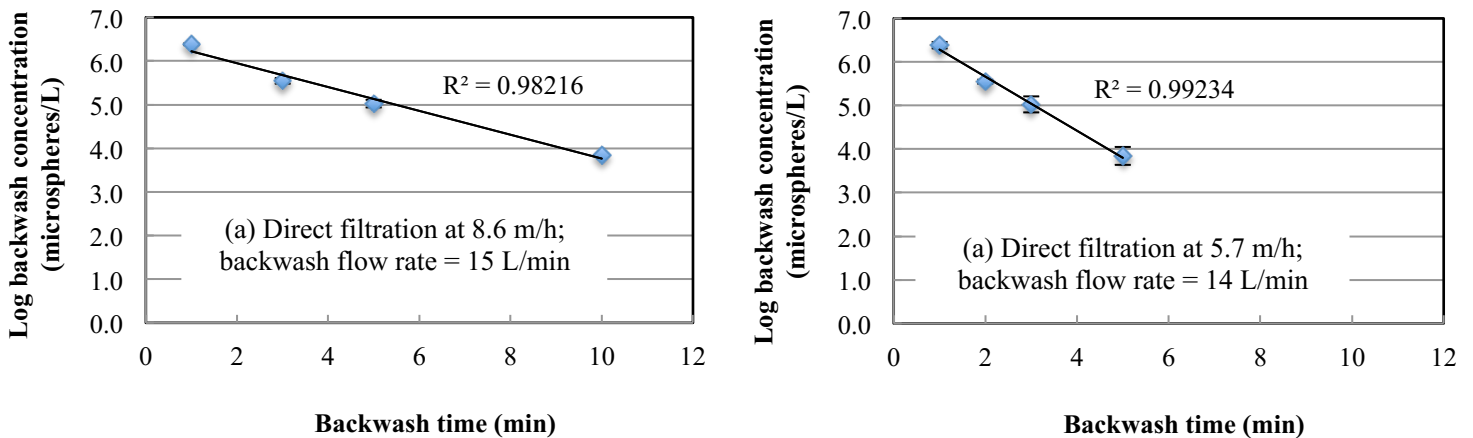


Figure 5.13 Log transformed backwash concentrations (\pm SD, $n=2$) for direct filtration pilot runs with filter loading rates of (a) 8.6 m/h, and (b) 5.7 m/h. Backwash flow rates and R^2 values for log-linear correlations are shown.

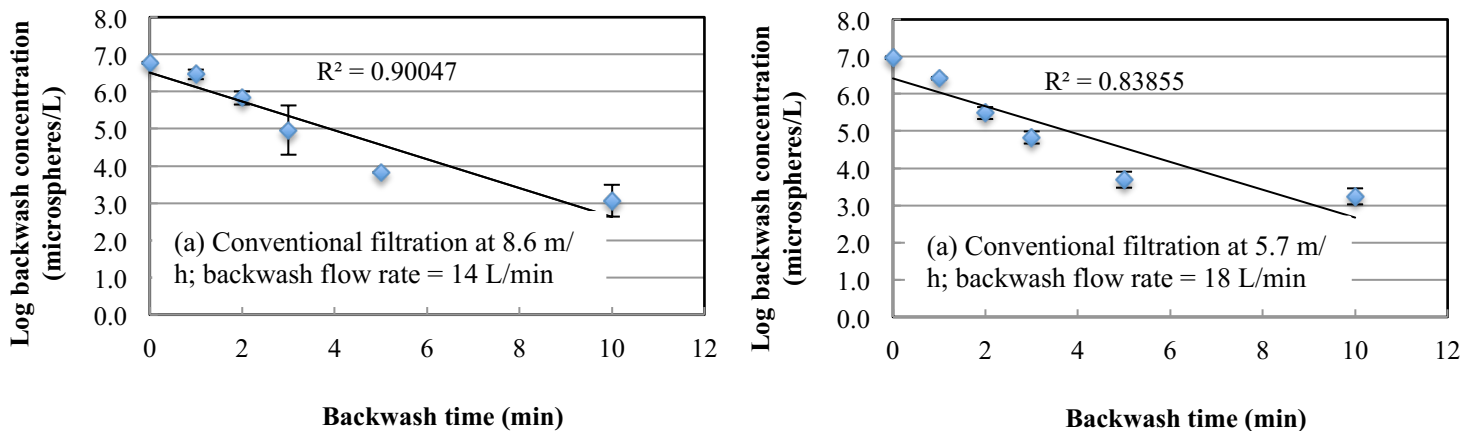


Figure 5.14 Log transformed backwash concentrations (\pm SD, $n=2$) for conventional filtration pilot runs with filter loading rates of (a) 8.6 m/h, and (b) 5.7 m/h. Backwash flow rates and R^2 values for log-linear correlations are shown.

The log-linear decrease in microsphere concentration is not unusual for what is expected from backwashing, which has been previously confirmed by evidence in the literature (Brouckaert, 2004). The backwash curves can be used to generate microsphere numbers accumulate in the filter media, and the backwash recovery. This is explored below in Section 5.3.7.

5.3.7 Mass balance, losses, and recovery

Mass balance for microspheres is an appropriate method for determining the losses and recovery of the experimental system used. The two points where this is applicable are (a) the losses incurred from the seeding solution to the influent directly above filter media, and (b) the microsphere recovery in backwashing. The total numbers of microspheres were calculated for each column at five different stages: seeding batch, influent, accumulated in filter media, effluent, and backwash. The losses and recovery were determined for each column (8 in total), and averaged for each experimental condition.

Microsphere counts were determined at five different points, using microsphere enumerations and Riemann sums for influent, effluent, and backwash.

1. Seeding batch microspheres
2. Influent microspheres
3. Effluent microspheres
4. Accumulated in filter media
5. Backwash microspheres

A more detailed description of methods is given in Appendix B. The seeding losses and backwash recovery are summarized below in Table 5.11, with percent loss and recovery are calculated as:

- Percent loss from seeding batch to influent = $\left(1 - \frac{\text{Influent}}{\text{Seeding Batch}}\right) \times 100$
- The accumulated microspheres recovered in the backwash = $\frac{\text{Backwash}}{\text{Accumulated}} \times 100$

Table 5.11 Percent loss (\pm SD, n=2) from seeding and backwash recovery for all experimental conditions.

	Direct Filtration	Conventional Filtration
Losses from seeding to influent	18.1 \pm 15	15.5 \pm 8
Backwash recovery	85.6 \pm 19	87.9 \pm 13

The results of the mass balance indicate losses that were better than expected between the seeding batch the influent. A 50% loss was expected as a conservative estimate when designing the experiment. This information is useful moving forward, as a more accurate estimate of losses may help to reduce the initial cost of seeding either microspheres, or other biological organisms and surrogates.

Backwash recovery is quite high, but is reasonable considering the non-biological nature of target particles. Other studies have found drinking water backwash recovery efficiencies of 80-87% for non-biological constituents (Thirunavukkarasu et al, 2003). It should be considered that the sample collection and enumeration process is much simpler compared to viable *C. parvum* oocysts. Previous studies report only 9.1% analytical recovery for backwash water samples seeded with viable oocysts (Di Giovanni et al, 1999). Backwash samples can typically be difficult to analyze due to the debris and floc

present (Karanis et al, 1996). Due to this difficulty in analysis, *Cryptosporidium* presence is not often reported concentrations or amounts, but simply as a percent of backwash samples with detected oocysts. For example, Karanis et al (1996) detected one or both of *Giardia* and *C. parvum* in 92% of backwash water samples. The evident implication of this is that non-biological surrogates, like microspheres, may only help to provide an indication of the quantity of oocysts in backwash. They do not provide any information regarding the viability and infectivity of biological pathogens in backwash discharge, such as *C. parvum*. This is an area that could deserve some additional consideration, possibly with the use of biological surrogates.

5.4 Summary and conclusions from pilot-scale experiments

The specific objectives of this study were achieved, as the removal of *Cryptosporidium* surrogates (glycopolymer-modified microspheres) was investigated, deposition profiles were developed, removal of microspheres was compared to traditional oocysts removal indicators, and the losses and recovery were analyzed.

To summarize, a brief review of main results are given in section 5.4.1. Conclusions and recommendations are given in section 5.4.2.

5.4.1 Summary of main results

- Main differences of influent conditions were particle counts and turbidity, which were higher in direct filtration compared to conventional. Conventional filtration influent also had PAC, which likely had a considerable impact on the results.

- While the range of influent concentrations were generally quite high (10^5 - 10^6 /L), the difference in concentration did not have an appreciable impact on log-removals.
- Conventional filtration influent conditions resulted in higher log removals of glycopolymer-modified microspheres compared to direct filtration at both high and low flow rate conditions. This is likely due to decreased turbidity and particle counts in the influent, and the presence of PAC.
- Flow rate had a negative impact on log-removal. This is likely a result of reduced transport of microspheres to media grain surfaces at higher flow rates.
- The impact of flow rate was more evident for conventional filtration; as higher turbidity and particle counts in direct filtration may have contributed to “unfavourable” conditions where transport of microspheres to media grain surfaces was reduced and adhesion sites were occupied by colloidal particles.
- Statistically significant differences were observed for main effects of flow rate and influent conditions, and also for the interaction of these main effects (ANOVA with 95% confidence limit).
- Deposition profiles and rate coefficients suggest that predominant removal mechanisms of sedimentation and interception are enhanced by the presence of PAC in “cleaner” influent conditions (i.e. conventional filtration). Sedimentation and interception are more prevalent with depth filtration, as evidenced by declined deposition rate coefficients.
- A cursory analysis of microsphere log-removal correlations with turbidity and particle counts showed substantial variability. This supports previously

established research that turbidity and particle counts may not be effective surrogates for *Cryptosporidium* removal.

- Backwash concentrations were typical of what is expected from drinking water filtration, with a strong log-linear correlation of microsphere concentration to backwash time.
- Mass balances demonstrate a better than expected loss from seeding (15-18% loss). Backwash recovery is also quite good (approximately 86%), but future consideration should be given to biological surrogates to understand infectivity in backwash waste streams.

5.5 References

- Abudalo, R. A., Bogatsu, Y. G., Ryan, J. N., Harvey, R. W., Metge, D. W., and Elimelech, M. Effect of ferric oxyhydroxide grain coatings on the transport of bacteriophage PRD1 and *Cryptosporidium parvum* oocysts in saturated porous media. *Environmental Science and Technology*, **2005** 39(17), 6412-6419.
- Amirtharajah, A. Some theoretical and conceptual views of filtration *Journal American Water Works Association*, **1988**. 36-46.
- Assavasilavasukul, P., Lau, B. L., Harrington, G. W., Hoffman, R. M., and M.A. Borchardt. Effect of pathogen concentrations on removal of *Cryptosporidium* and *Giardia* by conventional drinking water treatment. *Water Research*, 42(10), **2008**. 2678-2690.

- Betancourt, W. Q., and Rose, J. B. Drinking water treatment processes for removal of *Cryptosporidium* and *Giardia*. *Veterinary Parasitology*, **2004**. 126(1), 219-234.
- Bolto, B., and Gregory, J. Organic polyelectrolytes in water treatment. *Water Research*. **2007**, 41(11), 2301-2324
- Brouckaert, B.M. Hydrodynamic detachment of deposited particles in fluidized bed filter backwashing. PhD Dissertation. Georgia Institute of Technology. **2004**. pp.38-40
- Chung, J. Development of fluorescently labelled *Cryptosporidium* oocysts surrogates to test the efficacy of sand filtration processes. PhD Dissertation, University of New South Wales, Australia **2012**
- Crittenden, J. C., Trussell, R. R., Hand, D. W., Howe, K. J., and Tchobanoglous, G. *MWH Water Treatment: Principles and Design: Principles and Design 2nd edition*. John Wiley & Sons, Danvers, MA. **2005**. pp 870-873.
- Dai, X., and Hozalski, R. M. Evaluation of microspheres as surrogates for *Cryptosporidium parvum* oocysts in filtration experiments. *Environmental Science and Technology*. **2003**, 37(5), 1037-1042.
- Di Giovanni, G. D., Hashemi, F. H., Shaw, N. J., Abrams, F. A., LeChevallier, M. W., and Abbaszadegan, M. Detection of infectious *Cryptosporidium parvum* oocysts in surface and filter backwash water samples by immunomagnetic separation and integrated cell culture-PCR. *Applied and Environmental Microbiology*, **1999**. 65(8), 3427-3432.
- Elliot, A.C., and W.A Woodward. *Statistical Analysis Quick Reference Guide*. Sage Publications, Inc. Thousand Oaks, CA. **2007**. pp 167.

- Emelko, M. B. Removal of *Cryptosporidium parvum* by granular media filtration, PhD Dissertation. The University of Waterloo. Waterloo, Canada. **2001**
- Emelko, M. B. Removal of viable and inactivated *Cryptosporidium* by dual-and tri-media filtration. *Water Research*. **2003**, 37(12), 2998-3008.
- Emelko, M. B., Huck, P. M., and Coffey, B. M. A review of *Cryptosporidium* removal by granular media filtration. *American Water Works Association*, **2005**, 97(12), 101.
- Gitis, V. Rapid sand filtration of *Cryptosporidium parvum*: effects of media depth and coagulation. *Water Science & Technology: Water Supply*. **2008**. 8(2): 129-134.
- Huck, P. M., B. M. Coffey, M. B. Emelko, and C. R. O'Melia. The importance of coagulation for the removal of *Cryptosporidium* and surrogates by filtration. *Chemical Water and Wastewater Treatment VI*, Springer Berlin Heidelberg, **2000**. pp. 191-200.
- Karanis, P., Schoenen, D., and Seitz, H. M. *Giardia* and *Cryptosporidium* in backwash water from rapid sand filters used for drinking water production. *Zentralblatt für Bakteriologie*, **1996**. 284(1), 107-114.
- Lau, B. L., Harrington, G. W., Anderson, M. A., and Tejedor, I. Physicochemical aspects of *Cryptosporidium* surrogate removal in carbon block filtration. *American Water Works Association*, **2005**. 92-101.
- LeChevallier, M. W., Norton, W. D., and Lee, R. G. Occurrence of *Giardia* and *Cryptosporidium* spp. in surface water supplies. *Applied and Environmental Microbiology*, **1991**. 57(9), 2610-2616.
- Li, X., Scheibe, T. D., and Johnson, W. P. Apparent decreases in colloid deposition rate coefficients with distance of transport under unfavorable deposition conditions: A

- general phenomenon. *Environmental Science and Technology*, **2004**. 38(21), 5616-5625.
- Nelson, K. E., and Ginn, T. R. New collector efficiency equation for colloid filtration in both natural and engineered flow conditions. *Water Resources Research*, **2011**. 47(5).
- Park, Y., Atwill, E. R., Hou, L., Packman, A. I., and Harter, T. Deposition of *Cryptosporidium parvum* oocysts in porous media: a synthesis of attachment efficiencies measured under varying environmental conditions. *Environmental Science and Technology*, **2012**. 46(17), 9491-9500.
- Patania, N. L. Jacangelo, J. G., Cummings, L., Wilczak, A., Riley, K. and Oppenheimer, J. Optimization of filtration for cyst removal. *AWWA Research Foundation and American Water Works Association*, Denver **1995**
- Rajagopalan, R., and C. Tien. Trajectory analysis of deep-bed filtration with sphere-in-cell porous-media model. *AIChE*. **1976**. 22(3) 523-533
- Swertfeger, J., Metz, D. H., DeMarco, J., Braghetta, A., and Jacangelo, J. G. Effect of filter media on cyst and oocyst removal. *American Water Works Association Journal*, **1999**, 91(9), 90-100.
- Thirunavukkarasu, O. S., Viraraghavan, T., and Subramanian, K. S. Arsenic removal from drinking water using iron oxide-coated sand. *Water, Air, and Soil Pollution*, **2003**. 142(1-4), 95-111.
- Tufenkji, N., and M. Elimelech. Correlation equation for predicting single-collector efficiency in physicochemical filtration in saturated porous media. *Environmental Science and Technology*, **2004**. 38(2), 529-536.

Yao, K.M., Habibian, M.T., and O'Melia, C.R. Water and Waste Water Filtration: Concepts and Applications. *Environmental Science and Technology*. **1971**, 5(11), 1105-1112

Zeng, Y., Grandner, S., Oliveira, C. L., Thünemann, A. F., Paris, O., Pedersen, J. S., and von Klitzing, R. Effect of particle size and Debye length on order parameters of colloidal silica suspensions under confinement. *Soft Matter*,**2011**. 7(22), 10899-10909.

Chapter 6. Conclusions and future work

6.1 Major conclusions

Considering that the overarching objective of this study is to provide information that can be used to improve the overall operation of drinking water treatment, specifically with regards to *Cryptosporidium*, several conclusions can be drawn.

1. A Glycopolymers-modified microspheres were shown to have surface properties similar to viable *Cryptosporidium*, and cost significantly less to produce compared to AGP-modified microspheres. This type of microsphere modification was used as a *Cryptosporidium* surrogate for further bench- and pilot-scale filtration experiments.
2. Based on charge reversal and the interaction with SiO₂ surfaces, ECHA is a more effective cationic polyelectrolyte than pDADMAC as a filtration aid.
3. Based on pilot-scale filter experiments, influent conditions are very important in the removal of *Cryptosporidium* surrogates. This was clearly demonstrated by the differences in conventional and direct filtration, which was very much tied to pretreatment and removal mechanisms.
4. Deepening the filter bed, specifically the sand layer could increase the amount of depth removal for both direct and conventional filtration.
5. One option for optimization without deepening the filter bed is by increasing the enhancing the sedimentation and interception in the anthracite layer. This could be accomplished with higher doses of alum

and polymer, or possibly using a polymer that encourages particle bridging and enmeshment in during the rapid mix.

6.2 Future work

The present study identified an appropriate, cost effective *Cryptosporidium* surrogate; and the transport and removal of this surrogate in pilot-scale filter was investigated. With this as a starting point, there are several areas where future research is beneficial.

1. Comparisons using pilot-scale filtration experiments should be made of viable *Cryptosporidium* oocysts and glycopolymer-modified microspheres. It is necessary to understand if the proposed surrogates behave similarly to *Cryptosporidium* in filters, and if they are impacted similarly (or proportionally) by different filter operational parameters (chemical pretreatment doses, loading rate, filter media specifications, e.t.c.).
2. Further study regarding yeast as a potential surrogate will be useful, as biological surrogates may prove to be more representative, and perhaps quantitative, indicators of *Cryptosporidium* oocysts.
3. The effect of water temperature is an area that is of particular relevance in Canada, and the impact of temperature on chemical pretreatment and *Cryptosporidium* removal is not well understood. Pilot-scale experiments should be performed during winter and summer months to more fully understand temperature impacts.
4. More effective bench-scale methods for modeling the transport and removal of *Cryptosporidium* oocysts may be a good compliment to this

study, particularly QCM-D. This may involve experimental designs that represent the complexity of naturally occurring surface water, as opposed to the “clean” systems used in this study.

References

- Abudalo, R. A., Ryan, J. N., Harvey, R. W., Metge, D. W., & Landkamer, L. Influence of organic matter on the transport of *Cryptosporidium parvum* oocysts in a ferric oxyhydroxide-coated quartz sand saturated porous medium. *Water Research*, **2010**. 44(4), 1104-1113.
- Amirtharajah, A. Some theoretical and conceptual views of filtration. *American Water Works Association*, **1988**. 36-46.
- Arora, H., Giovanni, G.D., and Lechevallier, M. Spent filter backwash contaminants and treatment strategies. *American Water Works Association*. **2001**, 93(5), 100-112
- Assavasilavasukul, P., Lau, B. L., Harrington, G. W., Hoffman, R. M., and M.A. Borchardt. Effect of pathogen concentrations on removal of *Cryptosporidium* and *Giardia* by conventional drinking water treatment. *Water Research*, 42(10), **2008**. 2678-2690.
- Bangs Laboratories Inc. TechNote 205 – Covalent Coupling; Fishers, IN, Rev #5. **2013**. Vol KT/MM-03/2002, p. 6
- Behrens, S. H., Christl, D. I., Emmerzael, R., Schurtenberger, P., and Borkovec, M. Charging and aggregation properties of carboxyl latex particles: Experiments versus DLVO theory. *Langmuir*, **2000** 16(6), 2566-2575.
- Bergman, L.W. Chapter 2: Growth and Maintenance of Yeast. *In: Two-Hybrid Systems Methods and Protocols* (ed. MacDonald, P.N.) **2001**, 9-10
- Betancourt, W. Q., and Rose, J. B. Drinking water treatment processes for removal of *Cryptosporidium* and *Giardia*. *Veterinary Parasitology*, **2004**. 126(1), 219-234.

- Biolin Scientific. QCM-D Technology. **2014**. <http://www.biolinscientific.com/q-sense/technologies/> Accessed May 25, 2015
- Black, A. P., Birkner, F. B., and Morgan, J. J. The effect of polymer adsorption on the electrokinetic stability of dilute clay suspensions. *Journal of Colloid and Interface Science*, **1966**. 21(6), 626-648.
- Bolto, B., and Gregory, J. Organic polyelectrolytes in water treatment. *Water Research*. **2007**, 41(11), 2301-2324.
- Boström, M., Williams, D. R. M., and Ninham, B. W. Specific ion effects: why DLVO theory fails for biology and colloid systems. *Physical Review Letters*, **2001** 87(16), 168103.
- Brouckaert, B.M. Hydrodynamic detachment of deposited particles in fluidized bed filter backwashing. PhD Dissertation. Georgia Institute of Technology. **2004**. pp.38-40
- Brush, C. F., Ghiorse, W. C., Anguish, L. J., Parlange, J. Y., & Grimes, H. G. Transport of *Cryptosporidium parvum* oocysts through saturated columns. *Journal of Environmental Quality*, **1999**. 28(3), 809-815.
- Bukhari, Z., Marshall, M. M., Korich, D. G., Fricker, C. R., Smith, H. V., Rosen, J., & Clancy, J. L. Comparison of *Cryptosporidium parvum* viability and infectivity assays following ozone treatment of oocysts. *Applied and Environmental Microbiology*, **2000**. 66(7), 2972-2980.
- Bustamante, H. A., Shanker, S. R., Pashley, R. M., and Karaman, M. E. Interaction between *Cryptosporidium* oocysts and water treatment coagulants. *Water Research*, **2001** 35(13), 3179-3189.

- Caruso, F., and Möhwald, H. Preparation and characterization of ordered nanoparticle and polymer composite multilayers on colloids. *Langmuir*, **1999**, 15(23), 8276-8281.
- Centers for Disease Control and Prevention. Public Health Image Library #3386.
CDC/Alexander J. da Silva, PhD, Melanie Moser. **2002**.
- Chalmers, R. M. Chapter Sixteen - Cryptosporidium. *Microbiology of Waterborne Diseases (Second Edition)* Academic Press, London. **2014**, 287-326.
- Chung, J. Development of fluorescently labelled *Cryptosporidium* oocysts surrogates to test the efficacy of sand filtration processes. PhD Dissertation, University of New South Wales, Australia **2012**
- Clancy, J. L., Marshall, M. M., Hargy, T. M., & Korich, D. G. Susceptibility of five strains of *Cryptosporidium parvum* oocysts to UV light. *Journal American Water Works Association*, **2004**, [84-93.
- Considine, R. F., Dixon, D. R. and Drummond, C. J. Oocysts of *Cryptosporidium parvum* and model sand surfaces in aqueous solutions: an atomic force microscope (AFM) study. *Water Research*. **2002**, 36 (14): 3421-3428.
- Crittenden, J. C., Trussell, R. R., Hand, D. W., Howe, K. J., and Tchobanoglous, G. *MWH Water Treatment: Principles and Design: Principles and Design 2nd edition*. John Wiley & Sons, Danvers, MA. **2005**. pp 870-873.
- Dai, X., and Hozalski, R. M. Evaluation of microspheres as surrogates for *Cryptosporidium parvum* oocysts in filtration experiments. *Environmental Science and Technology*. **2003**, 37(5), 1037-1042.

- Di Giovanni, G. D., Hashemi, F. H., Shaw, N. J., Abrams, F. A., LeChevallier, M. W., and Abbaszadegan, M. Detection of infectious *Cryptosporidium parvum* oocysts in surface and filter backwash water samples by immunomagnetic separation and integrated cell culture-PCR. *Applied and Environmental Microbiology*, **1999**, 65(8), 3427-3432.
- Edzwald, James K., William C. Becker, and Steven J. Tambini. Organics, polymers, and performance in direct filtration. *Journal of Environmental Engineering* **1987**, 113, no. 1 167-185.
- Elliot, A.C., and W.A Woodward. *Statistical Analysis Quick Reference Guide*. Sage Publications, Inc. Thousand Oaks, CA. **2007**. pp 167.
- Emelko, M. B. Removal of *Cryptosporidium parvum* by granular media filtration, PhD Dissertation. The University of Waterloo. Waterloo, Canada. **2001**
- Emelko, M. B. Removal of viable and inactivated *Cryptosporidium* by dual-and tri-media filtration. *Water Research*. **2003**, 37(12), 2998-3008.
- Emelko, M. B., Huck, P. M., and Coffey, B. M. A review of *Cryptosporidium* removal by granular media filtration. *American Water Works Association*, **2005**, 97(12), 101.
- Fayer, R., and Ungar, B. L. *Cryptosporidium* spp. and cryptosporidiosis. *Microbiological Reviews*, **1986**, 50(4), 458.
- Fournier, T., Medjoubi-N, N., and Porquet, D. Alpha-1-acid glycoprotein. *Biochimica et Biophysica Acta (BBA)-Protein Structure and Molecular Enzymology*. **2000**, 1482(1), 157-171.
- Ghosh, M. M., Cox, C. D., and Prakash, T. M.. Polyelectrolyte selection for water treatment. *Journal American Water Works Association*, **1985** 67-73.

- Gitis, V. Rapid sand filtration of *Cryptosporidium parvum*: effects of media depth and coagulation. *Water Science & Technology: Water Supply*. **2008**. 8(2): 129-134
- Haas, C. N., Severin, B., Roy, D., Engelbrecht, R., Lalchandani, A., and Farooq, S. Field observations on the occurrence of new indicators of disinfection efficiency. *Water Research*. **1985**, 19(3), 323-329.
- Hagler, A.N. Yeasts as indicators of environmental quality. *In: Biodiversity and Ecophysiology of Yeasts* (eds. Rose, A.H., and Harrison, J.S.) **2006**, 515-532.
- Harter, T., Wagner, S., & Atwill, E. R. Colloid transport and filtration of *Cryptosporidium parvum* in sandy soils and aquifer sediments. *Environmental Science and Technology*, **2000**. 34(1), 62-70.
- Hayashi, H., Tsuneda, S., Hirata, A., and Sasaki, H. Soft particle analysis of bacterial cells and its interpretation of cell adhesion behaviors in terms of DLVO theory. *Colloids and Surfaces B: Biointerfaces*, **2001**. 22(2), 149-157.
- Health Canada. Guidelines for Canadian Drinking Water Quality—Summary Table **2012**
Water, Air and Climate Change Bureau, Healthy Environments and Consumer Safety Branch, Health Canada, Ottawa, Ontario.
- Hendricks, D.W. *Water Treatment Unit Processes: Physical and Chemical*. CRC Press. **2006**. pp 1020
- Hermansson, M. The DLVO theory in microbial adhesion. *Colloids and Surfaces B: Biointerfaces*, **1999**. 14(1), 105-119.
- Hsu, B. M., Huang, C., and Pan, J. R. Filtration behaviors of *Giardia* and *Cryptosporidium*—ionic strength and pH effects. *Water Research*, **2001**. 35(16), 3777-3782.

- Huck, P. M., Emelko, M. B., Coffey, B. M., Maurizio, D. D. and O'Melia, C. R. Filter operation effects on pathogen passage. AWWA Research Foundation and American Water Works Association, Denver **2001**
- Johal, M. S. *Understanding Nanomaterials*. **2011**. CRC Press. pp. 195-196
- Karanis, P., Schoenen, D., and Seitz, H. M. *Giardia* and *Cryptosporidium* in backwash water from rapid sand filters used for drinking water production. *Zentralblatt für Bakteriologie*, **1996**. 284(1), 107-114.
- Kuznar, Z. A., and Elimelech, M. Role of surface proteins in the deposition kinetics of *Cryptosporidium parvum* oocysts. *Langmuir*, **2005**. 21(2), 710-716.
- Lau, B. L., Harrington, G. W., Anderson, M. A., and Tejedor, I. Physicochemical aspects of *Cryptosporidium* surrogate removal in carbon block filtration. *American Water Works Association*, **2005**. 92-101.
- LeChevallier, M. W., Norton, W. D., and Lee, R. G. *Giardia* and *Cryptosporidium* spp. in filtered drinking water supplies. *Applied Environmental Microbiology*. **1991**, 57(9), 2617-2621.
- Li, X., Scheibe, T. D., and Johnson, W. P. Apparent decreases in colloid deposition rate coefficients with distance of transport under unfavorable deposition conditions: A general phenomenon. *Environmental Science and Technology*, **2004**. 38(21), 5616-5625.
- Logan, A. J., Stevik, T. K., Siegrist, R. L., and Rønn, R. M. Transport and fate of *Cryptosporidium parvum* oocysts in intermittent sand filters. *Water Research*, **2001**. 35(18), 4359-4369.

- MacKenzie, W. R., Hoxie, N. J., Proctor, M. E., Gradus, M. S., Blair, K. A., Peterson, D. E., and Davis, J. P. A massive outbreak in Milwaukee of *Cryptosporidium* infection transmitted through the public water supply. *New England Journal of Medicine*, **1994** 331(3), 161-167.
- Marcus, I. M., Herzberg, M., Walker, S. L., and Freger, V. *Pseudomonas aeruginosa* attachment on QCM-D sensors: the role of cell and surface hydrophobicities. *Langmuir*, **2012** 28(15), 6396-6402.
- Matilainen, A., Vepsäläinen, M., and Sillanpää, M. Natural organic matter removal by coagulation during drinking water treatment: A review. *Advances in Colloid and Interface Science*, **2010**. 159(2), 189-197.
- McCormick, R. F., and King, P. H. Factors that affect use of direct filtration in treating surface waters. *Journal American Water Works Association*, **1982**. 234-242.
- McEwan, J.B. *Treatment processes for particle removal*. American Water Works Association. CRC Press. Denver, CO. **1998**. pp 85
- Nelson, K. E., and Ginn, T. R. New collector efficiency equation for colloid filtration in both natural and engineered flow conditions. *Water Resources Research*, **2011**. 47(5).
- Pang, L., Nowostawska, U., Ryan, J. N., Williamson, W. M., Walshe, G., and Hunter, K. A. Modifying the surface charge of pathogen-sized microspheres for studying pathogen transport in groundwater. *Journal of Environmental Quality*, **2009** 38(6), 2210-2217.
- Pang, L., Nowostawska, U., Weaver, L., Hoffman, G., Karmacharya, A., Skinner, A., and Karki, N. Biotin-and Glycoprotein-Coated Microspheres: Potential Surrogates for

- Studying Filtration of *Cryptosporidium parvum* in Porous Media. *Environmental Science and Technology*. **2012**, 46(21), 11779-11787.
- Park, Y., Atwill, E. R., Hou, L., Packman, A. I., & Harter, T.. Deposition of *Cryptosporidium parvum* oocysts in porous media: a synthesis of attachment efficiencies measured under varying environmental conditions. *Environmental Science and Technology*, **2012**. 46(17), 9491-9500.
- Patania, N. L. Jacangelo, J. G., Cummings, L., Wilczak, A., Riley, K. and Oppenheimer, J. Optimization of filtration for cyst removal. American Water Works Association Research Foundation, Denver **1995**
- Pizzi, N.G. *Water Treatment 4th edition*. American Water Works Association. Denver, CO. **2011**. pp 106
- Poitras, C. and Tufenkji, N. A QCM-D-based biosensor for E. coli O157: H7 highlighting the relevance of the dissipation slope as a transduction signal. *Biosensors and Bioelectronics*, **2009**. 24(7), 2137-2142.
- Poitras, C., Fatisson, J., and Tufenkji, N. Real-time microgravimetric quantification of *Cryptosporidium parvum* in the presence of potential interferents. *Water Research*, **2009** 43(10), 2631-2638.
- Polysciences Fluoresbrite YG Carboxylate Microspheres 4.50µm. Polysciences Inc. Warrington, PA. **2015**. <http://www.polysciences.com/default/fluoresbrite-yg-carboxylate-microspheres-450-m>
- Rajagopalan, R., and C. Tien. Trajectory analysis of deep-bed filtration with sphere-in-cell porous-media model. *AIChE*. **1976**. 22(3) 523-533

- Rochelle, P. A., Marshall, M. M., Mead, J. R., Johnson, A. M., Korich, D. G., Rosen, J. S., and De Leon, R. Comparison of in vitro cell culture and a mouse assay for measuring infectivity of *Cryptosporidium parvum*. *Applied and Environmental Microbiology*, **2002**. 68(8), 3809-3817.
- Sauerbrey, G. Use of vibrating quartz for thin film weighing and microweighing. *Z. Phys*, **1959**. 155(2), 206-222.
- Sigma-Aldrich. Alpha-1-Acid Glycoprotein Product Information. Saint Louis, MO. ALF/RXR 9/02. http://www.sigmaaldrich.com/content/dam/sigmaaldrich/docs/Sigma/Product_Information_Sheet/2/g9885pis.pdf
- Stirling, R., Aramini, J., Ellis, A., Lim, G., Meyers, R., Fleury, M., and Werker, D. Waterborne Cryptosporidiosis Outbreak, North Battleford, Saskatchewan, April **2001**.
- Swertfeger, J., Metz, D. H., DeMarco, J., Braghetta, A., and Jacangelo, J. G. Effect of filter media on cyst and oocyst removal. *American Water Works Association Journal*, **1999**, 91(9), 90-100.
- Thirunavukkarasu, O. S., Viraraghavan, T., and Subramanian, K. S. Arsenic removal from drinking water using iron oxide-coated sand. *Water, Air, and Soil Pollution*, **2003**. 142(1-4), 95-111.
- Torkzaban, S., Bradford, S. A., and Walker, S. L. Resolving the coupled effects of hydrodynamics and DLVO forces on colloid attachment in porous media. *Langmuir*, **2007**. 23(19), 9652-9660.
- Treweek, Gordon P. Optimization of flocculation time prior to direct filtration. *Journal American Water Works Association* **1979**. 96-101.

- Tufenkji, N., and M. Elimelech. Correlation equation for predicting single-collector efficiency in physicochemical filtration in saturated porous media. *Environmental Science and Technology*. **2004**. 38(2), 529-536.
- Tufenkji, N. and Elimelech, M., Spatial distribution of *Cryptosporidium* oocysts in porous media: Evidence for dual mode deposition. *Environmental Science and Technology*. **2005**, 39, 3620-3629
- United States Environmental Protection Agency. Method 1623: *Cryptosporidium* and *Giardia* in Water by Filtration/IMS/FA **2005**
- United States Environmental Protection Agency. National Primary Drinking Water Regulations: Long Term 2 Enhanced Surface Water Treatment Rule. **2006**
<https://www.federalregister.gov/articles/2006/01/05/06-4/national-primary-drinking-water-regulations-long-term-2-enhanced-surface-water-treatment-rule#h-8> Retrieved January 27, 2015
- Vandamme, D., Foubert, I., and Muylaert, K. Flocculation as a low-cost method for harvesting microalgae for bulk biomass production. *Trends in Biotechnology*, **2013**. 31(4), 233-239.
- Wang, Y., Narain, R., and Liu, Y. Study of Bacterial Adhesion on Different Glycopolymer Surfaces by Quartz Crystal Microbalance with Dissipation. *Langmuir*, **2014**. 30(25), 7377-7387.
- Widerström M, Schönning C, Lilja M, Lebbad M, Ljung T, and Allestam G. Large outbreak of *Cryptosporidium hominis* infection transmitted through the public water supply, Sweden. *Emerging Infectious Diseases*

- http://wwwnc.cdc.gov/eid/article/20/4/12-1415_article. **2014** Retrieved October 20, 2014
- Yao, K.M., Habibian, M.T., and O'Melia, C.R. Water and Waste Water Filtration: Concepts and Applications. *Environmental Science and Technology*. **1971**, 5(11), 1105-1112
- Yang, R., Murphy, C., Song, Y., Ng-Hublin, J., Estcourt, A., Hijjawi, N., Chalmers, R., Hadfield, S., Bath, A., Gordon, C., and Ryan, U. Specific and quantitative detection and identification of *Cryptosporidium hominis* and *C. parvum* in clinical and environmental samples. *Experimental Parasitology*, **2013**, 135(1), 142-147.
- Zeng, Y., Grandner, S., Oliveira, C. L., Thünemann, A. F., Paris, O., Pedersen, J. S., and von Klitzing, R. Effect of particle size and Debye length on order parameters of colloidal silica suspensions under confinement. *Soft Matter*, **2011**. 7(22), 10899-10909.
- Zhu, H., Smith, D.W., Zhou, H., and Stanley, S.J. Selection of polymers as filter aid for E.L. Smith Water Treatment Plant Softened Water. *Environmental Engineering Technical Report*. University of Alberta. Edmonton, AB, Canada. **1995**
- Zilberman, A., Zimmels, Y., Starosvetsky, J., Zuckerman, U., and Armon, R. A two-phase separation method for recovery of *Cryptosporidium* oocysts from soil samples. *Water, Air, and Soil Pollution*, **2009**. 203(1-4), 325-334.

Appendix A

Assumption testing for two-way ANOVA

Assumptions of the 2x2 ANOVA are independence, homoscedasticity, and normality. Figure 5.15 of residuals versus observation order verifies that residuals are independent from one another.

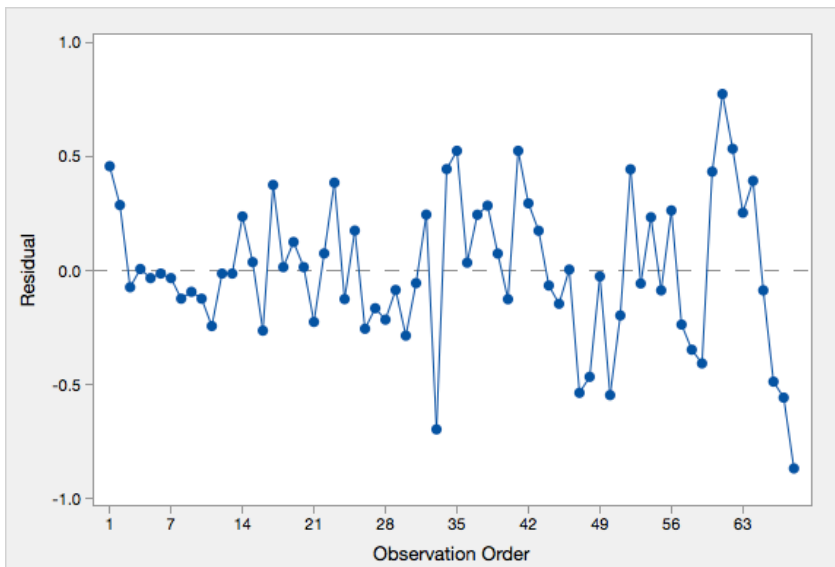


Figure 5.15 Observation order of log-removals versus model residuals

Figure 5.16 shows that the distribution of residuals may possibly have unequal variance. The most noticeable difference in variance is observed for direct filtration at 8.6 m/h (smallest variance) and conventional filtration at 5.7 m/h (highest variance). This represents a deviation from the assumptions for the 2x2 ANOVA. Several data transformations were attempted (log, natural log, square root), and all transformations resulted in a similar pattern of unequal variance between these two data sets. All data transformations resulted with the same conclusions from the 2x2 ANOVA (statistical significance for main effects and interaction). It was determined to present the non-transformed ANOVA results. It has been previously established that ANOVA models are

quite robust to reasonable departures from assumptions of equal variance (Elliot and Woodward, 2007).

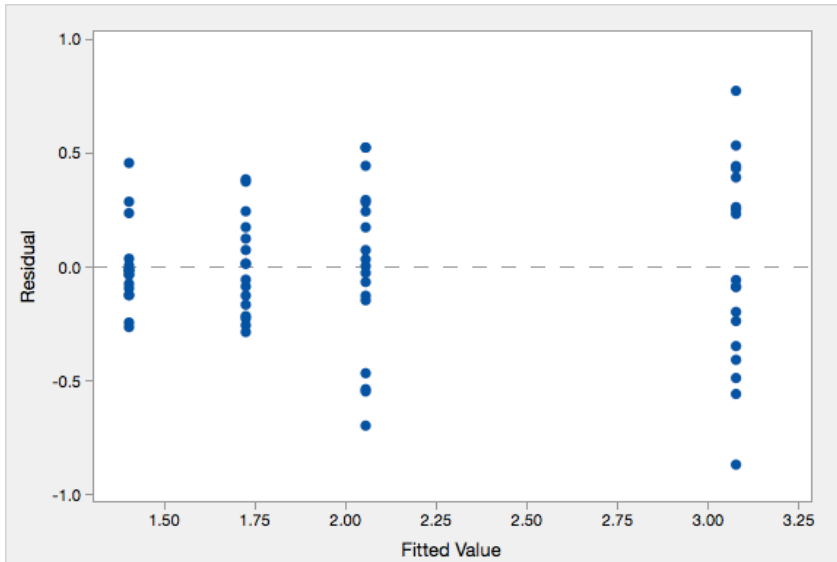


Figure 5.16 Fitted log-removal values versus model residuals

Normality of residuals is verified in Figure 5.17, where the model residuals fall on straight line and there is no discernable pattern. This was confirmed by Anderson-Darling (AD) tests for normality, where data for each pilot run resulted in $p > 0.05$. It can be concluded that the data follow a normal distribution. The AD-value and p-value are shown below in Table 5.12.

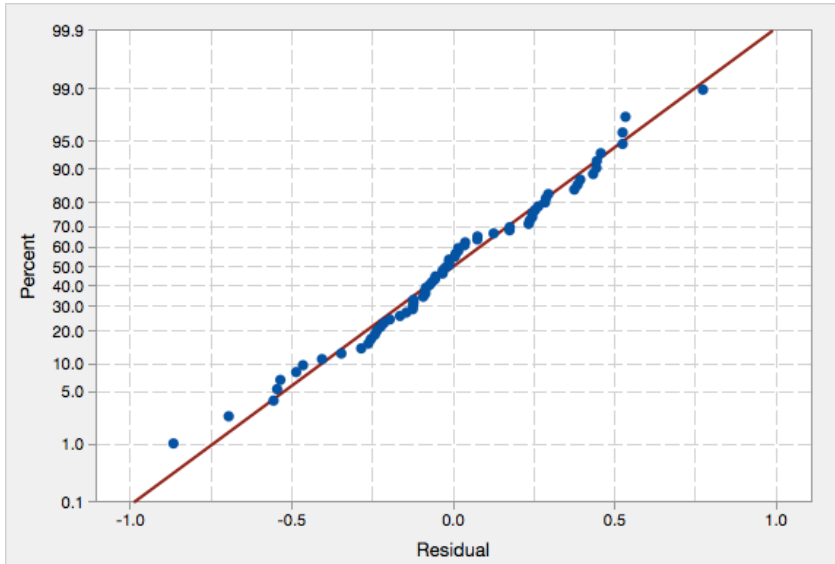


Figure 5.17 Normal probability plot for ANOVA of log-removals

Table 5.12 Anderson-Darling normality tests for log-removal data.

Filtration Mode	Flow Rate (m/h)	AD –value	p-value
Direct	8.6	0.58	0.0888
Direct	5.7	0.47	0.1713
Conventional	8.6	0.35	0.3738
Conventional	5.7	0.43	0.2310

Calculated values for normal effects plot (Figure 5.7)

The normal effects plot (Figure 5.7) was constructed using the average log-removals calculated over the duration of each pilot-column run. A 2-factor, 2-level approach was used. No zero-value midpoints were used due to limited resources and personnel resources. Settings for each experiment are given below in Table 5.13. The contrast and effects are calculated as follows:

Contrast = (sum of observations at high level) - (sum of observations at low level)

$$\text{Effects} = \frac{2 \times \text{contrast}}{n2^k}$$

n = # of replicates (1 in this case); k = # of factors (2 in this case)

The absolute value of the calculated effect was plotted against assigned n-scores determined from ascending rank.

Table 5.13 Contrast and effects table designations. For flow rate, (+) refers to 8.6 m/h, (-) refers to 5.7 m/h. For influent conditions, (+) refers direct filtration and (-) refers to conventional filtration.

Experiment #	A (flow rate)	B (influent condition)	AB	Average log-removal
Run 1	+	+	+	1.46
Run 2	-	+	-	1.73
Run 3	+	-	-	2.06
Run 4	-	-	+	3.08

Experiment #	A (flow rate)	B (influent condition)	AB
Run 1	1.46	1.46	1.46
Run 2	-1.73	1.73	-1.73
Run 3	2.06	-2.06	-2.06
Run 4	-3.08	-3.08	3.08
Contrast	-1.28	-1.95	0.76
Effects	-0.64	-0.97	0.38

Appendix B

Total microsphere count methods

1. Seeding batch microspheres

Microsphere concentration was multiplied by volume of seeding batch.

2. Influent microspheres

The total number of microspheres was approximated using a Riemann sum with microsphere concentration and corresponding volume of displaced water. Since the influent microspheres were not measured until the concentration was zero, the volume where this point was reached was estimated by extrapolating the influent concentration curve. This was done either visually, or determined by fitting the data points to a curve after seeding was finished (ie, microsphere concentration after 115 L) and finding the x-intercept.

3. Effluent microspheres

The effluent microspheres were determined by the same method as the influent.

4. Accumulated in filter media

Microspheres accumulated in the filter media was determined as the effluent microspheres subtracted from the influent microspheres.

5. Backwash microspheres

Backwash concentration is determined by the Riemann sum method using the plot of backwash concentration at certain backwash times. The calculated value was multiplied by the backwash flow rate to determine the total number of microspheres. For direct filtration, the concentration at the beginning of backwash (time=0) was not measured. This concentration was determined using the log-linear relationship of backwash concentration to backwash time (seen in Figure 5.14). The y-intercept of the best fit line for the first 3 data points was used to back calculate the concentration at $t=0$, this value was then adjusted by 10 seconds to account for the typical lag in turbidity concentrations noted for backwash (Brouckaert, 2004).

Table 5.14a Total microsphere counts at different points of the experimental system for direct filtration pilot-column trials

Loading rate	Direct Filtration		Direct Filtration	
	8.6 (m/h)		5.7 (m/h)	
	Column 1	Column 2	Column 1	Column 2
Seeding Batch	1.89×10^8	1.89×10^8	1.22×10^8	1.29×10^8
Influent	1.27×10^8	1.49×10^8	1.58×10^8	1.24×10^8
Effluent	5.05×10^6	7.01×10^6	2.82×10^6	3.17×10^6
Accumulated	1.22×10^8	1.42×10^8	1.55×10^8	1.21×10^8
Backwash	1.27×10^8	1.38×10^8	9.08×10^7	1.05×10^8

Table 5.14b Total microsphere counts at different points of the experimental system for conventional filtration pilot-column trials

Loading rate	Conventional Filtration		Conventional Filtration	
	8.6 (m/h)		5.7 (m/h)	
	Column 1	Column 2	Column 1	Column 2
Seeding Batch	8.57×10^7	9.13×10^7	1.22×10^8	1.33×10^8
Influent	7.79×10^7	8.41×10^7	9.15×10^7	1.07×10^8
Effluent	4.64×10^5	1.28×10^6	7.93×10^4	1.45×10^5
Accumulated	7.74×10^7	8.28×10^7	9.15×10^7	1.07×10^8
Backwash	5.70×10^7	8.46×10^7	8.81×10^7	8.50×10^7